Short Course on Electronically Scanned Reflectarrays - Introduction

Koen Van Caekenberghe, Ph.D.

April 15, 2011

Overview

Introduction

Electronically Scanned Arrays

Array Antennas

Feed Antennas
- Rectangular Horns
- Conical Horns
- Soft and Hard Surface Horns
- UWB Leaky Lens Antenna

Reflector Antennas
- Reflector Antennas
- Cassegrain & Gregorian Dual-Reflector Antennas
- Inverse Cassegrain Dual-Reflector Antennas

RF Components
- Linear-Circular Polarizers & Orthomode Transducers
- (TTD) Phase Shifters
- Transmitters

RF Technologies
- Ferrites
- Ferroelectrics
- MOSFET
- pHEMT (MODFET)
- p-i-n Diodes
- RF MEMS

Introduction

Archimedes Heat Ray (214 B.C. - Present)

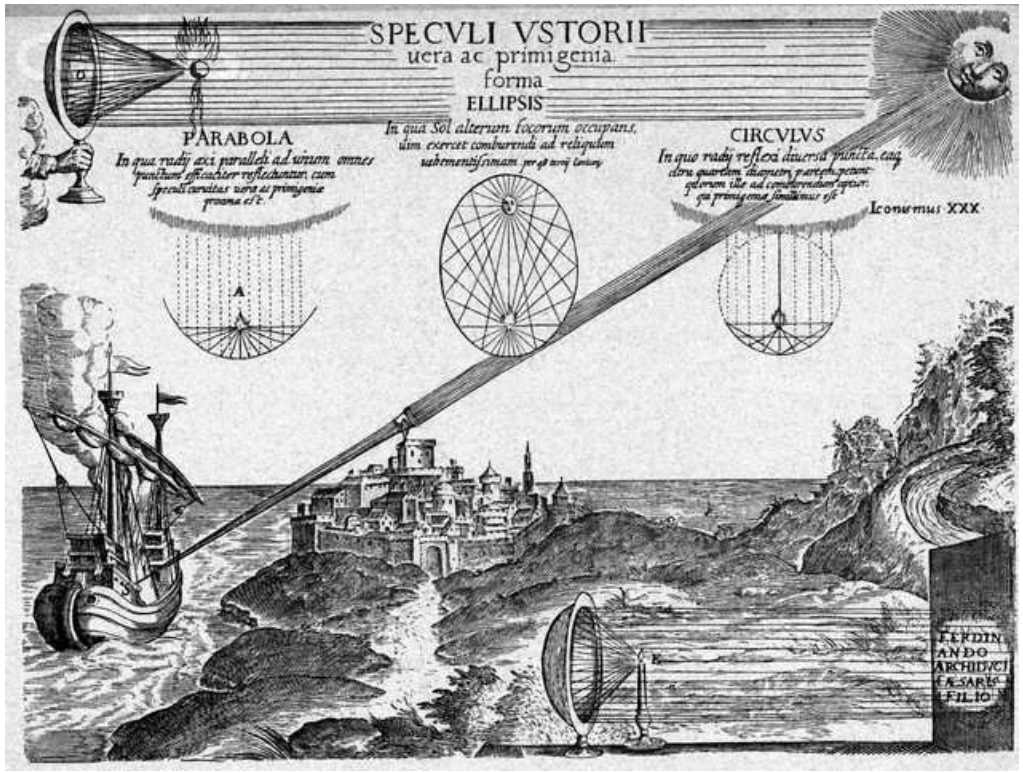

Figure 1: Engraving of Archimedes' Burning Mirror by Athanasius Kircher, German Renaissance Jesuit, 1602-1680

Figure 2: Stirling engine with parabolic reflector by Stirling Energy Systems

Electronically Scanned Arrays

Electronically Scanned Arrays

- Assume a line array of N identical antennas, fed by correlated replicas of a waveform, which are:
  - symmetrically attenuated across the aperture, with taper $|a_n|$
  - linearly phase shifted modulo 360° (or time delayed) across the aperture, with progressive phase shift $\beta = -k_0\, d_x\, \sin\theta_0$ (or with progressive time delay $\Delta\tau = \frac{d_x\, \sin\theta_0}{c}$)

- The normalized far field of the line array (along the x-axis), $\vec{E}(r,\theta,\phi)$, can be written as the product of the element factor, $\vec{f}(\theta,\phi)$, and a scalar array factor, $F(\theta,\phi)$.
  $\vec{E}(r,\theta,\phi) = \vec{f}(\theta,\phi)\, F(\theta,\phi) =$
  $\vec{f}(\theta,\phi) \sum_{n=-N/2}^{N/2} |a_n|\, e^{j\, k_0\, \frac{2\,n-1}{2}\, d_x\, (u-u_0)}$
  in which:
  - $k_0 = \frac{2\,\pi}{\lambda_0}$, $u = \sin\theta$, $u_0 = \sin\theta_0$
  - $r = \sqrt{x^2+y^2+z^2}$
  - The polarization of the line array is determined by the element factor, $\vec{f}(\theta,\phi)$

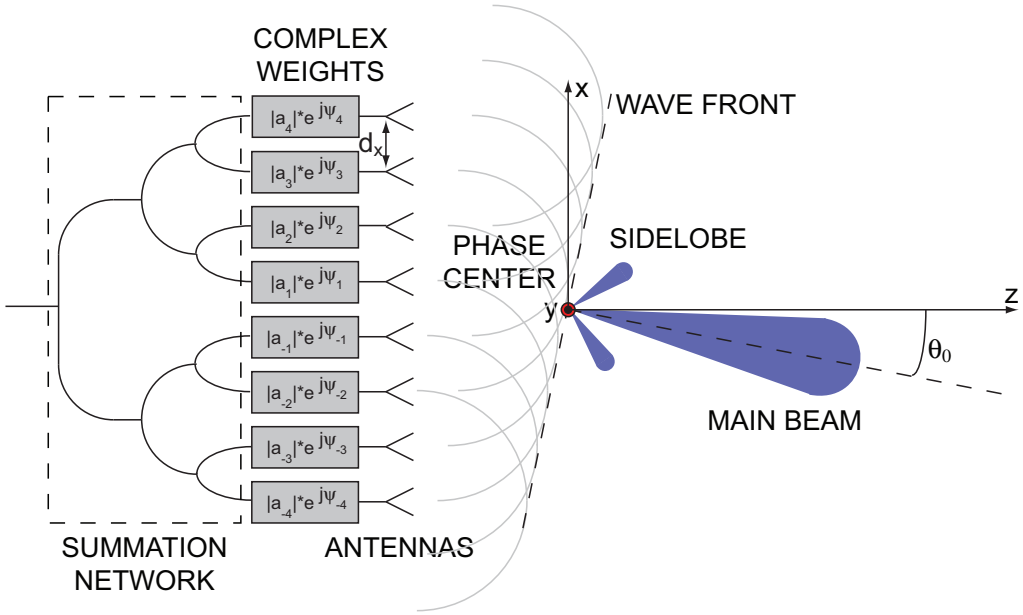

Figure 3: Electronically scanned array principle (line array along x-axis), in which $\psi_n = \frac{2\,n-1}{2}\,\beta$

Electronically Scanned Arrays

Derivation of expressions for the average directivity and the side lobe level variance in the presence of random (Gaussian distributed) phase errors, Φ_n. Assume a uniform taper ($|a_n| = 1$):

- **Average main beam radiation intensity**:
  - Assume $\theta_0 = 0°$:

$$F_e(\theta = 0°, \phi) = \sum_{n=1}^{N} e^{j\Phi_n} = \sum_{n=1}^{N} [\cos\Phi_n + j \sin\Phi_n]$$

  - Assume Φ_n is small ($\sum_{n=1}^{N} \sin\Phi_n \approx 0$):

$$\begin{aligned} F_e(\theta = 0°, \phi) &\approx \sum_{n=1}^{N} \cos\Phi_n \\ &\approx \sum_{n=1}^{N} [1 - \frac{1}{2}{\Phi_n}^2] \\ &= N - \frac{1}{2}\sum_{n=1}^{N} {\Phi_n}^2. \end{aligned}$$

- **Average main beam radiation intensity (continued)**:
  - The average main beam radiation intensity equals:

$$\begin{aligned} \overline{F_e^2(\theta = 0°, \phi)} &= \overline{\left(N - \frac{1}{2}\sum_{n=1}^{N} {\Phi_n}^2\right)^2} \\ &= N^2 - N\overline{\sum_{n=1}^{N} {\Phi_n}^2} + \\ &\quad \frac{1}{4}\overline{\sum_{k,l}^{N} {\Phi_n}^2 {\Phi_l}^2}. \end{aligned}$$

  - Assume a phase error variance $\Phi^2 = \overline{{\Phi_n}^2}$, which implies:

$$\overline{{\Phi_n}^2 {\Phi_l}^2} = \overline{\Phi^4} \ll 4N\Phi^2$$

  - The average main beam radiation intensity becomes:

$$\overline{F_e^2(\theta = 0°, \phi)} = N^2(1 - \Phi^2).$$

- **Sidelobe level variance**:
  - The perturbed array factor, evaluated at a null of the error-free array pattern, becomes:

$$\begin{aligned} F_e(\theta = \theta_{null}, \phi) &= \sum_{n=1}^{N} e^{j\beta_n} e^{j\Phi_n} \\ &= \sum_{n=1}^{N} e^{j\beta_n} [\cos\Phi_n + j \sin\Phi_n] \end{aligned}$$

    with $\beta_n = -k_0(n-1)d_x \sin\theta_{null}$.

  - At a null of the error-free array pattern, the $\sum_{n=1}^{N} e^{j\beta_n} \cos\Phi_n$ terms vanish[a]:

$$\begin{aligned} F_e(\theta = \theta_{null}, \phi) &\approx j \sum_{n=1}^{N} e^{j\beta_n} \sin\Phi_n \\ &\approx j \sum_{n=1}^{N} e^{j\beta_n} \Phi_n \end{aligned}$$

[a] $\cos x = \sum_{n=0}^{\infty} \frac{(-1)^n}{(2n)!} x^{2n} = 1 - \frac{x^2}{2!} + \frac{x^4}{4!} - \cdots$

- **Sidelobe level variance (continued)**:
  - The average radiation intensity, evaluated at the null of the error-free array pattern, becomes:

$$\begin{aligned} & \overline{|F_e(\theta = \theta_{null}, \phi)|^2} \\ &= \overline{\left[\sum_{n=1}^{N} e^{j\beta_n}\Phi_n\right]\left[\sum_{n=1}^{N} e^{-j\beta_n}\Phi_n\right]} \\ &= \sum_{n=1}^{N} \overline{\Phi_n^2} + \overline{\sum_{k\neq l} \Phi_n \Phi_l e^{j(\beta_n - \beta_l)}} \\ &= N\Phi^2 \end{aligned}$$

    with $\overline{\Phi_n}, \overline{\Phi_l}$ assumed uncorrelated.

  - The sidelobe level variance, evaluated at a null of the error-free array pattern, becomes:

$$\begin{aligned} \sigma^2 &= \frac{\overline{|F_e(\theta = \theta_{null}, \phi)|^2}}{D_0} = \frac{N\Phi^2}{N^2} \\ &= \frac{\Phi^2}{N} \end{aligned}$$

- **Average directivity**:
  - The average directivity D_e, can be calculated from:

$$\begin{aligned} D_e(\theta = 0^\circ, \phi) &= \frac{4\pi \overline{F_e^2(\theta = 0^\circ, \phi)}}{P_{rad}} \\ &= \frac{N^2\left(1 - \Phi^2\right)}{N + N\Phi^2} \\ &= N\frac{1 - \Phi^2}{1 + \Phi^2} \\ &\approx N\frac{1}{1 + \Phi^2} \end{aligned}$$

  - The average directivity and gain loss become:

$$\begin{aligned} \frac{D_e}{D} &= \frac{1}{1 + \Phi^2} \\ \frac{G_e}{G} &= \frac{1}{1 + \Phi^2} \end{aligned}$$

- **Example**:
  - Assume a 4-bit phase shifter; the maximum phase error is now $\pm 11.25^\circ$. The phase error variance becomes:

$$\Phi^2 = \frac{\pi^2}{3(2^{2P})} = 0.0129\ [rad^2]$$

    which yields a phase error standard deviation of 6.5°.
  - Assume 64 antennas; the sidelobe level variance and the average directivity loss become:

$$\begin{aligned} \sigma^2 &= \frac{\Phi^2}{N} = -36.956\ [dB] \\ \frac{D_e}{D} &= \frac{1}{1 + \Phi^2} = -0.0557\ [dB] \end{aligned}$$

Electronically Scanned Arrays

Figures of merit [1–5]:

- Bandwidth
  - Radar range resolution:

    $r = \frac{c}{2\,BW}$

- Beam pointing error:

  $\Delta^2 = \Phi^2 \frac{\sum A_i^2\, x_i^2}{\left(\sum A_i\, x_i^2\right)^2}$

- EIRP $\times$ G_r/T
  - Radar range equation:

    $R_{max} = \sqrt[4]{\frac{\lambda_0^2\, EIRP\, G_r/T\, \sigma}{64\,\pi^3\, k_B\, BW\, SNR_{min}}}$

  - Scan loss:

    $\frac{G_e}{G} = \frac{(\cos\theta)^n}{1+\delta^2+\Phi^2}$

- Field of view:

  $\frac{d}{\lambda_0} \leq \frac{1}{1+\sin\theta_{max}}$

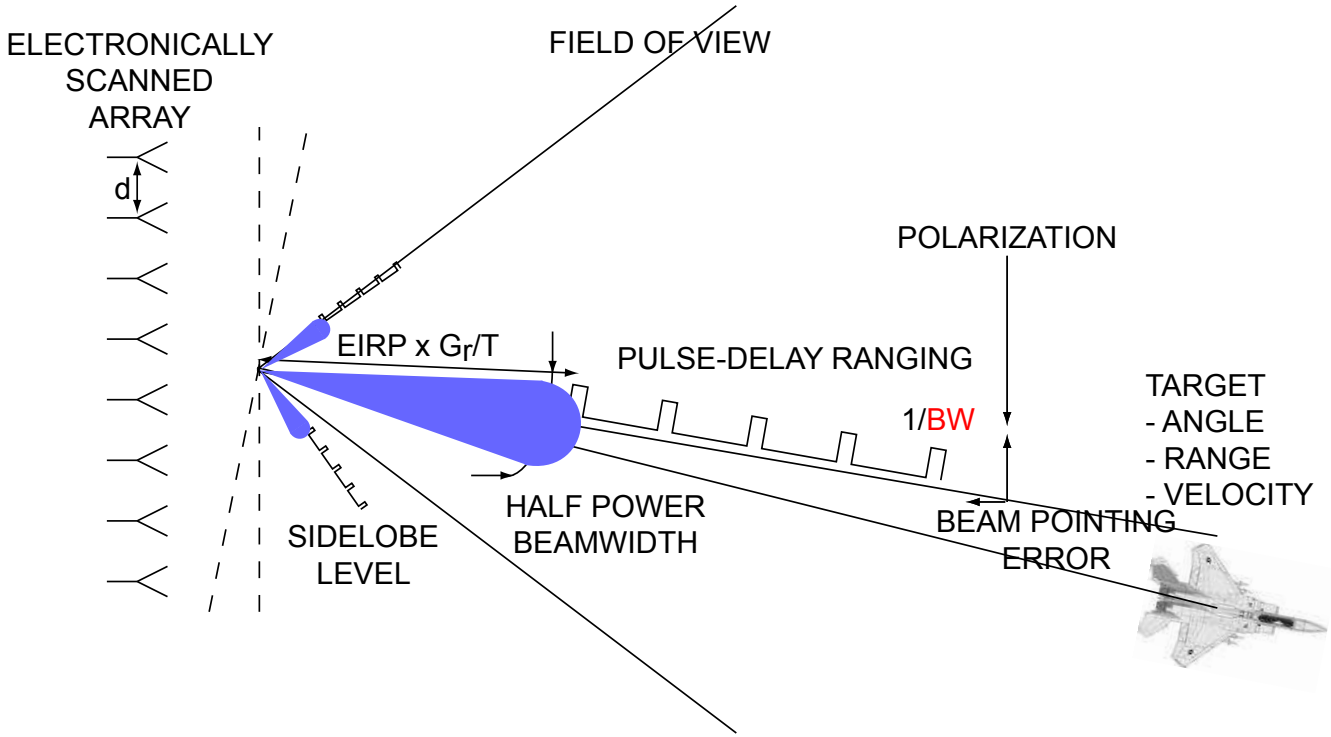

Figure 4: Figures of merit for an electronically scanned array set the radar's ability to search and track targets.

Electronically Scanned Arrays

Figures of merit [1–5]:

- Bandwidth
  - Radar range resolution:

    $r = \frac{c}{2\,BW}$

- Beam pointing error:

  $\Delta^2 = \Phi^2 \frac{\sum A_i^2\, x_i^2}{\left(\sum A_i\, x_i^2\right)^2}$

- EIRP $\times$ G_r/T
  - Radar range equation:

    $R_{max} = \sqrt[4]{\frac{\lambda_0^2\, EIRP\, G_r/T\, \sigma}{64\,\pi^3\, k_B\, BW\, SNR_{min}}}$

  - Scan loss:

    $\frac{G_e}{G} = \frac{(\cos\theta)^n}{1+\delta^2+\Phi^2}$

- Field of view:

  $\frac{d}{\lambda_0} \leq \frac{1}{1+\sin\theta_{max}}$

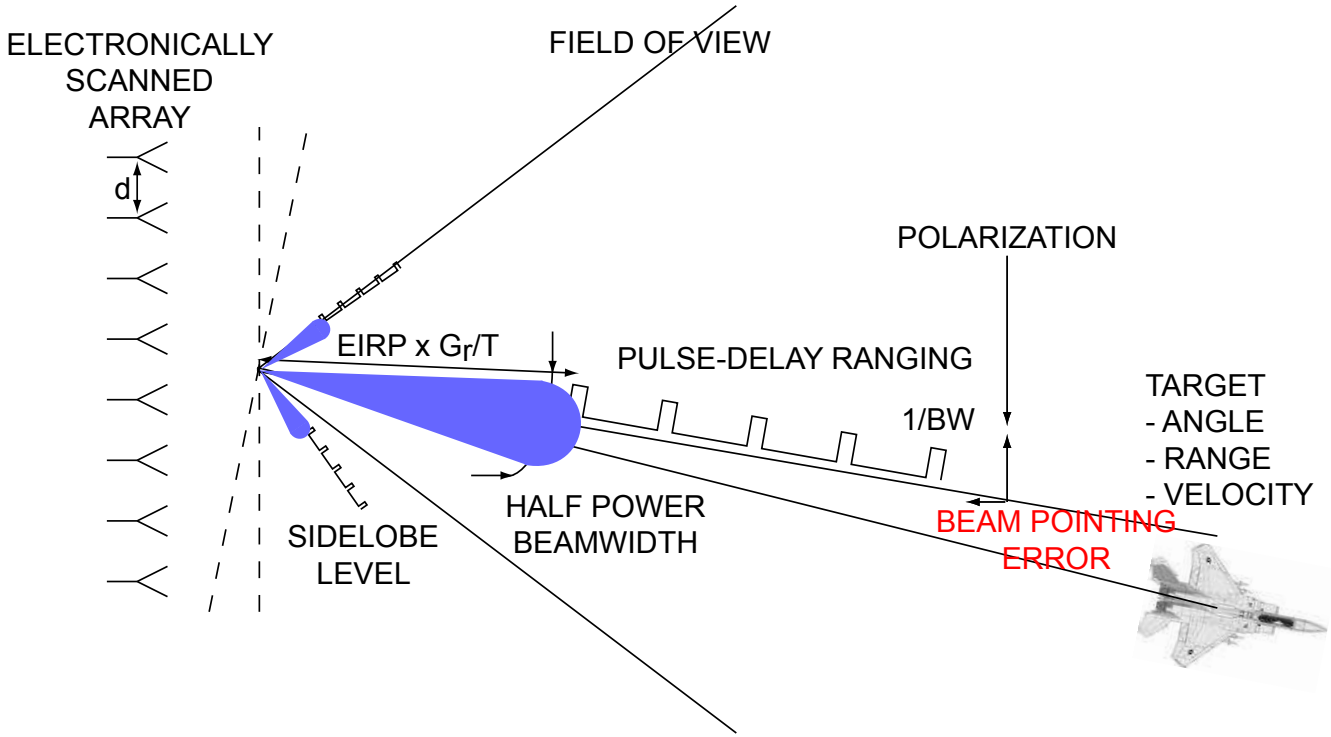

Figure 5: Figures of merit for an electronically scanned array set the radar's ability to search and track targets.

Electronically Scanned Arrays

Figures of merit [1–5]:

- Bandwidth
  - Radar range resolution:

    $r = \frac{c}{2\,BW}$

- Beam pointing error:

  $\Delta^2 = \Phi^2 \frac{\sum A_i^2\, x_i^2}{\left(\sum A_i\, x_i^2\right)^2}$

- EIRP $\times$ G_r/T
  - Radar range equation:

    $R_{max} = \sqrt[4]{\frac{\lambda_0^2\, EIRP\, G_r/T\, \sigma}{64\,\pi^3\, k_B\, BW\, SNR_{min}}}$

  - Scan loss:

    $\frac{G_e}{G} = \frac{(\cos\theta)^n}{1+\delta^2+\Phi^2}$

- Field of view:

  $\frac{d}{\lambda_0} \leq \frac{1}{1+\sin\theta_{max}}$

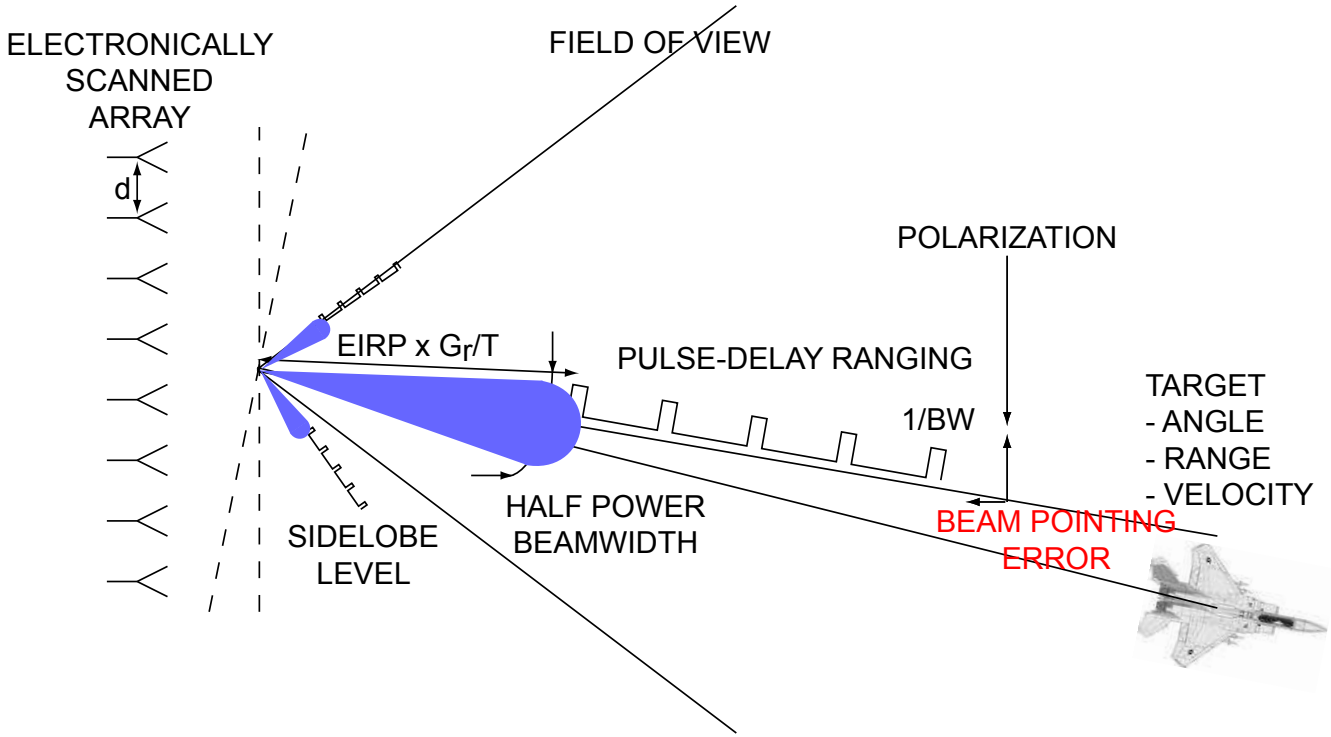

Figure 5: Figures of merit for an electronically scanned array set the radar's ability to search and track targets.

- Amplitude error variance:

  $\hat{\delta}^2 = S^2_{A_{ATT}} + S^2_{A_{PS}}$

- Phase error variance:

  $\hat{\Phi}^2 = S^2_{P_{ATT}} + S^2_{P_{PS}} + \frac{1}{3}\frac{\pi^2}{2^{2P}}$

Electronically Scanned Arrays

Figures of merit [1–5]:

- Bandwidth
  - Radar range resolution:

    $r = \frac{c}{2\,BW}$

- Beam pointing error:

  $\Delta^2 = \Phi^2 \frac{\sum A_i^2\, x_i^2}{\left(\sum A_i\, x_i^2\right)^2}$

- EIRP $\times$ G_r/T
  - Radar range equation:

    $$R_{max} = \sqrt[4]{\frac{\lambda_0^2\, EIRP\, G_r/T\, \sigma}{64\,\pi^3\, k_B\, BW\, SNR_{min}}}$$

  - Scan loss:

    $\frac{G_e}{G} = \frac{(\cos\theta)^n}{1+\delta^2+\Phi^2}$

- Field of view:

  $\frac{d}{\lambda_0} \leq \frac{1}{1+\sin\theta_{max}}$

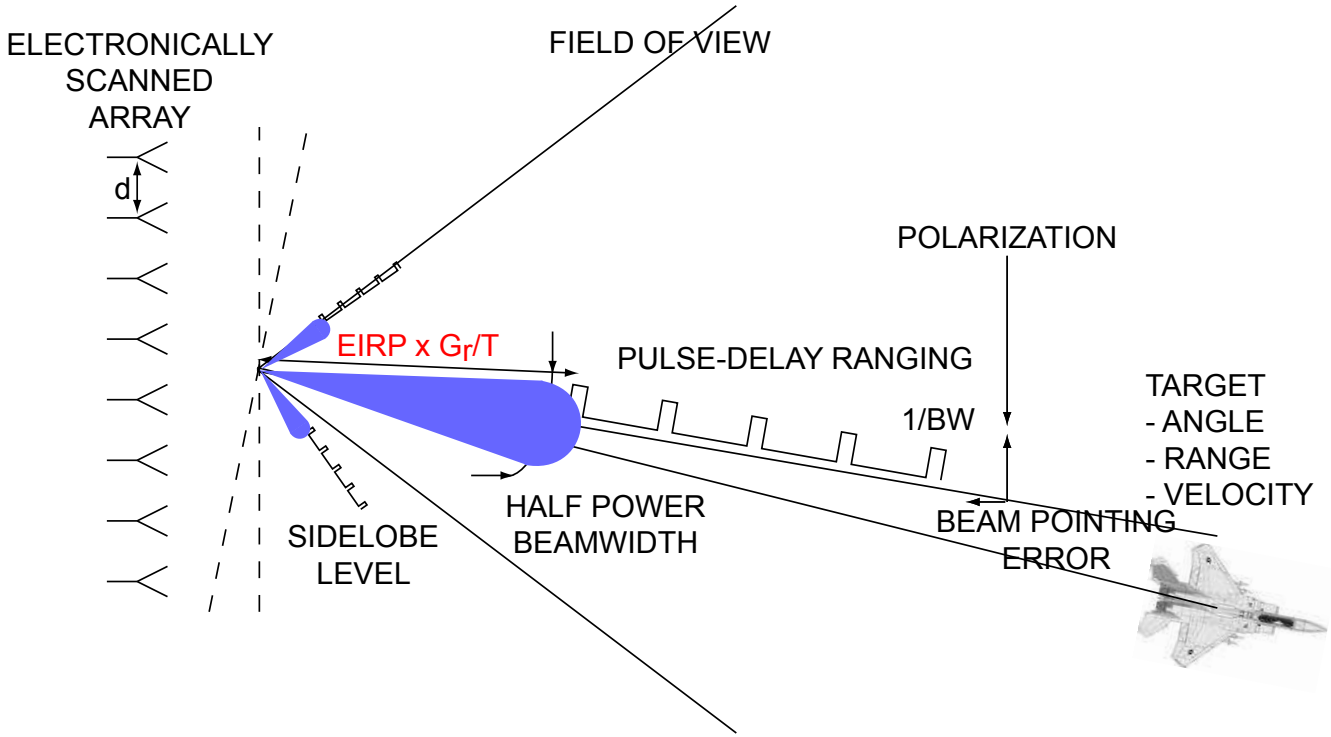

Figure 6: Figures of merit for an electronically scanned array set the radar's ability to search and track targets.

Electronically Scanned Arrays

Figures of merit [1–5]:

- Bandwidth
  - Radar range resolution:

    $r = \frac{c}{2\,BW}$

- Beam pointing error:

  $\Delta^2 = \Phi^2 \frac{\sum A_i^2\, x_i^2}{\left(\sum A_i\, x_i^2\right)^2}$

- EIRP $\times$ G_r/T
  - Radar range equation:

    $R_{max} = \sqrt[4]{\frac{\lambda_0^2\, EIRP\, G_r/T\, \sigma}{64\,\pi^3\, k_B\, BW\, SNR_{min}}}$

  - Scan loss:

    $\frac{G_e}{G} = \frac{(\cos\theta)^n}{1+\delta^2+\Phi^2}$

- Field of view:

  $\frac{d}{\lambda_0} \leq \frac{1}{1+\sin\theta_{max}}$

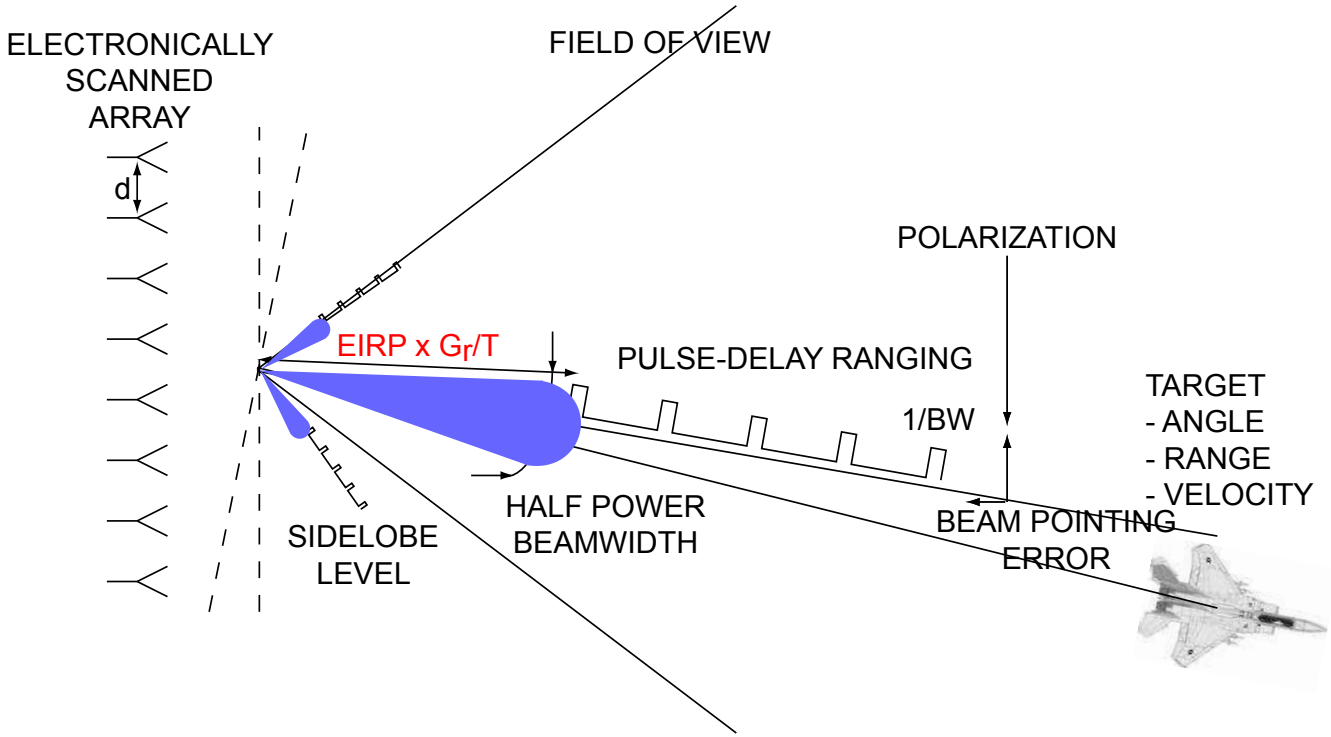

Figure 6: Figures of merit for an electronically scanned array set the radar's ability to search and track targets.

Electronically Scanned Arrays

Figures of merit [1–5]:

- Bandwidth
  - Radar range resolution:

    $r = \frac{c}{2\,BW}$

- Beam pointing error:

  $\Delta^2 = \Phi^2 \frac{\sum A_i^2\, x_i^2}{\left(\sum A_i\, x_i^2\right)^2}$

- EIRP $\times$ G_r/T
  - Radar range equation:

    $R_{max} = \sqrt[4]{\frac{\lambda_0^2\, EIRP\, G_r/T\, \sigma}{64\,\pi^3\, k_B\, BW\, SNR_{min}}}$

  - Scan loss:

    $\frac{G_e}{G} = \frac{(\cos\theta)^n}{1+\delta^2+\Phi^2}$

- Field of view:

  $\frac{d}{\lambda_0} \leq \frac{1}{1+\sin\theta_{max}}$

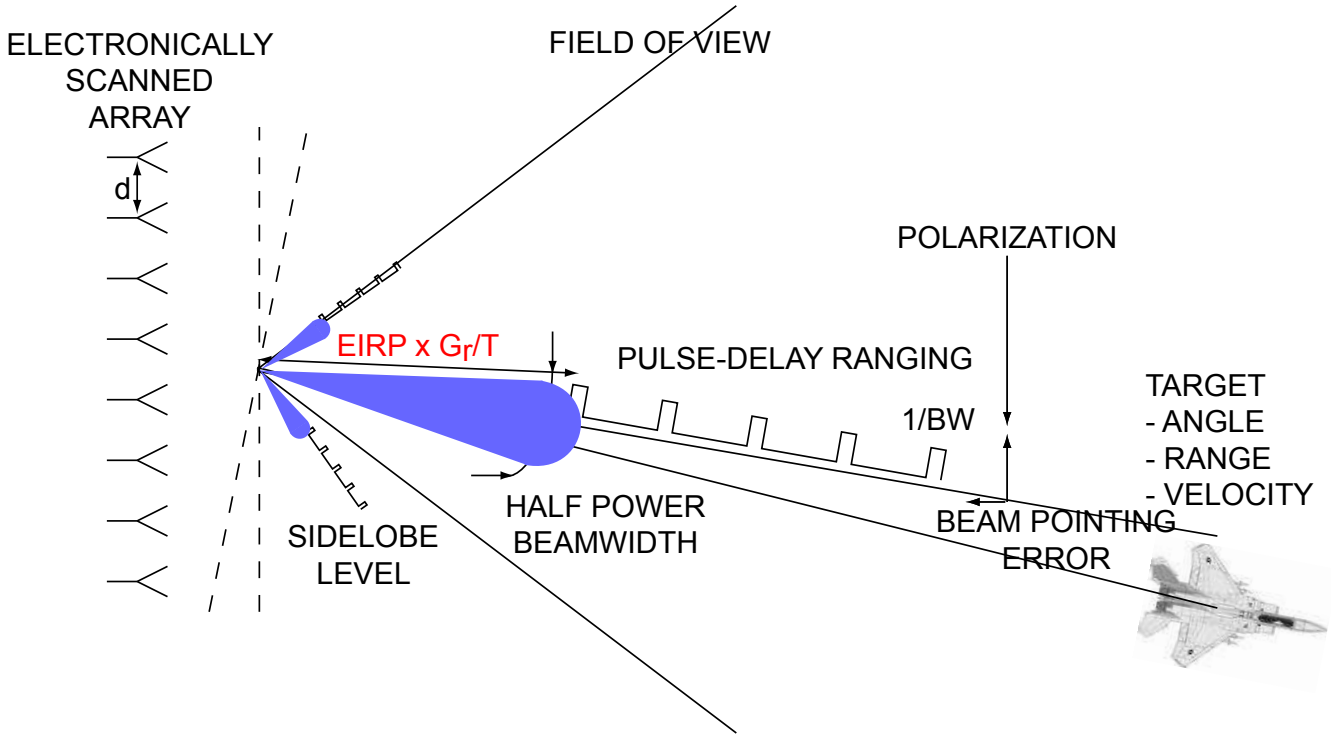

Figure 6: Figures of merit for an electronically scanned array set the radar's ability to search and track targets.

- Amplitude error variance:

  $\hat{\delta}^2 = S_{A_{ATT}}^2 + S_{A_{PS}}^2$

- Phase error variance:

  $\hat{\Phi}^2 = S_{P_{ATT}}^2 + S_{P_{PS}}^2 + \frac{1}{3}\frac{\pi^2}{2^{2P}}$

Electronically Scanned Arrays

Figures of merit [1–5]:

- Bandwidth
  - Radar range resolution:

    $r = \frac{c}{2\,BW}$

- Beam pointing error:

  $\Delta^2 = \Phi^2 \frac{\sum A_i^2\, x_i^2}{\left(\sum A_i\, x_i^2\right)^2}$

- EIRP $\times$ G_r/T
  - Radar range equation:

    $R_{max} = \sqrt[4]{\frac{\lambda_0^2\, EIRP\, G_r/T\, \sigma}{64\,\pi^3\, k_B\, BW\, SNR_{min}}}$

  - Scan loss:

    $\frac{G_e}{G} = \frac{(\cos\theta)^n}{1+\delta^2+\Phi^2}$

- Field of view:

  $\frac{d}{\lambda_0} \leq \frac{1}{1+\sin\theta_{max}}$

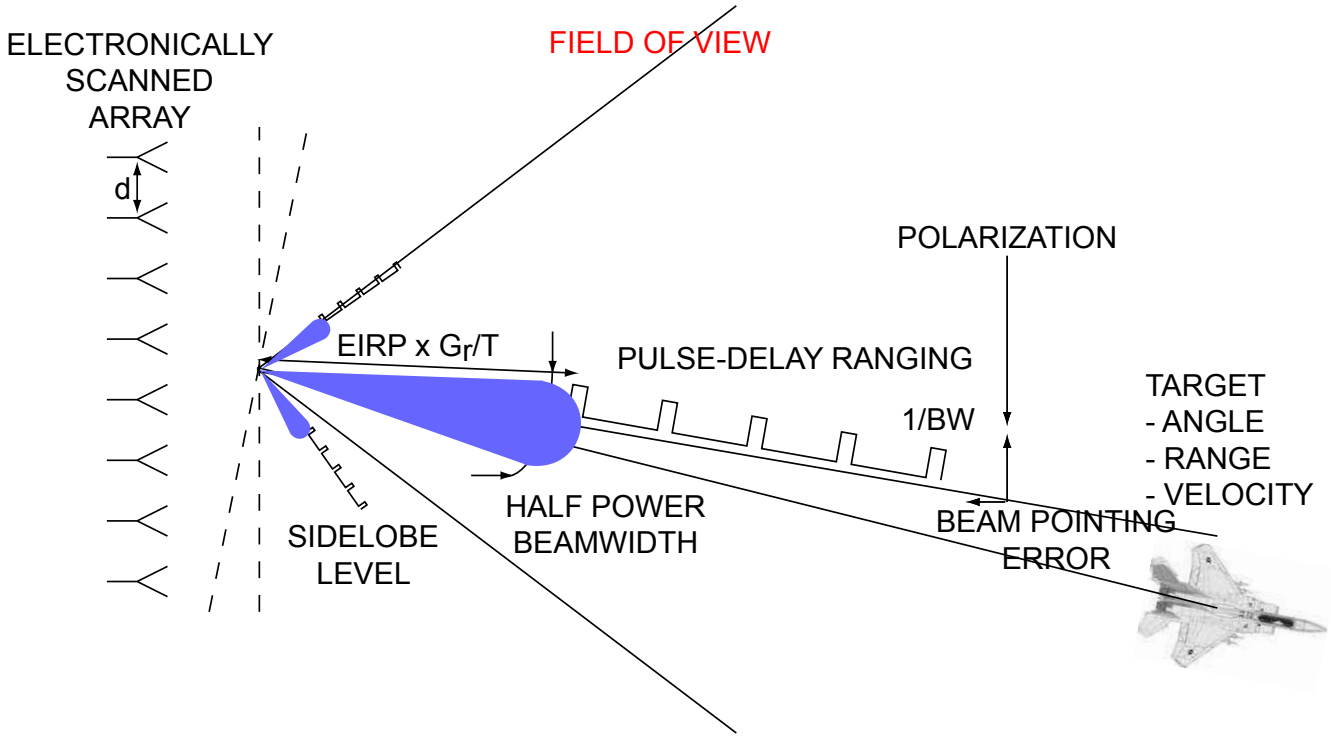

Figure 7: Figures of merit for an electronically scanned array set the radar's ability to search and track targets.

Electronically Scanned Arrays

Figures of merit (continued):

- Half-power beamwidth:

  $HPBW = 0.886\, B_b\, \frac{\lambda_0}{L}$

- Phase center stability
- Polarization purity
- Radar cross section
- Scalability (2-D, 3-D)
- Sidelobe level:

  $SL_{dB} = 10\, log_{10} \frac{\delta^2 + \Phi^2}{N\, \epsilon_A}$

- Size
- Thermal dissipation
- Weight

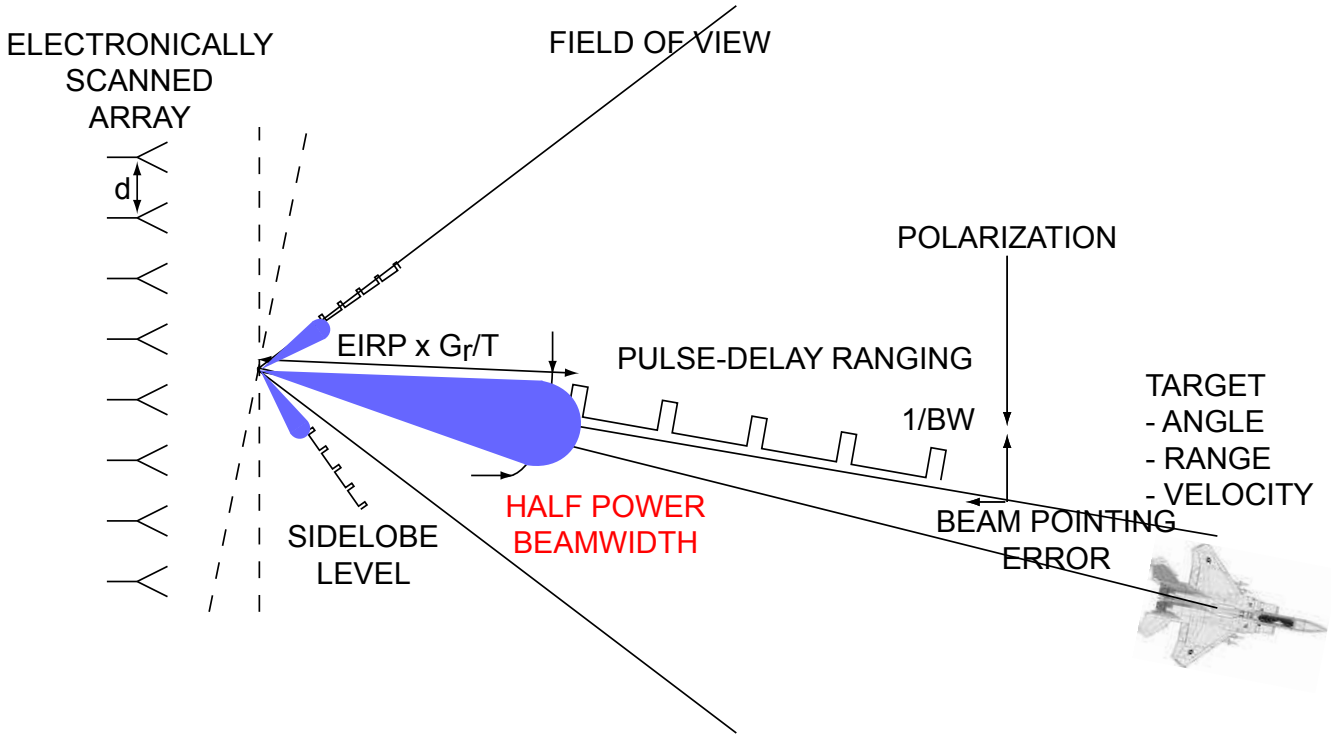

Figure 8: Figures of merit for an electronically scanned array set the radar's ability to search and track targets.

Electronically Scanned Arrays

Figures of merit (continued):

- Half-power beamwidth:
  $HPBW = 0.886\, B_b\, \frac{\lambda_0}{L}$
- Phase center stability
- Polarization purity
- Radar cross section
- Scalability (2-D, 3-D)
- Sidelobe level:
  $SL_{dB} = 10\, log_{10} \frac{\delta^2 + \Phi^2}{N\, \epsilon_A}$
- Size
- Thermal dissipation
- Weight

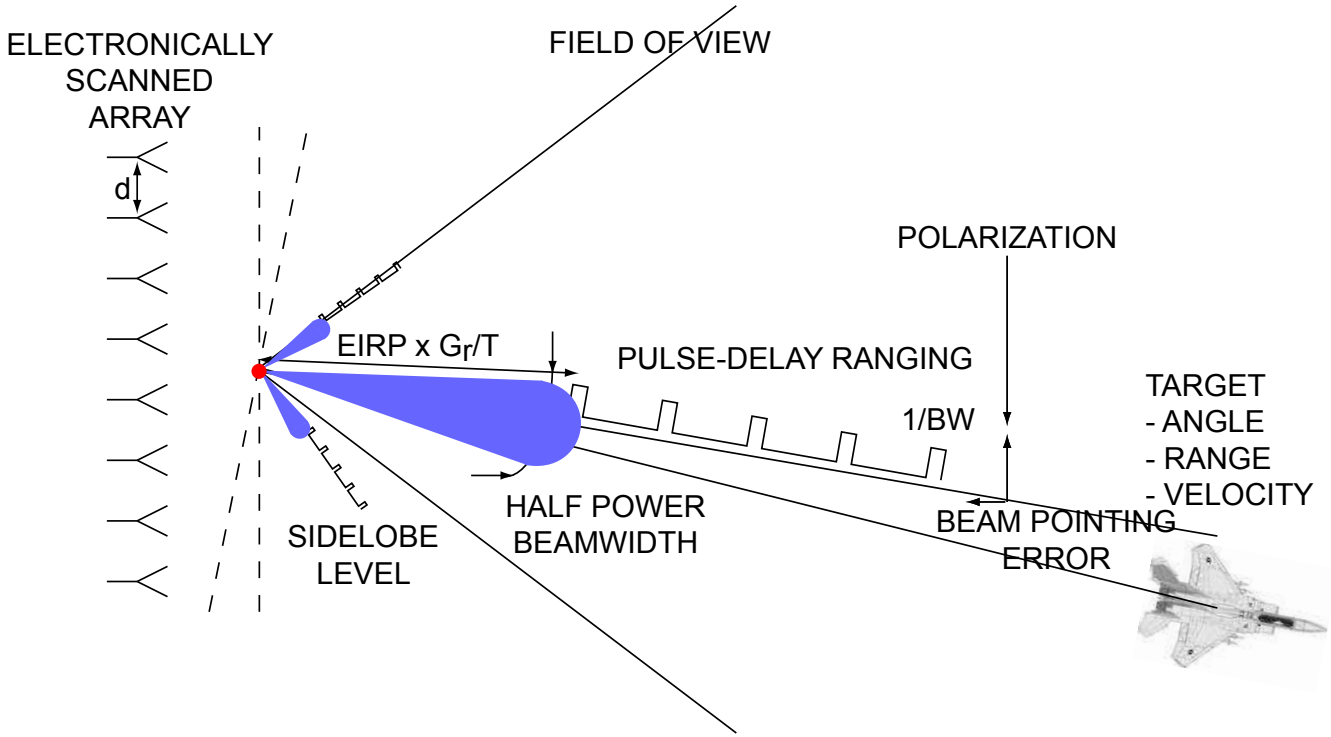

Figure 9: Figures of merit for an electronically scanned array set the radar's ability to search and track targets.

- The distance between the phase center and a point on the mean beam axis is $\frac{\lambda_0}{2\,\pi} \frac{\mathrm{d}^2\, \psi(\theta,\phi)}{\mathrm{d}\, \theta^2} |_{\theta=\theta_0}$, in which $\psi(\theta, \phi)$ is the far field phase pattern, and is often frequency-variant.

Electronically Scanned Arrays

Figures of merit (continued):

- Half-power beamwidth:
  $HPBW = 0.886\, B_b\, \frac{\lambda_0}{L}$
- Phase center stability
- Polarization purity
- Radar cross section
- Scalability (2-D, 3-D)
- Sidelobe level:
  $SL_{dB} = 10\, log_{10}\, \frac{\delta^2 + \Phi^2}{N\, \epsilon_A}$
- Size
- Thermal dissipation
- Weight

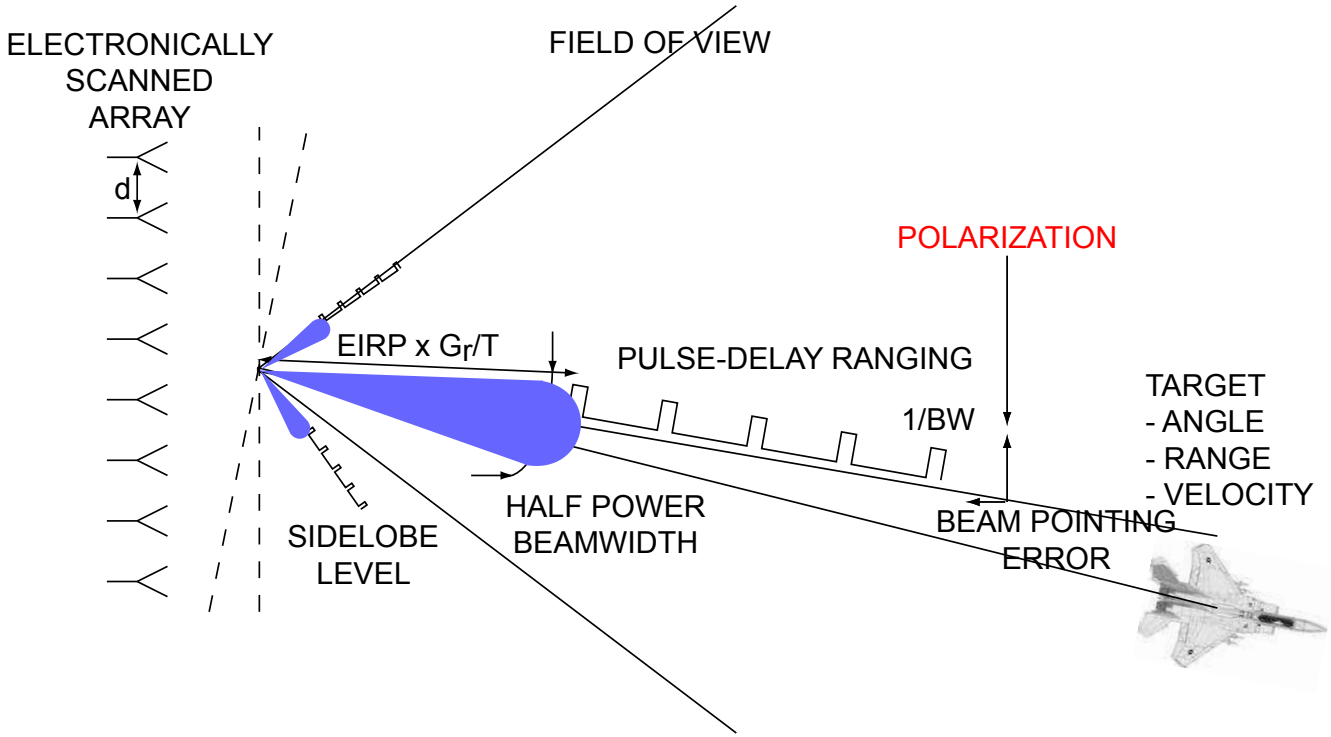

Figure 10: Figures of merit for an electronically scanned array set the radar's ability to search and track targets.

Electronically Scanned Arrays

Figures of merit (continued):

- ☐ Half-power beamwidth:
  $HPBW = 0.886\, B_b\, \frac{\lambda_0}{L}$
- ☐ Phase center stability
- ☐ Polarization purity
- ☐ Radar cross section
- ☐ Scalability (2-D, 3-D)
- ☐ Sidelobe level:
  $SL_{dB} = 10\, log_{10}\, \frac{\delta^2 + \Phi^2}{N\, \epsilon_A}$
- ☐ Size
- ☐ Thermal dissipation
- ☐ Weight

Electronically Scanned Arrays

Figures of merit (continued):

- Half-power beamwidth:

  $HPBW = 0.886\, B_b\, \frac{\lambda_0}{L}$

- Phase center stability
- Polarization purity
- Radar cross section
- Scalability (2-D, 3-D)
- Sidelobe level:

  $SL_{dB} = 10\, log_{10}\, \frac{\delta^2 + \Phi^2}{N\, \epsilon_A}$

- Size
- Thermal dissipation
- Weight

Electronically Scanned Arrays

Figures of merit (continued):

- Half-power beamwidth:
  $HPBW = 0.886\, B_b\, \frac{\lambda_0}{L}$
- Phase center stability
- Polarization purity
- Radar cross section
- Scalability (2-D, 3-D)
- Sidelobe level:
  $SL_{dB} = 10\, log_{10}\, \frac{\delta^2 + \Phi^2}{N\, \epsilon_A}$
- Size
- Thermal dissipation
- Weight

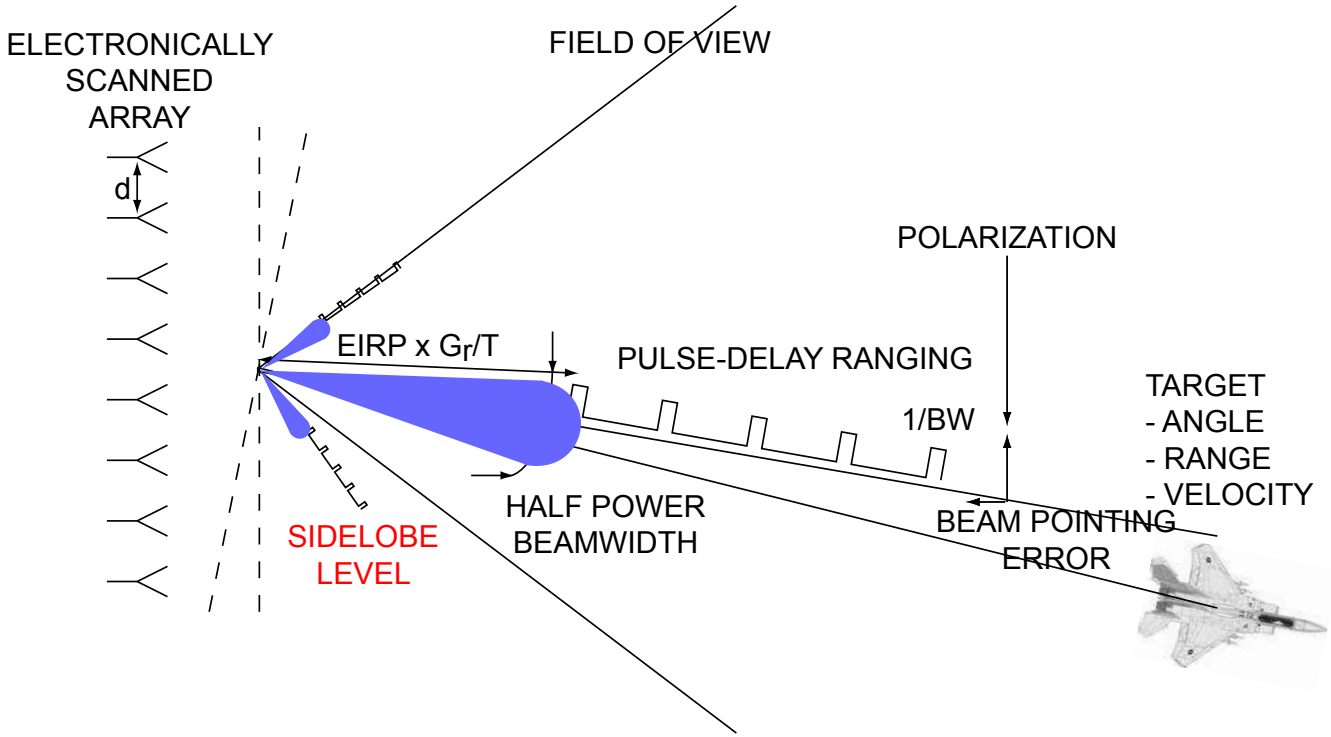

Figure 11: Figures of merit for an electronically scanned array set the radar's ability to search and track targets.

Electronically Scanned Arrays

Figures of merit (continued):

- Half-power beamwidth:
  $HPBW = 0.886\, B_b\, \frac{\lambda_0}{L}$
- Phase center stability
- Polarization purity
- Radar cross section
- Scalability (2-D, 3-D)
- Sidelobe level:
  $SL_{dB} = 10\, log_{10} \frac{\delta^2 + \Phi^2}{N\, \epsilon_A}$
- Size
- Thermal dissipation
- Weight

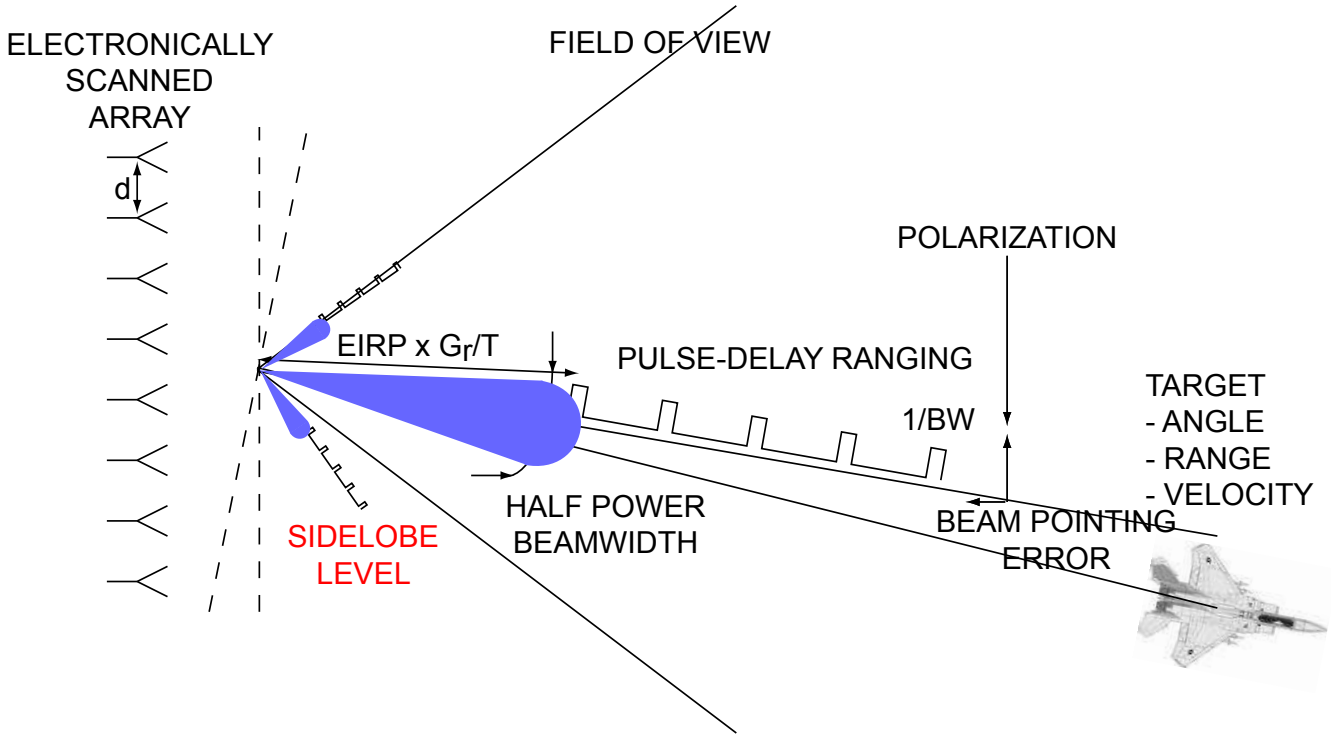

Figure 11: Figures of merit for an electronically scanned array set the radar's ability to search and track targets.

- Amplitude error variance:
  $\hat{\delta}^2 = S^2_{A_{ATT}} + S^2_{A_{PS}}$
- Phase error variance:
  $\hat{\Phi}^2 = S^2_{P_{ATT}} + S^2_{P_{PS}} + \frac{1}{3}\frac{\pi^2}{2^{2P}}$

Electronically Scanned Arrays

Figures of merit (continued):

- Half-power beamwidth:

  $HPBW = 0.886\, B_b\, \frac{\lambda_0}{L}$

- Phase center stability
- Polarization purity
- Radar cross section
- Scalability (2-D, 3-D)
- Sidelobe level:

  $SL_{dB} = 10\, log_{10}\, \frac{\delta^2 + \Phi^2}{N\, \epsilon_A}$

- Size
- Thermal dissipation
- Weight

Electronically Scanned Arrays

Figures of merit (continued):

- Half-power beamwidth:
  $HPBW = 0.886\, B_b\, \frac{\lambda_0}{L}$
- Phase center stability
- Polarization purity
- Radar cross section
- Scalability (2-D, 3-D)
- Sidelobe level:
  $SL_{dB} = 10\, log_{10}\, \frac{\delta^2 + \Phi^2}{N\, \epsilon_A}$
- Size
- Thermal dissipation
- Weight

Electronically Scanned Arrays

Figures of merit (continued):

- Half-power beamwidth:
  $HPBW = 0.886\, B_b\, \frac{\lambda_0}{L}$
- Phase center stability
- Polarization purity
- Radar cross section
- Scalability (2-D, 3-D)
- Sidelobe level:
  $SL_{dB} = 10\, log_{10}\, \frac{\delta^2 + \Phi^2}{N\, \epsilon_A}$
- Size
- Thermal dissipation
- Weight

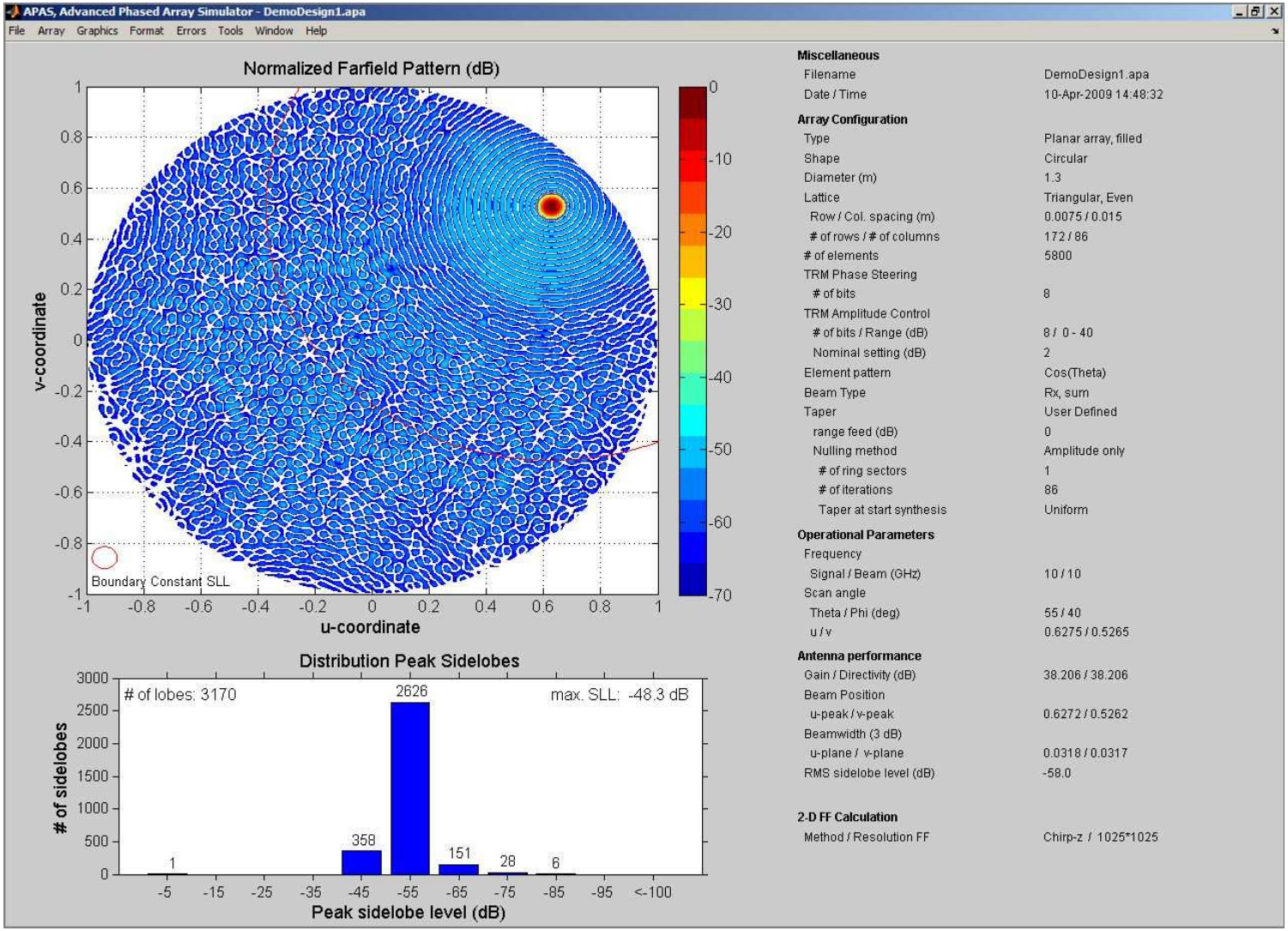

Figure 12: Array factor, $F(\theta, \phi)$, realized with 8 bit attenuators (40 dB attenuation range), and 8 bit phase shifters. The main beam is scanned to $\theta = 55°$, $\phi = 40°$. Calculated with APAS [6].

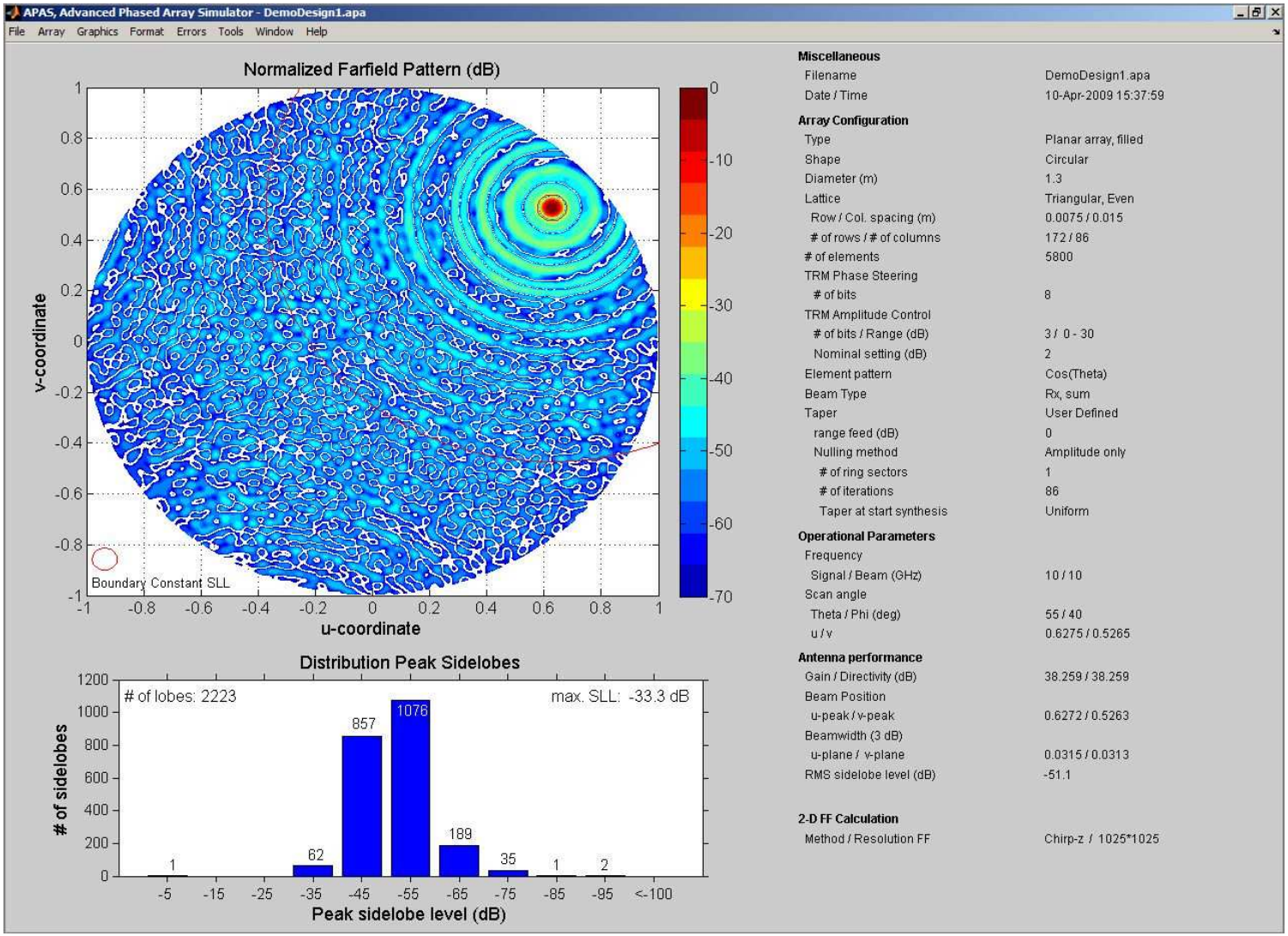

Figure 13: Array factor, $F(\theta, \phi)$, realized with 3 bit attenuators (30 dB attenuation range), and 8 bit phase shifters. The main beam is scanned to $\theta = 55°$, $\phi = 40°$. Calculated with APAS [6].

Electronically Scanned Arrays

Design trade-offs are necessary in the selection of:

- Aperture: real beam or synthetic aperture (SAR)
- Antenna: connected or folded dipole, microstrip, tapered slot, or waveguide antenna
- Beamforming: analog (IF, optical, RF), digital (DBF)
- Feed network: constrained (corporate, series) or space-fed (lens array, reflect array). Extensions include calibration, monopulse, and SLB feed networks.
- Grid: periodic (hexagonal, rectangular, or triangular) or aperiodic (sparse)
- Manufacturing: 2-D arrays: brick, stick, tile [7] or tray, 3-D arrays: geodesic dome, multifaceted (pyramidal frusta)
- Polarization: vertical (taking advantage of Brewster angle for ground-based and naval platforms), polarimetric (all-weather, speckle reduction (FOPEN SAR))
- RF power amplification: active (SSPA) [8], passive subarrays, passive (VED)
- Scanning: frequency-, space-, or time-orthogonal waveform-coherent pencil beams, or multiple input multiple output (MIMO) waveform-orthogonal wide beams

Electronically Scanned Arrays

Design trade-offs are necessary in the selection of:

- Aperture: real beam or synthetic aperture (SAR)
- Antenna: connected or folded dipole, microstrip, tapered slot, or waveguide antenna
- Beamforming: analog (IF, optical, RF), digital (DBF)
- Feed network: constrained (corporate, series) or space-fed (lens array, reflect array). Extensions include calibration, monopulse, and SLB feed networks.
- Grid: periodic (hexagonal, rectangular, or triangular) or aperiodic (sparse)
- Manufacturing: 2-D arrays: brick, stick, tile [7] or tray, 3-D arrays: geodesic dome, multifaceted (pyramidal frusta)
- Polarization: vertical (taking advantage of Brewster angle for ground-based and naval platforms), polarimetric (all-weather, speckle reduction (FOPEN SAR))
- RF power amplification: active (SSPA) [8], passive subarrays, passive (VED)
- Scanning: frequency-, space-, or time-orthogonal waveform-coherent pencil beams, or multiple input multiple output (MIMO) waveform-orthogonal wide beams

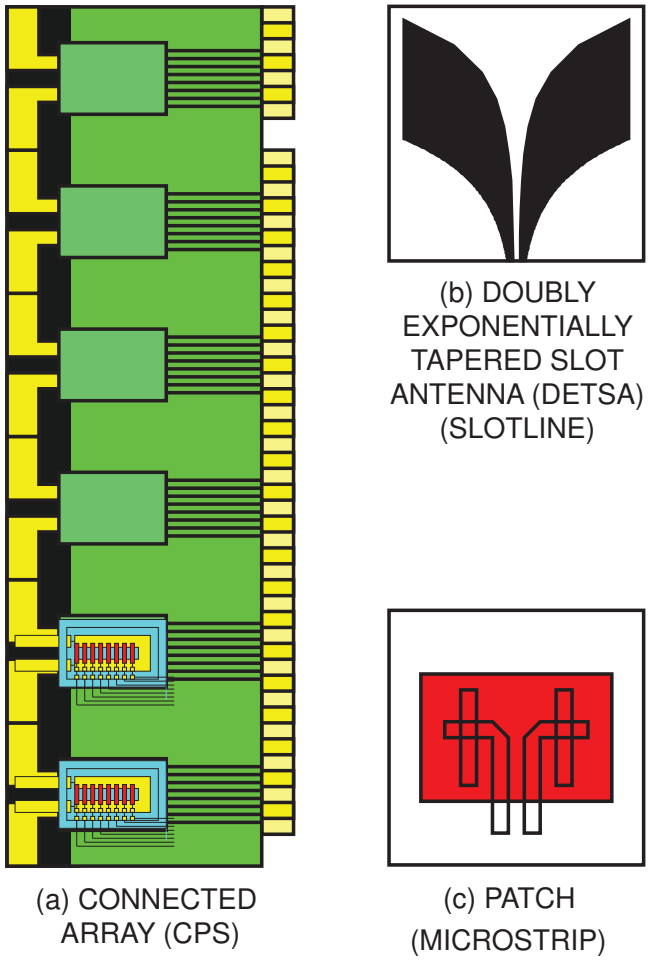

Figure 14: Antennas: (a) Connected array, (b) DETSA, and (c) microstrip.

Electronically Scanned Arrays

Design trade-offs are necessary in the selection of:

- ☐ Aperture: real beam or synthetic aperture (SAR)
- ☐ Antenna: connected or folded dipole, microstrip, tapered slot, or waveguide antenna
- ☐ Beamforming: analog (IF, optical, RF), digital (DBF)
- ☐ Feed network: constrained (corporate, series) or space-fed (lens array, reflect array). Extensions include calibration, monopulse, and SLB feed networks.
- ☐ Grid: periodic (hexagonal, rectangular, or triangular) or aperiodic (sparse)
- ☐ Manufacturing: 2-D arrays: brick, stick, tile [7] or tray, 3-D arrays: geodesic dome, multifaceted (pyramidal frusta)
- ☐ Polarization: vertical (taking advantage of Brewster angle for ground-based and naval platforms), polarimetric (all-weather, speckle reduction (FOPEN SAR))
- ☐ RF power amplification: active (SSPA) [8], passive subarrays, passive (VED)
- ☐ Scanning: frequency-, space-, or time-orthogonal waveform-coherent pencil beams, or multiple input multiple output (MIMO) waveform-orthogonal wide beams

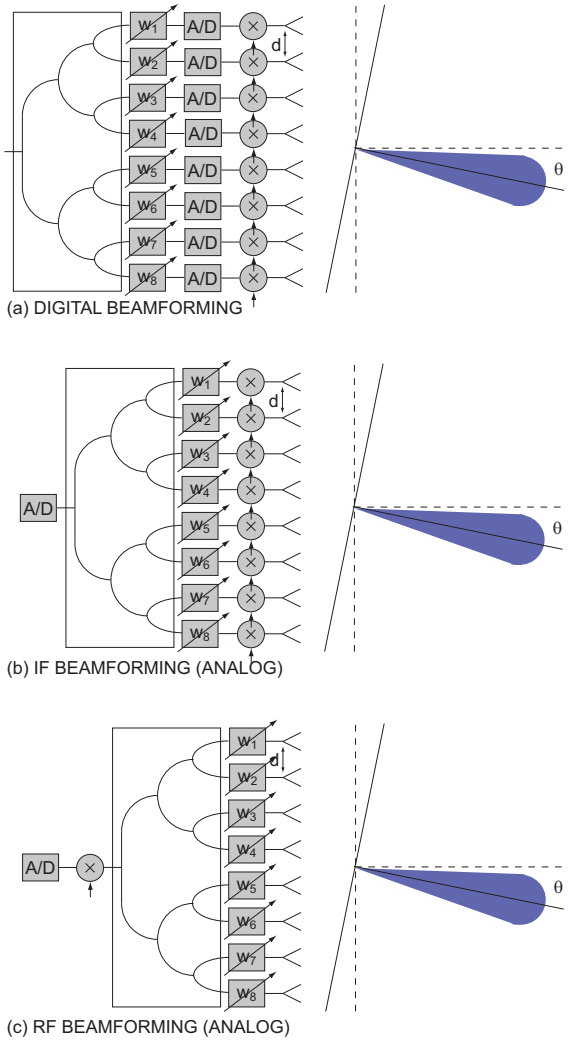

Figure 15: Beamforming networks: (a) DBF, (b) IF, and (c) RF

Electronically Scanned Arrays

Design trade-offs are necessary in the selection of:

- Aperture: real beam or synthetic aperture (SAR)
- Antenna: connected or folded dipole, microstrip, tapered slot, or waveguide antenna
- Beamforming: analog (IF, optical, RF), digital (DBF)
- Feed network: constrained (corporate, series) or space-fed (lens array, reflect array). Extensions include calibration, monopulse, and SLB feed networks.
- Grid: periodic (hexagonal, rectangular, or triangular) or aperiodic (sparse)
- Manufacturing: 2-D arrays: brick, stick, tile [7] or tray, 3-D arrays: geodesic dome, multifaceted (pyramidal frusta)
- Polarization: vertical (taking advantage of Brewster angle for ground-based and naval platforms), polarimetric (all-weather, speckle reduction (FOPEN SAR))
- RF power amplification: active (SSPA) [8], passive subarrays, passive (VED)
- Scanning: frequency-, space-, or time-orthogonal waveform-coherent pencil beams, or multiple input multiple output (MIMO) waveform-orthogonal wide beams

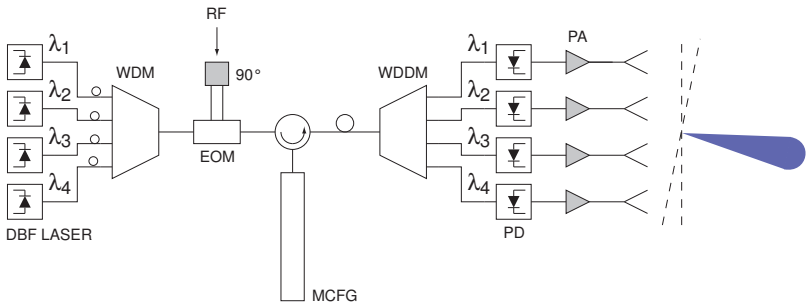

Figure 16: Beamforming networks: optical (Tx)

Electronically Scanned Arrays

Design trade-offs are necessary in the selection of:

- Aperture: real beam or synthetic aperture (SAR)
- Antenna: connected or folded dipole, microstrip, tapered slot, or waveguide antenna
- Beamforming: analog (IF, optical, RF), digital (DBF)
- Feed network: constrained (corporate, series) or space-fed (lens array, reflect array). Extensions include calibration, monopulse, and SLB feed networks.
- Grid: periodic (hexagonal, rectangular, or triangular) or aperiodic (sparse)
- Manufacturing: 2-D arrays: brick, stick, tile [7] or tray, 3-D arrays: geodesic dome, multifaceted (pyramidal frusta)
- Polarization: vertical (taking advantage of Brewster angle for ground-based and naval platforms), polarimetric (all-weather, speckle reduction (FOPEN SAR))
- RF power amplification: active (SSPA) [8], passive subarrays, passive (VED)
- Scanning: frequency-, space-, or time-orthogonal waveform-coherent pencil beams, or multiple input multiple output (MIMO) waveform-orthogonal wide beams

Receiver calibration:

- **Function**: Equalisation of the receiver transfer functions, H_k^{Rx}, is performed during radar operation to cope with aging or temperature variations [9–11].

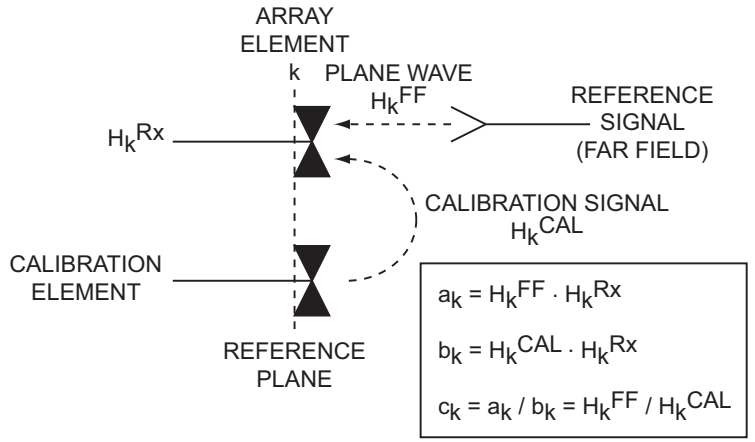

Figure 17: The multi-element phase toggling (MEP) technique [11] calibrates groups of elements simultaneously. It uses a calibration network or exploits mutual coupling.

Electronically Scanned Arrays

Design trade-offs are necessary in the selection of:

- ☐ Aperture: real beam or synthetic aperture (SAR)
- ☐ Antenna: connected or folded dipole, microstrip, tapered slot, or waveguide antenna
- ☐ Beamforming: analog (IF, optical, RF), digital (DBF)
- ☐ Feed network: constrained (corporate, series) or space-fed (lens array, reflect array). Extensions include calibration, monopulse, and SLB feed networks.
- ☐ Grid: periodic (hexagonal, rectangular, or triangular) or aperiodic (sparse)
- ☐ Manufacturing: 2-D arrays: brick, stick, tile [7] or tray, 3-D arrays: geodesic dome, multifaceted (pyramidal frusta)
- ☐ Polarization: vertical (taking advantage of Brewster angle for ground-based and naval platforms), polarimetric (all-weather, speckle reduction (FOPEN SAR))
- ☐ RF power amplification: active (SSPA) [8], passive subarrays, passive (VED)
- ☐ Scanning: frequency-, space-, or time-orthogonal waveform-coherent pencil beams, or multiple input multiple output (MIMO) waveform-orthogonal wide beams

Figure 18: Grid: (a) rectangular (periodic), (b) triangular (periodic), (c) sparse (aperiodic).

Electronically Scanned Arrays

Design trade-offs are necessary in the selection of:

- Aperture: real beam or synthetic aperture (SAR)
- Antenna: connected or folded dipole, microstrip, tapered slot, or waveguide antenna
- Beamforming: analog (IF, optical, RF), digital (DBF)
- Feed network: constrained (corporate, series) or space-fed (lens array, reflect array). Extensions include calibration, monopulse, and SLB feed networks.
- Grid: periodic (hexagonal, rectangular, or triangular) or aperiodic (sparse)
- Manufacturing: 2-D arrays: brick, stick, tile [7] or tray, 3-D arrays: geodesic dome, multifaceted (pyramidal frusta)
- Polarization: vertical (taking advantage of Brewster angle for ground-based and naval platforms), polarimetric (all-weather, speckle reduction (FOPEN SAR))
- RF power amplification: active (SSPA) [8], passive subarrays, passive (VED)
- Scanning: frequency-, space-, or time-orthogonal waveform-coherent pencil beams, or multiple input multiple output (MIMO) waveform-orthogonal wide beams

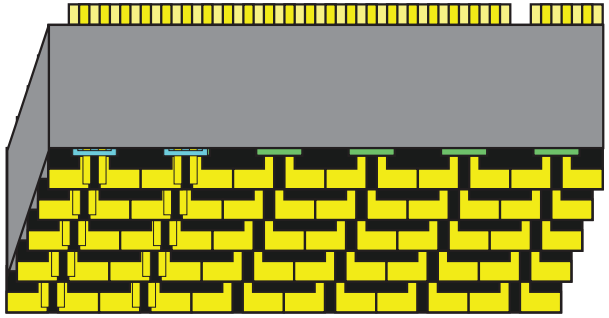

Figure 19: Manufacturing: brick assembly.

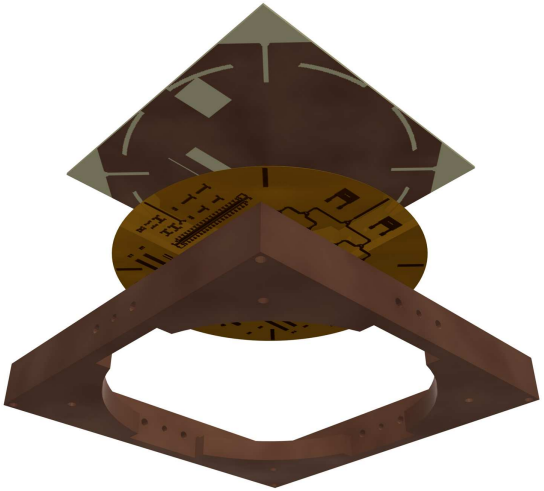

Figure 20: Manufacturing: tile assembly.

Electronically Scanned Arrays

Design trade-offs are necessary in the selection of:

- Aperture: real beam or synthetic aperture (SAR)
- Antenna: connected or folded dipole, microstrip, tapered slot, or waveguide antenna
- Beamforming: analog (IF, optical, RF), digital (DBF)
- Feed network: constrained (corporate, series) or space-fed (lens array, reflect array). Extensions include calibration, monopulse, and SLB feed networks.
- Grid: periodic (hexagonal, rectangular, or triangular) or aperiodic (sparse)
- Manufacturing: 2-D arrays: brick, stick, tile [7] or tray, 3-D arrays: geodesic dome, multifaceted (pyramidal frusta)
- Polarization: vertical (taking advantage of Brewster angle for ground-based and naval platforms), polarimetric (all-weather, speckle reduction (FOPEN SAR))
- RF power amplification: active (SSPA) [8], passive subarrays, passive (VED)
- Scanning: frequency-, space-, or time-orthogonal waveform-coherent pencil beams, or multiple input multiple output (MIMO) waveform-orthogonal wide beams

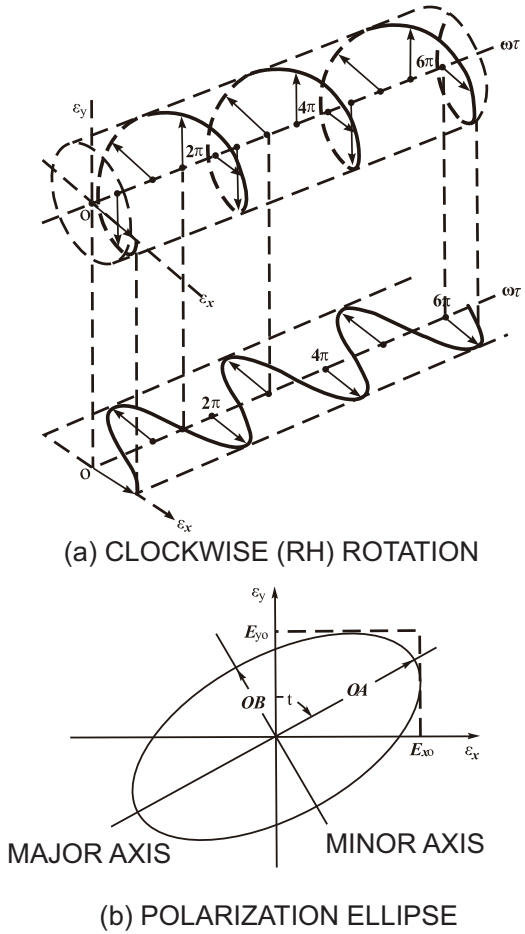

Figure 21: Polarization: (a) rotation of plane electromagnetic wave, (b) polarization ellipse at $z = 0$ as a function of time [12].

Electronically Scanned Arrays

Design trade-offs are necessary in the selection of:

- Aperture: real beam or synthetic aperture (SAR)
- Antenna: connected or folded dipole, microstrip, tapered slot, or waveguide antenna
- Beamforming: analog (IF, optical, RF), digital (DBF)
- Feed network: constrained (corporate, series) or space-fed (lens array, reflect array). Extensions include calibration, monopulse, and SLB feed networks.
- Grid: periodic (hexagonal, rectangular, or triangular) or aperiodic (sparse)
- Manufacturing: 2-D arrays: brick, stick, tile [7] or tray, 3-D arrays: geodesic dome, multifaceted (pyramidal frusta)
- **Polarization: vertical (taking advantage of Brewster angle for ground-based and naval platforms), polarimetric (all-weather, speckle reduction (FOPEN SAR))**
- RF power amplification: active (SSPA) [8], passive subarrays, passive (VED)
- Scanning: frequency-, space-, or time-orthogonal waveform-coherent pencil beams, or multiple input multiple output (MIMO) waveform-orthogonal wide beams

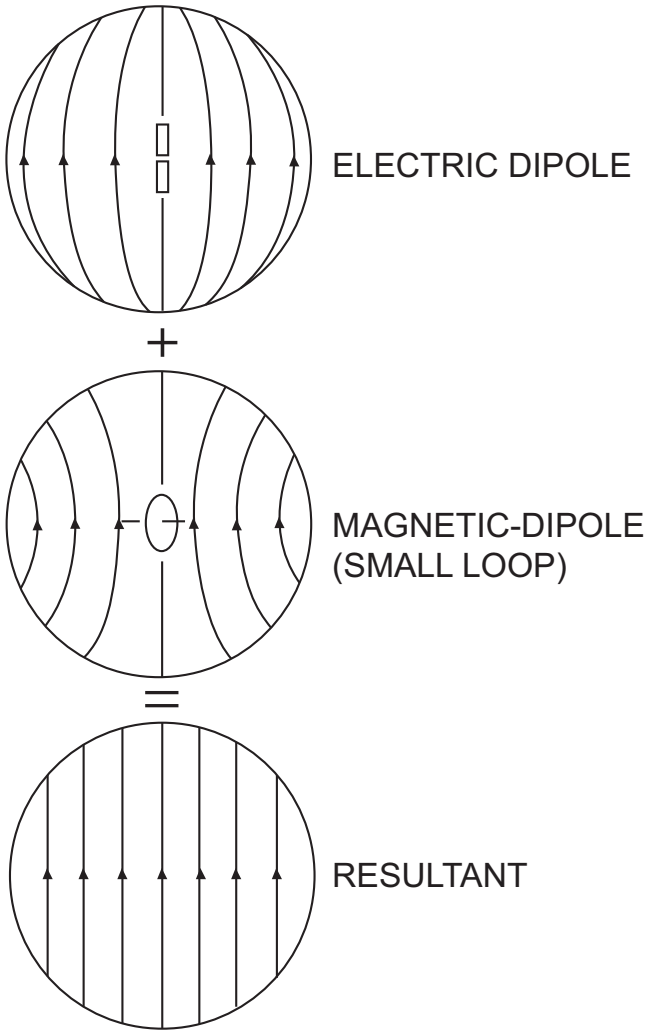

Figure 22: Polarization: Huygens' source [13].

Electronically Scanned Arrays

Design trade-offs are necessary in the selection of:

- ☐ Aperture: real beam or synthetic aperture (SAR)
- ☐ Antenna: connected or folded dipole, microstrip, tapered slot, or waveguide antenna
- ☐ Beamforming: analog (IF, optical, RF), digital (DBF)
- ☐ Feed network: constrained (corporate, series) or space-fed (lens array, reflect array). Extensions include calibration, monopulse, and SLB feed networks.
- ☐ Grid: periodic (hexagonal, rectangular, or triangular) or aperiodic (sparse)
- ☐ Manufacturing: 2-D arrays: brick, stick, tile [7] or tray, 3-D arrays: geodesic dome, multifaceted (pyramidal frusta)
- ☐ Polarization: vertical (taking advantage of Brewster angle for ground-based and naval platforms), polarimetric (all-weather, speckle reduction (FOPEN SAR))
- ☐ RF power amplification: active (SSPA) [8], passive subarrays, passive (VED)
- ☐ Scanning: frequency-, space-, or time-orthogonal waveform-coherent pencil beams, or multiple input multiple output (MIMO) waveform-orthogonal wide beams

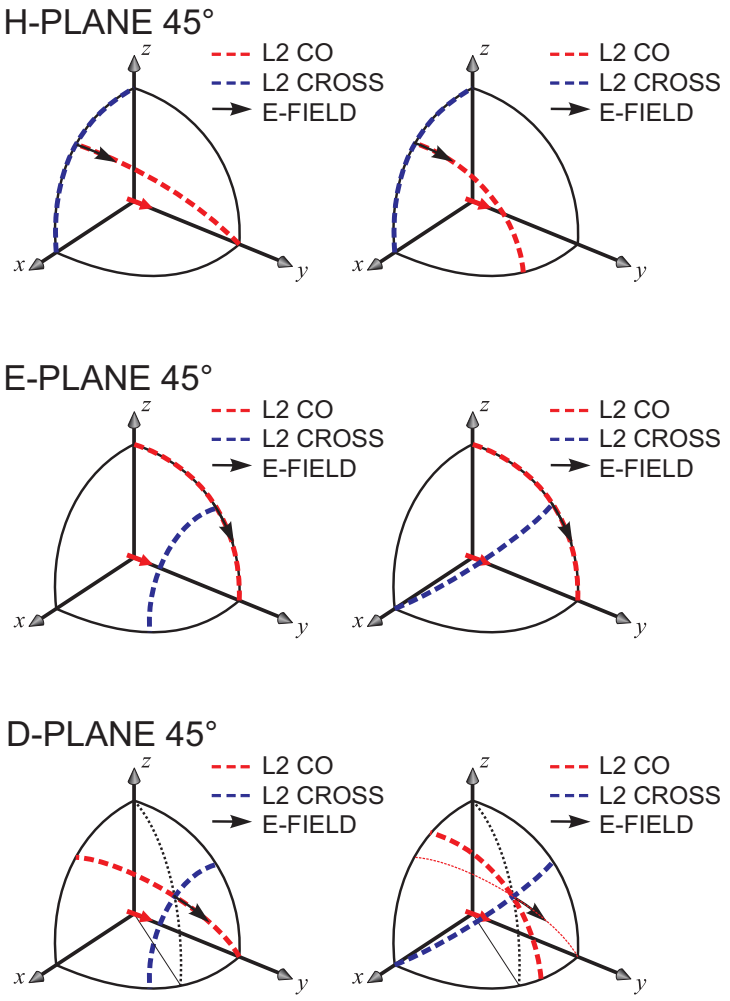

Figure 23: Polarization: Ludwig 2 & 3 definition of co- and crosspolarization for a dipole along the y-axis.

Electronically Scanned Arrays

Design trade-offs are necessary in the selection of:

- ☐ Aperture: real beam or synthetic aperture (SAR)
- ☐ Antenna: connected or folded dipole, microstrip, tapered slot, or waveguide antenna
- ☐ Beamforming: analog (IF, optical, RF), digital (DBF)
- ☐ Feed network: constrained (corporate, series) or space-fed (lens array, reflect array). Extensions include calibration, monopulse, and SLB feed networks.
- ☐ Grid: periodic (hexagonal, rectangular, or triangular) or aperiodic (sparse)
- ☐ Manufacturing: 2-D arrays: brick, stick, tile [7] or tray, 3-D arrays: geodesic dome, multifaceted (pyramidal frusta)
- ☐ Polarization: vertical (taking advantage of Brewster angle for ground-based and naval platforms), polarimetric (all-weather, speckle reduction (FOPEN SAR))
- ☐ RF power amplification: active (SSPA) [8], passive subarrays, passive (VED)
- ☐ Scanning: frequency-, space-, or time-orthogonal waveform-coherent pencil beams, or multiple input multiple output (MIMO) waveform-orthogonal wide beams

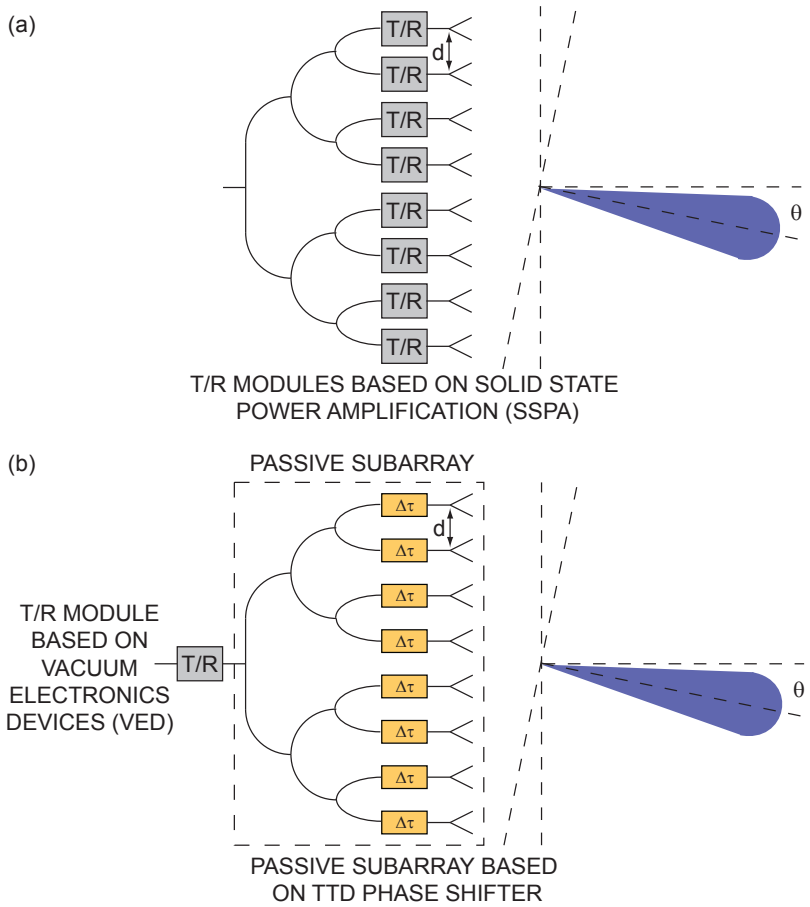

Figure 24: RF power amplification: (a) An active electronically scanned array (AESA), and (b) a passive electronically scanned array (PESA).

Electronically Scanned Arrays

Design trade-offs are necessary in the selection of:

- Aperture: real beam or synthetic aperture (SAR)
- Antenna: connected or folded dipole, microstrip, tapered slot, or waveguide antenna
- Beamforming: analog (IF, optical, RF), digital (DBF)
- Feed network: constrained (corporate, series) or space-fed (lens array, reflect array). Extensions include calibration, monopulse, and SLB feed networks.
- Grid: periodic (hexagonal, rectangular, or triangular) or aperiodic (sparse)
- Manufacturing: 2-D arrays: brick, stick, tile [7] or tray, 3-D arrays: geodesic dome, multifaceted (pyramidal frusta)
- Polarization: vertical (taking advantage of Brewster angle for ground-based and naval platforms), polarimetric (all-weather, speckle reduction (FOPEN SAR))
- RF power amplification: active (SSPA) [8], passive subarrays, passive (VED)
- Scanning: frequency-, space-, or time-orthogonal waveform-coherent pencil beams, or multiple input multiple output (MIMO) waveform-orthogonal wide beams

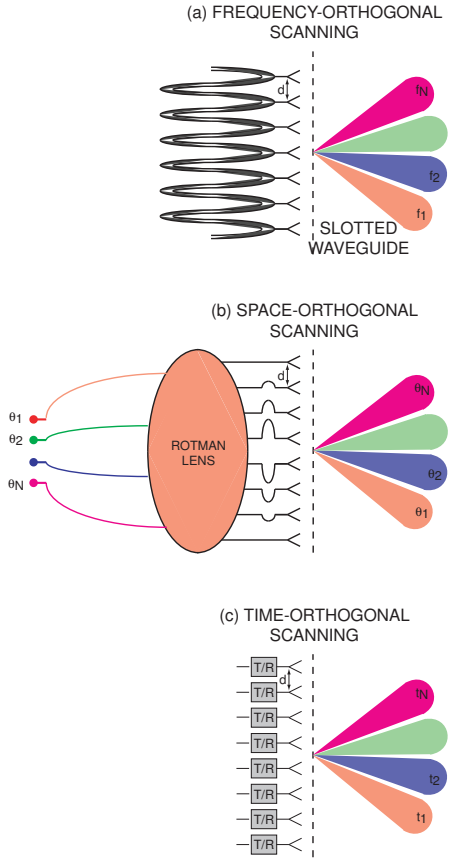

Figure 25: Electronically scanned array architectures: (a) frequency-orthogonal scanning with a slotted waveguide, (b) spatially-orthogonal scanning with a Rotman lens, (c) time-orthogonal scanning with RF (TTD) phase shifters.

Electronically Scanned Arrays: References

[1] D. Parker and D. C. Zimmermann, "Phased arrays - Part I: Theory and architectures," *IEEE Trans. Microwave Theory Tech.*, vol. 50, no. 3, pp. 678–687, March 2002.

[2] ——, "Phased arrays - Part II: Implementations, applications, and future trends," *IEEE Trans. Microwave Theory Tech.*, vol. 50, no. 3, pp. 688–698, March 2002.

[3] R. J. Mailloux, *Phased Array Antenna Handbook*. Artech House, 2005.

[4] E. Brookner, "Phased array radars: Past, astounding breakthroughs and future trends," *Microwave Journal*, vol. 51, no. 1, p. 30, January 2008.

[5] T. W. Jeffrey, *Phased-Array Radar Design*. SciTech Publishing, 2009.

[6] W. Keizer, "Low-sidelobe pattern synthesis using iterative fourier techniques coded in MATLAB [EM programmer's notebook]," *IEEE Antennas Propagat. Mag.*, vol. 51, no. 2, pp. 137 –150, April 2009.

[7] A. M. Puzella, J. M. Crowder, P. S. Dupuis, M. C. Fallica, J. B. Francis, and J. A. Licciardello, "Tile sub-array and related circuits and techniques," U.S. Patent 7,348,932 B1, September 21, 2006.

[8] M. Smith, M. Sarcione, and R. Conilogue, "Pioneering phased array systems & technologies. active electronically steered antennas," *Technology Today (Highlighting Raytheon's Technology)*, vol. 3, no. 1, pp. 19–23, 2004.

[9] R.-S. Chu and K. M. Lee, "Analysis and development of a signal injection technique using transmission lines embedded at phased array aperture," *IEEE Trans. Antennas Propagat.*, vol. 41, no. 10, pp. 1464–1469, Oct. 1993.

[10] K. M. Lee, R. S. Chu, and S. C. Liu, "A built-in performance monitoring/fault isolation and correction (PM/FIC) system for active phased-array antennas," *IEEE Trans. Antennas Propagat.*, vol. 41, no. 11, pp. 1530–1540, Nov. 1993.

[11] A. B. Smolders and G. Hampson, "Deterministic RF nulling in phased arrays for the next generation of radio telescopes," *IEEE Antennas Propagat. Mag.*, vol. 44, no. 4, pp. 13–22, Aug. 2002.

[12] C. A. Balanis, *Antenna Theory, Analysis and Design, 2nd Ed.* John Wiley & Sons, 1997.

[13] A. W. Love, "Some highlights in reflector antenna development," *Radio Science*, vol. 11, no. 8, pp. 671–684, Nov. 1976.

Design trade-offs are necessary in the selection of (continued):

- RF technology: III-V compound semiconductor (AlN, GaAs, GaN [1], InP, InSb), ferrite, ferroelectric, RF MEMS, silicon-based semiconductor (LDMOS, RF CMOS, SiC and SiGe), and vacuum electronics

Table I: RF technology versus AESA architecture

			Active Electronically Scanned Array (AESA)			
			Analog Beamforming			DBF (Rx) [2]
			IF (T/R)	RF (T/R)	Optical [3–6]	
III/V Compound Semiconductors	GaAs HBT, mHEMT & pHEMT	T/R	HPA, LNA, MFC[a]		EAM/EOM Driver, HPA, LNA, TIA	LNA
	GaN HEMT	T/R	HPA, Limiter, LNA, T/R Switch		Limiter, LNA	
	InP DHBT & HEMT	Rx	LNA	LNA	LNA, TIA	LNA
	p-n & p-i-n Diodes	T/R	Limiter	Limiter	Limiter, Photodiode	Limiter
Ferroelectrics		T/R				
Ferrites		T/R	Circulator	Circulator		
Packaging	Ceramic	T/R	LTCC	LTCC	LTCC	LTCC
	Organic	Rx	LCP, QFN	LCP, QFN	LCP, QFN	LCP, QFN
RF MEMS		T/R	T/R switch	MFC, T/R Switch		
Silicon-Based Semiconductors	LDMOS	Tx	HPA (L/S-band)			
	p-n & p-i-n Diodes	T/R	Limiter		Limiter, Photodiode	Limiter
	RF CMOS & SiGe:C BiCMOS	T/R	A/D, Control Loops, DDS I^2C/SPI, LNA, MFC, Mixer, VCO		A/D, Control Loops, DDS, I^2C/SPI, LNA, Mixer, VCO	A/D, Control Loops, I^2C/SPI, LNA, Mixer, STC Pulse Compression, VCO

[a] MFC: A multi-function chip contains an attenuator, a (true-time-delay) phase shifter, and SPDT switches, as well as amplifiers.

Electronically Scanned Arrays

Design trade-offs are necessary in the selection of (continued):

- RF technology: III-V compound semiconductor (AlN, GaAs, GaN [1], InP, InSb), ferrite, ferroelectric, RF MEMS, silicon-based semiconductor (LDMOS, RF CMOS, SiC and SiGe), and vacuum electronics

Table II: RF technology versus PESA architecture

			Passive Subarray	Passive Electronically Scanned Array (PESA)		
			Analog Beamforming RF (T/R)	Analog Beamforming RF (T/R)		
				Lens Arrays	Reflect Arrays	Switched BFN[a]
III/V Compound Semiconductors	GaAs HBT, mHEMT & pHEMT	T/R				
	GaN HEMT	T/R				
	InP DHBT & HEMT	Rx				
	p-n & p-i-n Diodes	T/R	(TTD) Phase Shifter	(TTD) Phase Shifter		SPNT Switch
Ferroelectrics		T/R	(TTD) Phase Shifter	(TTD) Phase Shifter		
Ferrites		T/R	Phase Shifter	Phase Shifter		
Packaging	Ceramic	T/R	LTCC			
	Organic	Rx	LCP/Duroid, QFN			
RF MEMS		T/R	(TTD) Phase Shifter	(TTD) Phase Shifter		SPNT Switch
Silicon-Based Semiconductors	LDMOS	Tx				
	p-n & p-i-n Diodes	T/R	(TTD) Phase Shifter	(TTD) Phase Shifter		SPNT Switch
	RF CMOS & SiGe:C BiCMOS	T/R				
Vacuum Electronics Devices		Tx		Klystron TWT	Klystron TWT	Klystron TWT

[a] A switched beamformer is a cascade of a single pole N throw (SPNT) switch and a beamformer (beamforming matrix (Butler matrix) or lens (Luneburg lens, Rotman lens) or reflector based focal plane scanner).

Electronically Scanned Arrays: References

[1] N. Kolias, "RF systems - the benefits of gallium nitride technology," *Technology Today (Highlighting Raytheon's Technology)*, no. 2, pp. 27–28, 2007.

[2] O. Adrian, "M3R AESA technology for extended air defence," *IEEE Aerosp. Electron. Syst. Mag*, vol. 25, no. 8, pp. 11–16, August 2010.

[3] J. J. Lee, R. Y. Loo, S. Livingston, V. I. Jones, J. B. Lewis, H.-W. Yen, G. L. Tangonan, and M. Wechsberg, "Photonic wideband array antennas," *IEEE Trans. Antennas Propagat.*, vol. 43, no. 9, pp. 966–982, September 1995.

[4] A. Meijerink, C. G. H. Roeloffzen, R. Meijerink, L. Zhuang, D. Marpaung, M. J. Bentum, M. Burla, J. Verpoorte, P. Jorna, A. Hulzinga, and W. van Etten, "Novel ring resonator-based integrated photonic beamformer for broadband phased array receive antennas – part I: Design and performance analysis," *J. Lightwave Technol.*, vol. 28, no. 1, pp. 33–18, Jan. 2010.

[5] L. Zhuang, C. G. H. Roeloffzen, A. Meijerink, M. Burla, D. Marpaung, A. Leinse, M. Hoekman, R. G. Heideman, and W. van Etten, "Novel ring resonator-based integrated photonic beamformer for broadband phased array receive antennas – part II: Experimental prototype," *J. Lightwave Technol.*, vol. 28, no. 1, pp. 19–31, Jan. 2010.

[6] C. Schow, F. Doany, and J. Kash, "Get on the optical bus," *IEEE Spectrum*, vol. 47, no. 9, pp. 32–56, September 2010.

Array Antennas

- **Function**: Antennas transform guided waves into space waves.

Table III: Comparison of Antenna Elements for Wide-Angle Electronically Scanned Arrays

	narrowband		wideband			ideal
	microstrip Touchard, et al. [1], 2009	waveguide & ind. iris Keizer, et al. [2,3], 1991	bowtie Smolders, et al. [4], 2002	bunny ear Lee, et al. [5–7], 2003	connected dipole Neto, et al. [8,9], 2009	connected Huygens' source
Design characteristics						
Directionality[a]	unidirectional	unidirectional	bidirectional		bidirectional	bidirectional
Feed, Z_{IN}	microstrip, 50 Ω	waveguide, $Z_{TE_{10}}$	twin-line,[b] 115 Ω	slotline, 50π Ω	CPS, 120π Ω	CPS, 120π Ω
Feed mode[c]	single-ended	TE_{10}	*differential*[b]	*differential*	*differential*	*differential*
Manufacturing	tile, laminate	brick, waveguide	brick	brick	brick	tile, laminate
Mutual coupling usage[d]	no, metal fence & cavity backing	yes, WAIM	no	no	yes, connected	yes, connected
Polarization[e]	single-polarized	single-polarized	single-polarized	dual-polarized	single-polarized	dual-polarized

[a] Front to back ratio: The front to back ratio of bidirectional broadside radiators can be improved using cavity or reflector (ground (GND) plane) backing, or dielectric lens, resonator or superstrate front-ends, at the expense of bandwidth, group velocity dispersion (GVD) and phase center stability.

[b] Feed mode: A hockey stick balun is used in [4] to transit the *differential* twin-line mode to a single-ended microstrip mode.

[c] Bandwidth: *Wideband antenna elements have differential feeds*. Differentially-fed antenna elements might suffer from common mode radiation and resonances.

[d] Mutual coupling usage: best friend (wide angle impedance matching (WAIM) layers induce leaky surface waves to reduce the scan loss), or worst enemy (cavity backing, metal fence, or pseudo-differential feeding prevent substrate mode and surface wave propagation and scan blindness due to edge radiation)

[e] Cross polarization level: The minimum achievable Ludwig-3 cross polarization level (θ=45°,ϕ=45°) of an array of single-polarized and dual-polarized electrical dipoles is -17 dB and -20 dB respectively. *An array of connected Huygens' sources is perfectly polarized over an infinite bandwidth and at all scanning angles.*

Table III: Comparison of Antenna Elements for Wide-Angle Electronically Scanned Arrays (continued)

	narrowband		wideband			ideal
	microstrip Touchard, et al. [1], 2009	waveguide & ind. iris Keizer, et al. [2, 3], 1991	bowtie Smolders, et al. [4], 2002	bunny ear Lee, et al. [5–7], 2003	connected dipole Neto, et al. [8], 2009	connected Huygens' source
Figures of merit (VSWR < 2)						
Active gain	$\approx 0.9\pi$ @ f_c	$\approx 0.9\pi$ @ f_c	[3, 6] dBi	[-8, 6] dBi	$\approx 0.9\pi$ @ f_c	$< \pi$ @ f_c [a]
Active RL (VSWR)	10 dB	9.5 dB (2:1)	9.5 dB (2:1)	15 dB	10 dB	∞
Bandwidth	2.7-3.3 GHz (20%)	30%	1.5-4.5 GHz (3:1)[b,c]	1-5 GHz (5:1)[c]	6-9 GHz (40%)[c]	$\rightarrow \infty$ for $L \rightarrow \infty$
Cross polarization[e]	$>$ -17 dB	-	-	-15 dB	$>$ -17 dB	0
Field of view	$\pm$ 60°	$\pm$ 60°	$\pm$ 50°	$\pm$ 45°	$\pm$ 45°	$\pm$ 70°
Phase center stability	instable, Yagi-Uda[f]	instable, WAIM	instable[a]	stable[a]	stable[a]	stable
RCS	-	-	-	-	-	0
Scan loss, $(\cos\theta)^n$	-	n=1.1 (E)	n=1.3 (E)	n=1.2 (E)	n=1.3 (E)	n=1 (E)
	-	n=1.1 (H)	n=1.3 (H)	n=1.2 (H)	n=1.3 (H)	n=1 (H)
Thickness, from GND plane	-	N/A	$\lambda_{min}/4$	$\lambda_{min}/4$	$\lambda_{min}/4$	N/A, no GND plane

[f] Yagi-Uda directors (multi-stacked patches for example) with varying resonant length increase the bandwidth and the gain, but the GVD, the phase center instability, and the scan loss as well. On-line calibration can be used to stabilize the phase center.

Figure 26: Connecting antenna elements in a revolutionary way could allow UWB antenna arrays with 100:1 bandwidth, capable of replacing as many as five conventional antennas, inventors James Maloney (left) and Paul Friederich (right) of Georgia Tech Research Institute, Atlanta, GA [10].

Array Antennas: References

[1] S. Touchard and O. Maas, "Low loss multifunction building block panel for S-band radar," *International Radar Conference Digest, Bordeaux, France*, Oct. 12–16 2009.

[2] W. Keizer, A. P. de Hek, and A. Smolders, "Theoretical and experimental performance of a wideband wide-scan-angle rectangular waveguide phased array [for radar application]," *IEEE AP-S International Symposium Digest, London, Ontario, Canada*, vol. 3, pp. 1724–1727, June 24–28 1991.

[3] A. B. Smolders, "Design and construction of a broadband wide-scan angle phased-array antenna with 4096 radiating elements," in *Proc. IEEE Int. Symp. on Phased Array Systems and Technology*, October 1996, pp. 87–92.

[4] A. B. Smolders and G. Hampson, "Deterministic RF nulling in phased arrays for the next generation of radio telescopes," *IEEE Antennas Propagat. Mag.*, vol. 44, no. 4, pp. 13–22, Aug. 2002.

[5] J. J. Lee and S. Livingston, "Wide-band bunny-ear radiating element," in *IEEE AP-S International Symposium Digest, Ann Arbor, MI*, June 1993, pp. 1604–1607.

[6] J. J. Lee and S. W. Livingston, "Wide band dipole radiating element with a slot line feed having a Klopfenstein impedance taper," U.S. Patent 5,428,364, May 20, 1993.

[7] J. J. Lee, S. Livingston, and R. Koenig, "A low-profile wide-band (5:1) dual-pol array," *IEEE Antennas Wireless Propagat. Lett.*, vol. 2, pp. 46–49, December 2003.

[8] A. Neto, D. Cavallo, G. Gerini, and G. Toso, "Scanning performances of wideband connected arrays in the presence of a backing reflector," *IEEE Trans. Antennas Propagat.*, vol. 57, no. 10, Part 2, pp. 3092–3102, October 2009.

[9] D. Cavallo, A. Neto, and G. Gerini, "PCB slot based transformers to avoid common-mode resonances in connected arrays of dipoles," *IEEE Trans. Antennas Propagat.*, vol. 58, no. 8, pp. 2767–2771, Aug. 2010.

[10] 100-to-1 Bandwidth: New Planar Design Allows Fabrication of Ultra Wideband Phased Array Antennas. Georgia Tech Research Institute. [Online]. Available: http://www.gtri.gatech.edu/casestudy/100-1-bandwidth

Feed Antennas

Rectangular Horns

Mono-mode pyramidal horn with smooth walls (1897, J. C. Bose [11])

- **Aperture field distribution**: flared out TE_{10} mode with quadratic phase error distribution in both directions. The amplitude taper is uniform in the E-plane direction, and cosine in the H-plane direction.
- **Advantages**:
  - Bandwidth (impedance): limited by cut-off frequency of TE_{10} mode, and cut-off frequency of higher order modes
- **Disadvantages**:
  - Aperture efficiency: low due to cosine taper in H-plane direction
  - Distortion
  - Polarization: single-polarized. Perfectly straight field lines yield *zero* Ludwig-3 cross-polarization in *all* planes
  - Phase center: frequency-(in)variant (depends on flare angle and length)
  - Quadratic phase error distribution: yields directivity loss and higher sidelobe levels, primarily in the E-plane due to the uniform tapper. The quadratic phase error distribution requires correction or an optimum gain design approach, which depends on flare angle and length.
  - Radiation pattern: asymmetrical due to asymmetrical taper
- **Applications**:
  - Antenna measurements: standard gain pyramidal horn

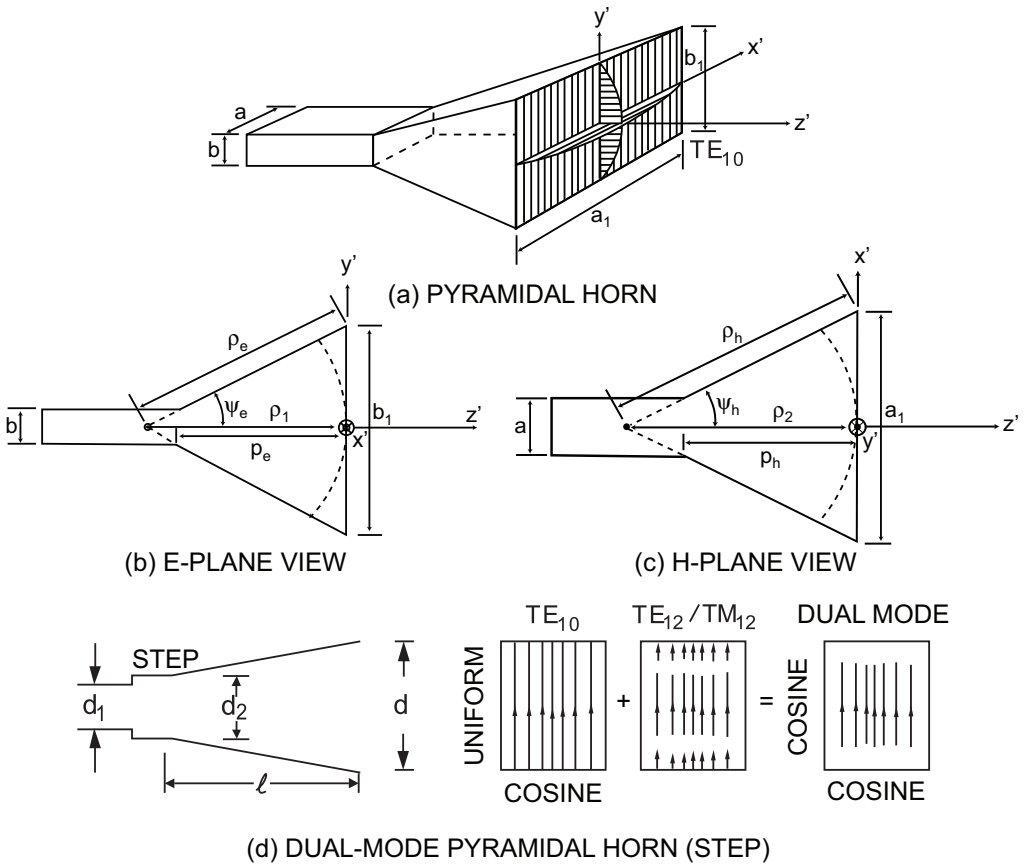

Figure 27: (a) Mono-mode pyramidal horn with smooth wall [1], (b) Dual-mode pyramidal horn with smooth wall, in which the step excites the TE_{12}/TM_{12} mode. At the center frequency (narrowband), the TE_{12}/TM_{12} mode adds up in phase with the TE_{10} mode in the aperture plane, to yield an aperture field distribution which is cosine tapered in both directions and which has perfectly straight field lines [11].

Conical Horns

Mono-mode conical horn with smooth wall (1950, A. P. King [3])

- **Aperture field distribution**: flared out TE_{11} mode with quadratic phase error distribution in both directions. The amplitude taper is uniform in the E-plane direction, and cosine in the H-plane direction.
- **Advantages**:
  - Bandwidth (impedance): limited by cut-off frequency of TE_{11} mode, and cut-off of higher order modes
- **Disadvantages**:
  - Aperture efficiency: low due to cosine taper in H-plane direction
  - Distortion
  - Polarization: H, V, LHCP, RHCP possible. Significant cross-polarization
  - Phase center: frequency-(in)variant (depends on flare angle and length)
  - Quadratic phase error distribution: yields directivity loss and higher sidelobe levels, primarily in the E-plane due to the uniform tapper. It requires correction or an optimum gain design approach, which depends on flare angle and length.
  - Radiation pattern: asymmetrical due to asymmetrical taper, despite physical symmetry
- **Applications**:
  - Antenna measurements: standard gain conical horn

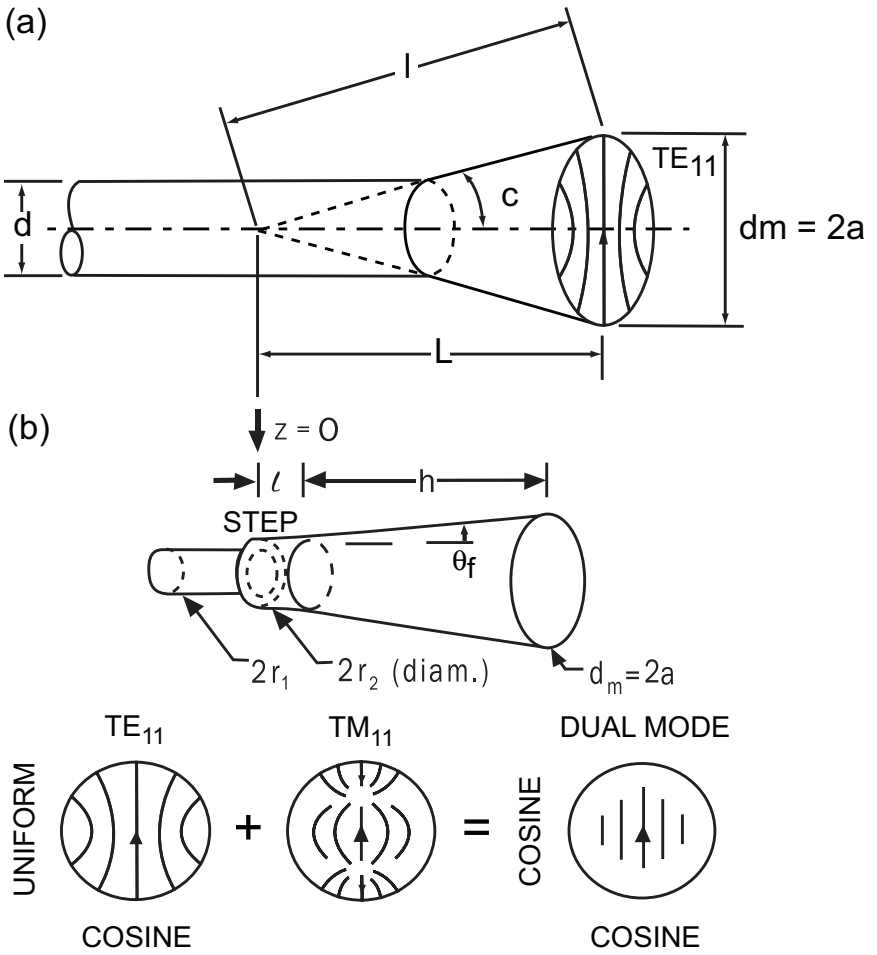

Figure 28: (a) Mono-mode conical horn with smooth wall [3], (b) Dual-mode conical horn with smooth wall (Potter horn), in which the step excites the TM_{11} mode. At the center frequency, the TM_{11} mode adds up in phase with the TE_{11} mode in the aperture plane, to yield an aperture field distribution which is cosine tapered in both directions and which has perfectly straight field lines [10].

Soft and Hard Surface Horns

Hybrid-mode soft horn (Scalar feed horn: 1964, A. F. Kay [2, 11, 12])

- **Aperture field distribution**: Flared-out balanced HE_{11} mode, which resembles the Hermite-Gaussian TEM_{00} mode, and is supported by a soft surface conical horn. The soft surface represents a perfect magnetic conductor boundary condition for the TM component and is obtained using transversal (axial) corrugations in a metal wall or metal strips on a dielectric wall. The aperture distribution is Gaussian tapered in both directions.
- **Advantages**:
  - Bandwidth (radiation pattern): 1.8:1
  - Distortion: HE_{11} mode has no cut-off frequency, allows distortion-free transmission *when* supported by soft surface
  - Polarization: H, V, LHCP, RHCP possible. Perfectly straight field lines yield *zero* Ludwig-3 cross-polarization in *all* planes
  - Radiation pattern: perfectly symmetrical (equal beamwidths)
  - Sidelobes: low due to Gaussian amplitude taper
- **Disadvantages**:
  - Aperture efficiency: low due to Gaussian amplitude taper
  - Phase center: frequency-(in)variant (depends on flare angle and length)
  - Quadratic phase error distribution
- **Applications**:
  - Single feed for reflector antenna (scalar feed horn)

Hybrid-mode hard horn (1987, E. Lier and P.-S. Kildal [4–7, 11])

- **Aperture field distribution**: Flared-out TEM mode (degenerated TE_{11}, TM_{11}, HE_{11} mode), which is supported by a hard surface cylindrically-shaped horn. The hard surface represents a PMC boundary condition for the TE component and is obtained using longitudinal (radial) corrugations in a metal wall or metal strips on a dielectric wall, *and* dielectric filling. The aperture field distribution is uniformly tapered in both directions.
- **Advantages**:
  - Aperture efficiency: high due to uniform amplitude taper
  - Bandwidth (radiation pattern): $<$ 1.8:1
  - Distortion: TEM mode has no cut-off frequency, allows distortion-free transmission *when* supported by hard surface
  - Polarization: H, V, LHCP, RHCP possible. Perfectly straight field lines yield *zero* Ludwig-3 cross-polarization in *all* planes
  - Radiation pattern: perfectly symmetrical (equal beamwidths)
- **Disadvantages**:
  - Phase center: frequency-(in)variant (depends on flare angle and length)
  - Quadratic phase error distribution
  - Sidelobes: high due to uniform amplitude taper
- **Applications**:
  - Focal plane array feed for multi-beam reflector antennas

Soft and Hard Surface Horns

Figure 29: Soft surface horn

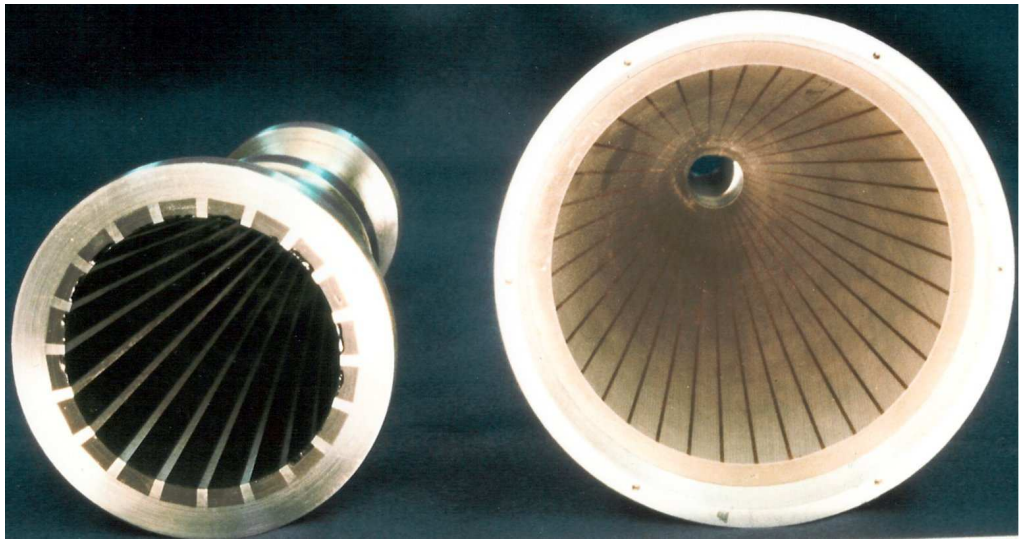

Figure 30: Hard surface horns (Courtesy of Dr. Lier [5])

UWB Leaky Lens Antenna

UWB leaky lens antenna (2010, A. Neto [8, 9])

- **Principle**: TEM mode leaky-wave radiation collimated by plano-convex ellipsoidal lens
- **Advantages**:
  - Bandwidth (radiation pattern): 5:1
  - Distortion: TEM mode has no cut-off and allows distortion-free transmission
  - Phase center: frequency-invariant
  - Quadratic phase error distribution: not applicable
  - Radiation pattern: nearly symmetrical (equal beamwidths)
  - Sidelobe level: low due to non-uniform taper
- **Disadvantages**:
  - Aperture efficiency: low due to non-uniform taper. The ellipsoidal lens can be shaped to yield a more uniform taper, at the expense of bandwidth
  - Polarization: single-polarized. Ludwig-3 cross-polarization level of -15 dB.
- **Applications**:
  - Single feed (UWB, non-uniform taper)
  - Focal plane array feed (wideband, uniform taper)

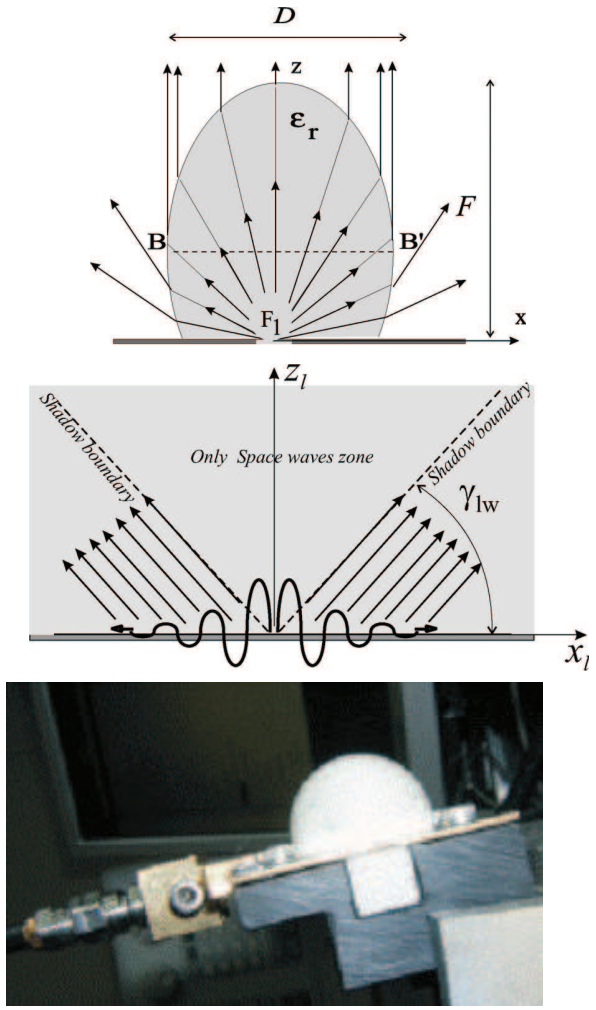

Figure 31: (a) Cross section of the UWB leaky lens antenna, showing the transmitted rays which focus energy toward broad side. (b) Side view (H-plane cut) of the near field ray picture, highlighting leaky waves existence zones, and the leaky wave angle, γ_{LW}, for a standard leaky wave slot. (c) Photograph.

Feed Antennas: References

[1] Constantine A. Balanis. *Antenna Theory, Analysis and Design, 2nd Ed.* John Wiley & Sons, 1997.

[2] P.-S. Kildal. Gaussian beam model for aperture-controlled and flareangle-controlled corrugated horn antennas. *Microwaves, Antennas and Propagation, IEE Proceedings H*, 135(4):237 – 240, August 1988.

[3] A. P. King. The radiation characteristics of conical horn antennas. *Proceedings of the IRE*, 38(3):249 – 251, March 1950.

[4] E. Lier. Analysis of soft and hard strip-loaded horns using a circular cylindrical model. *IEEE Trans. Antennas Propagat.*, 38(6):783 –793, June 1990.

[5] E. Lier. Review of soft and hard horn antennas, including metamaterial-based hybrid-mode horns. *IEEE Antennas Propagat. Mag.*, 52(2):31–39, April 2010.

[6] E. Lier and P.-S. Kildal. Soft and hard horn antennas. *IEEE Trans. Antennas Propagat.*, 36(8):1152 –1157, August 1988.

[7] E. Lier and P.-S. Kildal. A novel type of high-gain horn antenna. In *Proc. of the 5th International Conference on Antennas and Propagation, ICAP 87, York, England*, pages 431–433, March 30–April 2, 1987.

[8] A. Neto. UWB, non dispersive radiation from the planarly fed leaky lens antenna - part I: Theory and design. *IEEE Trans. Antennas Propagat.*, 58(7):2238 –2247, July 2010.

[9] A. Neto, S. Monni, and F. Nennie. UWB, non dispersive radiation from the planarly fed leaky lens antenna - part II: Demonstrators and measurements. *IEEE Trans. Antennas Propagat.*, 58(7):2248 –2258, July 2010.

[10] P. D. Potter. A new horn antenna with suppressed side lobes and equal beamwidths. *Microwave Journal*, 6:71–78, June 1963.

[11] John L. Volakis. *Antenna Engineering Handbook, Fourth Edition*. McGraw-Hill, 2007.

[12] Z. Ying, A.A. Kishk, and P.-S. Kildal. Broadband compact horn feed for prime-focus reflectors. *Electronics Letters*, 31(14):1114 –1115, July 1995.

Reflector Antennas

Reflector Antennas

Reflectors (214 B.C., Archimedes)

- **Principle**: A reflector antenna collimates RF energy (rays), emanating from a feed antenna, of which the phase center coincides with a focal point (caustic) of the reflector. Reflector antennas (and horn feed antennas) are aperture antennas, of which the aperture field distribution is related to the far field radiation pattern by the inverse 2-D fourier transform. Ideally, the aperture field distribution has:
  - Amplitude distribution: 2-D symmetrical with low edge taper in order to prevent spill-over [1]
  - Phase distribution: planar
  - Polarization: perfectly straight field lines

  Deviation from an ideal aperture field distribution yields amplitude and phase errors, and Ludwig-3 cross-polarizaton.

- **Advantages**:
  - EIRP

- **Disadvantages**:
  - Planar UWB electronically scanned reflectarrays require a Mizuguchi-compensated offset inverse Cassegrain configuration, or a fixed quadratic time delay distribution across the aperture to emulate a parabolic reflector.
  - Size, weight and wind resistance

- **Applications**:
  - Microwave communication links, radar, radio astronomy

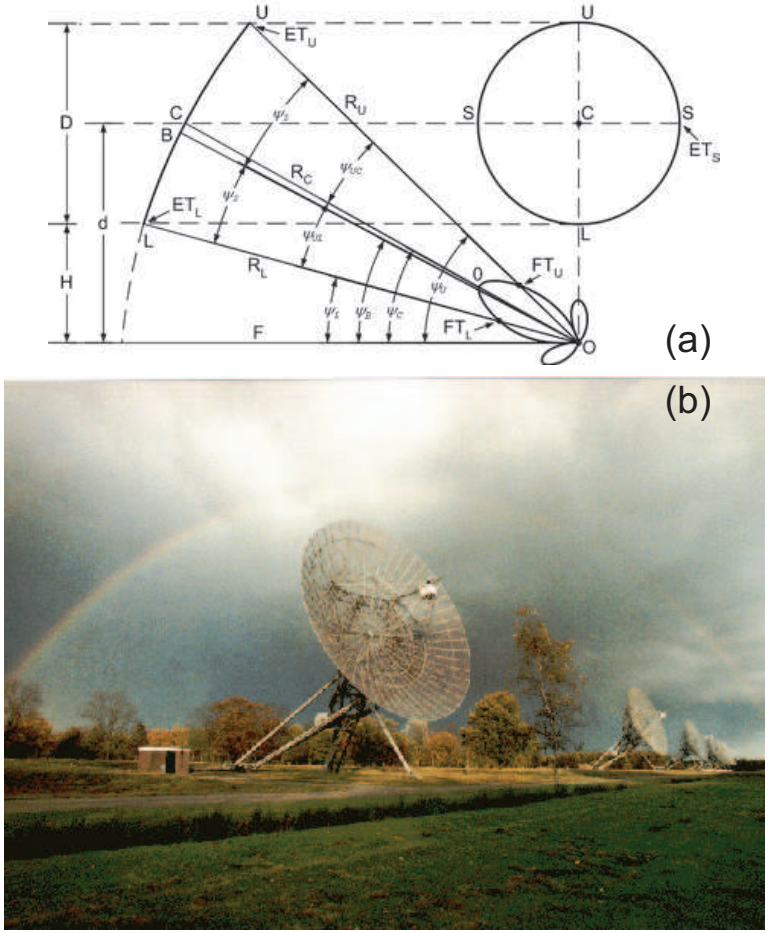

Figure 32: (a) A Mizuguchi-compensated offset-reflector has no aperture blockage, *zero* Ludwig-3 cross-polarization in *all* planes, no second order astigmatism, and minimal spill-over. (b) An axially-symmetric reflector provides the highest effective aperture multiplication factor, but has *non-zero* Ludwig-3 cross-polarization in the non-principal planes, which depends on the f/D ratio. Picture of Westerbork Synthesis Radio Telescope (WSRT).

Cassegrain & Gregorian Dual-Reflector Antennas

Cassegrain & Gregorian dual-reflector antennas (1961, P. Hannan [3–12])

- **Principle**: Folded optics; in a Cassegrain dual-reflector antenna, the focal point of the concave main reflector is located behind the convex (flat) subreflector, whereas in a Gregorian reflector system, the focal point of the concave main reflector is located between the main reflector and the concave subreflector [a]
- **Advantages**:
  - Feed location: Cassegrain and Gregorian subreflectors are used in order to put the feed and the bulky RF electronics (feed antenna(s), polarizer(s), OMT(s), klystron) at the gravitational center of the main reflector, and behind the main reflector.
  - Gain and sidelobe level: reduction of spillover and minor lobe radiation, by using additional degrees of freedom to shape the aperture field distribution of the main reflector
  - Size: ability to obtain an equivalent focal length much greater than the physical length (Cassegrain)
  - Cross-polarization level: low (Gregorian)
- **Disadvantages**:
  - Size (Gregorian)
- **Applications**:
  - Microwave communication links, radar, radio astronomy

[a] Not discussed: Dragonian (low cross-polarization level) and Schwarzschild (low comatic aberration for focal plane scanning) forms.

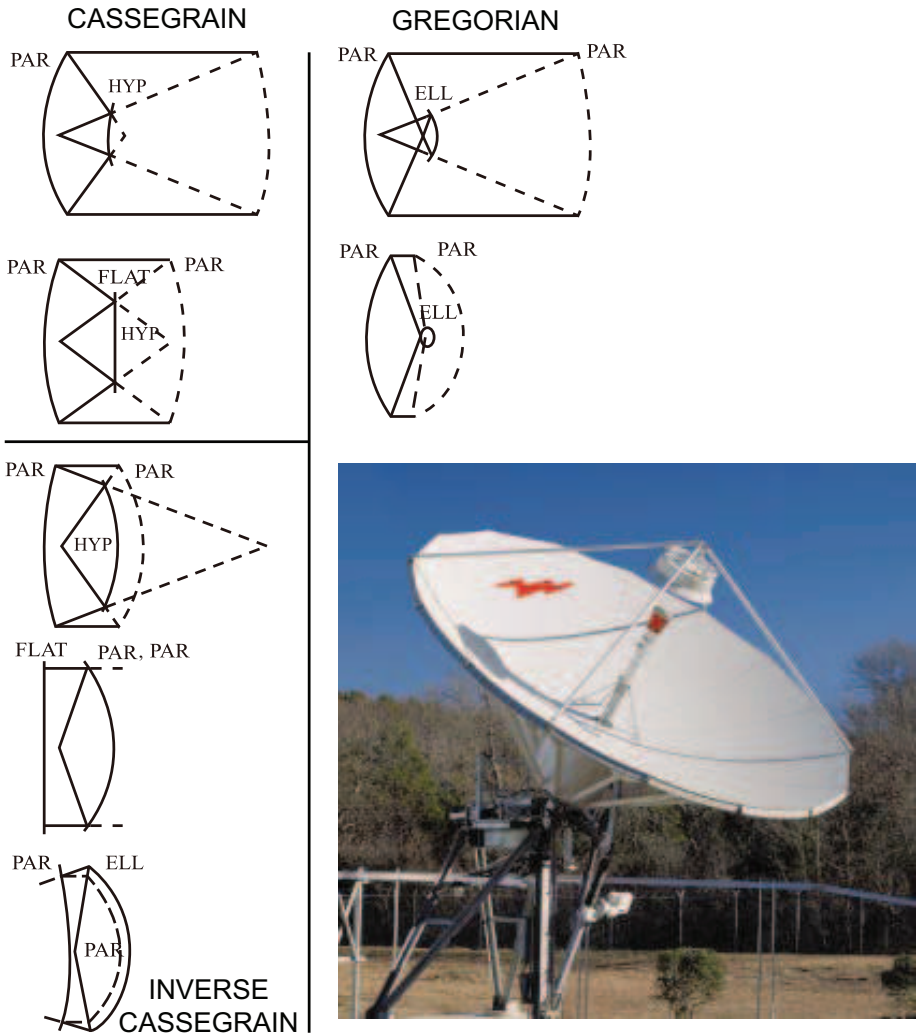

Figure 33: Cassegrain (left) and Gregorian (right) dual-reflector antennas [3]. Equivalent parabolas (dashed). Andrew Corp. 7.3 meter Gregorian dual-reflector earth station antenna with C-, Ku-band capabilities [2] (inset).

Inverse Cassegrain Dual-Reflector Antennas

Inverse Cassegrain (1961, P. Hannan [3, 8, 10, 13–15])

- **Principle**: Folded optics; in an inverse Cassegrain dual-reflector antenna, the focal point of the concave subreflector is located behind the convex (flat) main reflector.
- **Advantages**:
  - Advantages of Cassegrain dual-reflector antennas
  - Electronic scanning: The main reflector can be a planar electronically scanned reflectarray.
  - Size: very compact
  - No need for waveguide rotary joint
- **Disadvantages**:
  - Bandwidth: The axially-symmetric inverse Cassegrain dual-reflector antenna requires a planar reflect array with polarization twist (narrowband)
- **Applications**:
  - Radar
  - Radio astronomy

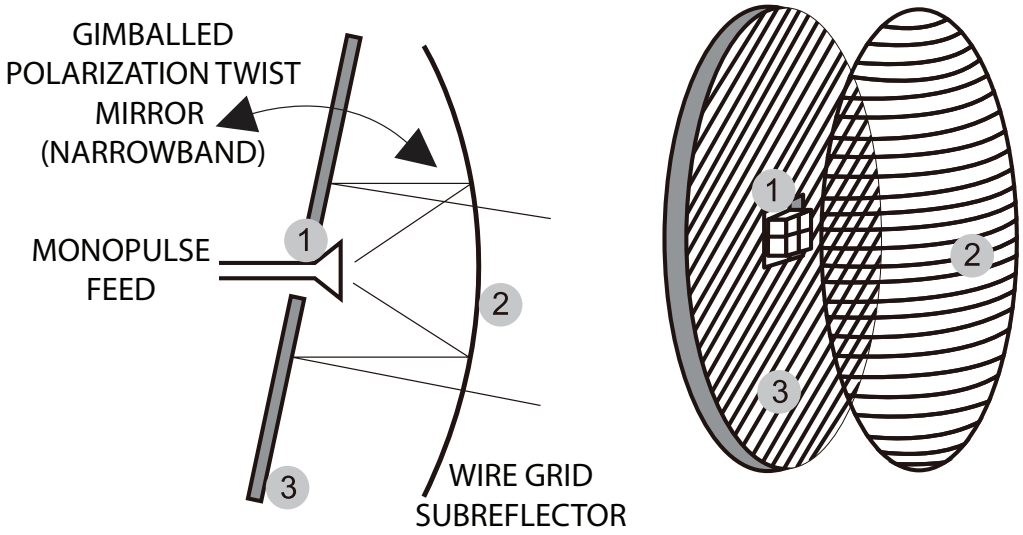

Figure 34: An inverse Cassegrain antenna comprises a feed illuminating a polarization-selective wire grid subreflector, which collimates the RF field to illuminate a polarization twisting mirror [15].

Inverse Cassegrain Dual-Reflector Antennas

343-756.
10-28-75 OR 3,916,416 SR

United States Patent [19]
Lewis

[11] **3,916,416**
[45] **Oct. 28, 1975**

[54] **360° AZIMUTH SCANNING ANTENNA WITHOUT ROTATING RF JOINTS**

[75] Inventor: **Bernard L. Lewis,** Oxon Hill, Md.

[73] Assignee: **The United States of America as represented by the Secretary of the Navy,** Washington, D.C.

[22] Filed: **Sept. 24, 1974**

[21] Appl. No.: **508,777**

[52] **U.S. Cl.** **343/756;** 343/761; 343/779; 343/840; 343/872

[51] **Int. Cl.**[2] **H01Q 19/00;** H01Q 19/12

[58] **Field of Search** 343/756, 761, 779, 839, 343/840, 872

[56] **References Cited**
UNITED STATES PATENTS

3,261,020 7/1966 Kay 343/756

Primary Examiner—Eli Lieberman
Attorney, Agent, or Firm—R. S. Sciascia; Arthur L. Branning; Norman V. Brown

[57] **ABSTRACT**

A 360° scanning radar antenna has a plurality of primary focusing-structures arranged in a circular fashion illuminating corresponding secondary focusing-structures which in turn are arranged about, and directed toward, a rotating multi-sided half-wave plane reflector. Radar energy is switched to radiate from a given primary focusing-structure during the time when the plane reflector is in position to reflect all of the energy collimated by the corresponding secondary focusing-structure. The secondary focusing-structure may be made to appear transparent to the beam reflected by the plane reflector.

6 Claims, 3 Drawing Figures

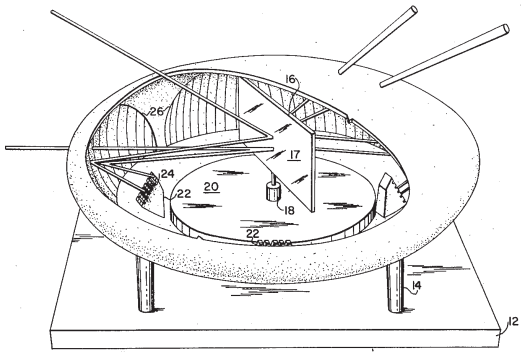

343-756 SR
2/24/81 OR 4,253,100

United States Patent [19]
Commault et al.

[11] **4,253,100**
[45] **Feb. 24, 1981**

[54] **INVERSE CASSEGRAIN ANTENNA FOR MULTIPLE FUNCTION RADAR**

[75] Inventors: **Yves Commault; Francois Gautier; Robert Pierrot,** all of Paris, France

[73] Assignee: **Thomson-CSF,** Paris, France

[21] Appl. No.: **116,661**

[22] Filed: **Jan. 29, 1980**

[30] **Foreign Application Priority Data**

Feb. 2, 1979 [FR] France 79 02768

[51] **Int. Cl.**[3] **H01Q 3/12;** H01Q 19/19; B01Q 19/195

[52] **U.S. Cl.** ..... **343/756;** 343/761; 343/781 CA

[58] **Field of Search** ..... 343/756, 761, 781 P, 343/781 CA, 837, 839, 914

[56] **References Cited**
U.S. PATENT DOCUMENTS

3,254,342 5/1966 Miller ..... 343/781 CA
3,771,160 11/1973 Laverick ..... 343/781 CA

Primary Examiner—Eli Lieberman
Attorney, Agent, or Firm—Cushman, Darby & Cushman

[57] **ABSTRACT**

Inverse Cassegrain antenna making it possible to use on the one hand the qualities of a conventional fine beam for look-out and tracking functions and making it possible on the other hand to have a widened beam either in the elevation plane or in the bearing plane. According to one embodiment, this antenna is provided with a mirror constituted by two reflector - polarizer elements joined to one another by a hinge which permits the articulation thereof, a remote control device regulating their relative orientation.

11 Claims, 10 Drawing Figures

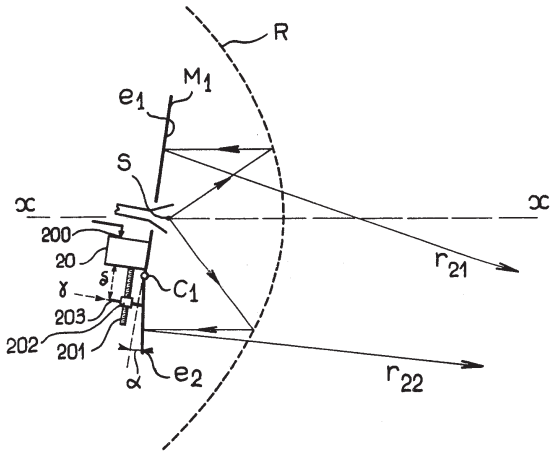

Reflector Antennas: References

[1] N. Llombart, A. Neto, G. Gerini, M. Bonnedal, and P. De Maagt, "Leaky wave enhanced feed arrays for the improvement of the edge of coverage gain in multibeam reflector antennas," *IEEE Trans. Antennas Propagat.*, vol. 56, no. 5, pp. 1280 –1291, May 2008.

[2] Specialized Turnkey Systems. [Online]. Available: http://www.stssa.com/

[3] P. Hannan, "Microwave antennas derived from the cassegrain telescope," *Antennas and Propagation, IRE Transactions on*, vol. 9, no. 2, pp. 140 –153, Mar. 1961.

[4] C. Granet, "Designing axially symmetric cassegrain or gregorian dual-reflector antennas from combinations of prescribed geometric parameters," *IEEE Antennas Propagat. Mag.*, vol. 40, no. 2, pp. 76 –82, Apr. 1998.

[5] ——, "Designing axially symmetric cassegrain or gregorian dual-reflector antennas from combinations of prescribed geometric parameters. 2. minimum blockage condition while taking into account the phase-center of the feed," *IEEE Antennas Propagat. Mag.*, vol. 40, no. 3, pp. 82 –89, June 1998.

[6] ——, "A simple procedure for the design of classical displaced-axis dual-reflector antennas using a set of geometric parameters," *IEEE Antennas Propagat. Mag.*, vol. 41, no. 6, pp. 64 –72, Dec. 1999.

[7] ——, "Designing classical dragonian offset dual-reflector antennas from combinations of prescribed geometric parameters," *IEEE Antennas Propagat. Mag.*, vol. 43, no. 6, pp. 100 –107, Dec. 2001.

[8] S. Chang and J. Prata, A., "A design procedure for classical offset inverse cassegrain antennas with circular apertures," in *IEEE AP-S International Symposium Digest , Boston, MA*, vol. 1, July 8-13 2001, pp. 534 –537 vol.1.

[9] C. Granet, "Designing classical offset cassegrain or gregorian dual-reflector antennas from combinations of prescribed geometric parameters," *IEEE Antennas Propagat. Mag.*, vol. 44, no. 3, pp. 114 – 123, June 2002.

[10] ——, "Designing classical offset inverse-cassegrain dual-reflector antennas from combinations of prescribed geometric parameters," *IEEE Antennas Propagat. Mag.*, vol. 45, no. 3, pp. 102 – 108, June 2003.

[11] ——, "Designing classical offset cassegrain or gregorian dual-reflector antennas from combinations of prescribed geometric parameters. part 2: feed-horn blockage conditions," *IEEE Antennas Propagat. Mag.*, vol. 45, no. 6, pp. 86 – 89, Dec. 2003.

[12] ——, "Designing schwarzschild dual-reflector systems," *IEEE Antennas Propagat. Mag.*, vol. 48, no. 3, pp. 68 –74, June 2006.

[13] B. L. Lewis, "360° azimuth scanning antenna without rotating RF joints," U.S. Patent 3,916,416, September 24, 1974.

[14] Y. Commault, F. Gautier, and R. Pierrot, "Inverse cassegrain antenna for multiple function radar," U.S. Patent 4,253,100, January 29, 1980.

[15] D. Howard and D. Cross, "Mirror antenna dual-band lightweight mirror design," *IEEE Trans. Antennas Propagat.*, vol. 33, no. 3, pp. 286 – 294, Mar. 1985.

RF Components

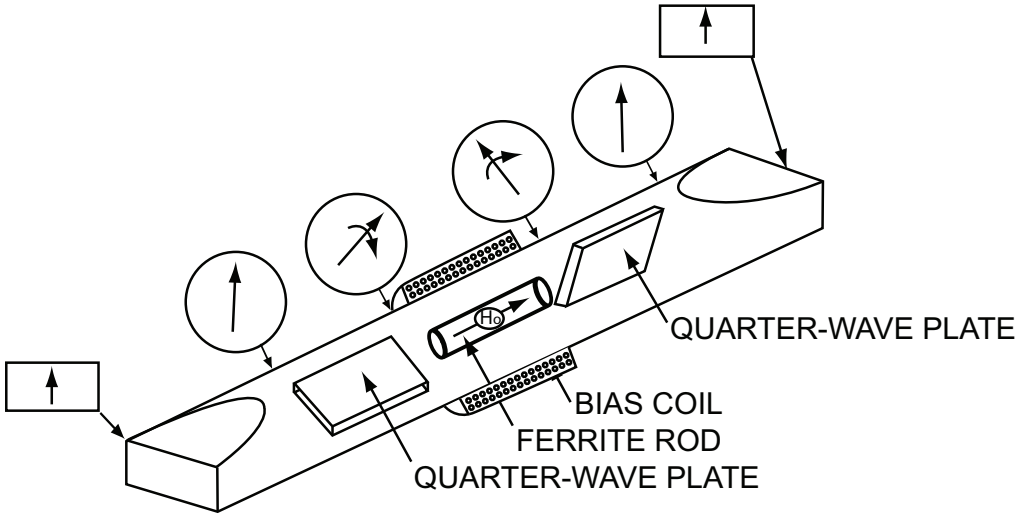

Figure 35: Linear circular polarizer in a ferrite Faraday rotation phase shifter [1].

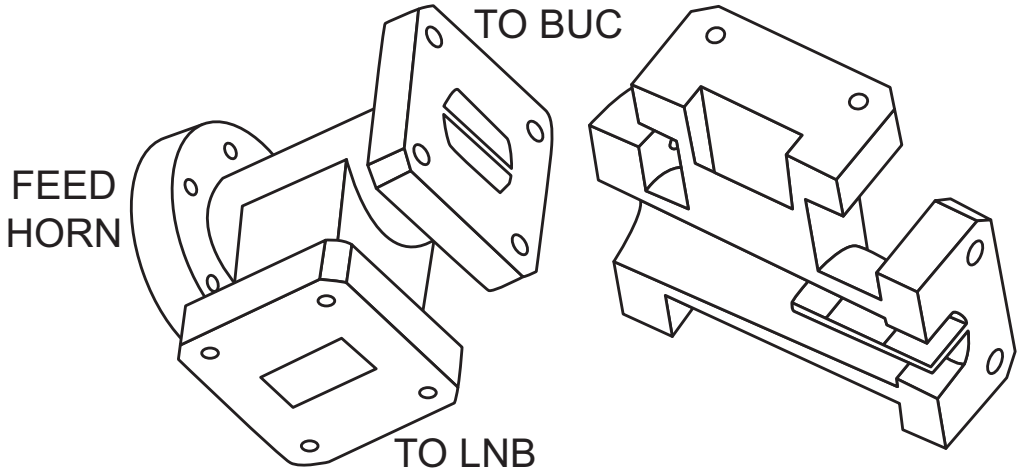

Figure 36: Orthomode transducer for conical feed horn. The drawing refers to a very small aperture terminal (VSAT) application. BUC stands for block up-converter. LNB stands for low noise block converter.

(True-Time-Delay) Phase Shifters

- **Function**: TTD phase shifters provide (TTD) phase shift to steer the beam of an RF beamforming ESA.
- Design trade-offs are necessary in the selection of:
  - Biasing: current-controlled, voltage-controlled (electrodynamic (current flow), electrostatic (no current flow))
  - Design: (distributed) loaded-line [2–5], reflect-type [6], switched LC network (high-pass, low-pass) [7], switched-line [8–11], vector modulator
  - Differential (CPS, slotline) or single-ended (CPW, microstrip) transmission line
  - Phase shift versus time delay
  - Quantization: analog or digital (4b, 5b)
  - RF power amplification: active (unilateral) or passive (reciprocal)

(True-Time-Delay) Phase Shifters

- **Function**: TTD phase shifters provide (TTD) phase shift to steer the beam of an RF beamforming ESA.
- Design trade-offs are necessary in the selection of:
  - Biasing: current-controlled, voltage-controlled (electrodynamic (current flow), electrostatic (no current flow))
  - Design: (distributed) loaded-line [2–5], reflect-type [6], switched LC network (high-pass, low-pass) [7], switched-line [8–11], vector modulator
  - Differential (CPS, slotline) or single-ended (CPW, microstrip) transmission line
  - Phase shift versus time delay
  - Quantization: analog or digital (4b, 5b)
  - RF power amplification: active (unilateral) or passive (reciprocal)

(True-Time-Delay) Phase Shifters

- **Function**: TTD phase shifters provide (TTD) phase shift to steer the beam of an RF beamforming ESA.
- Design trade-offs are necessary in the selection of:
  - Biasing: current-controlled, voltage-controlled (electrodynamic (current flow), electrostatic (no current flow))
  - Design: (distributed) loaded-line [2–5], reflect-type [6], switched LC network (high-pass, low-pass) [7], switched-line [8–11], vector modulator
  - Differential (CPS, slotline) or single-ended (CPW, microstrip) transmission line
  - Phase shift versus time delay
  - Quantization: analog or digital (4b, 5b)
  - RF power amplification: active (unilateral) or passive (reciprocal)

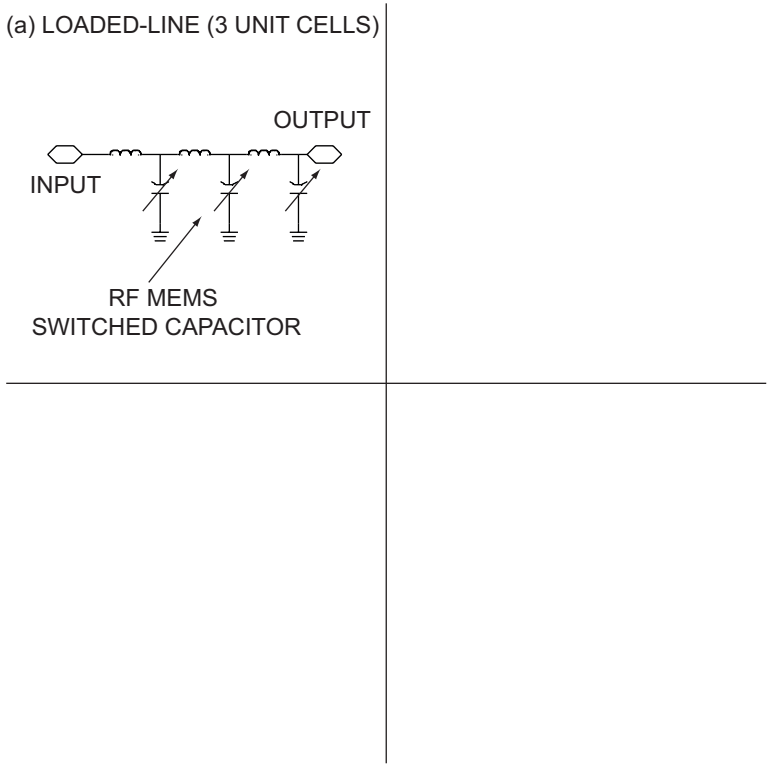

(True-Time-Delay) Phase Shifters

- **Function**: TTD phase shifters provide (TTD) phase shift to steer the beam of an RF beamforming ESA.
- Design trade-offs are necessary in the selection of:
  - Biasing: current-controlled, voltage-controlled (electrodynamic (current flow), electrostatic (no current flow))
  - Design: (distributed) loaded-line [2–5], reflect-type [6], switched LC network (high-pass, low-pass) [7], switched-line [8–11], vector modulator
  - Differential (CPS, slotline) or single-ended (CPW, microstrip) transmission line
  - Phase shift versus time delay
  - Quantization: analog or digital (4b, 5b)
  - RF power amplification: active (unilateral) or passive (reciprocal)

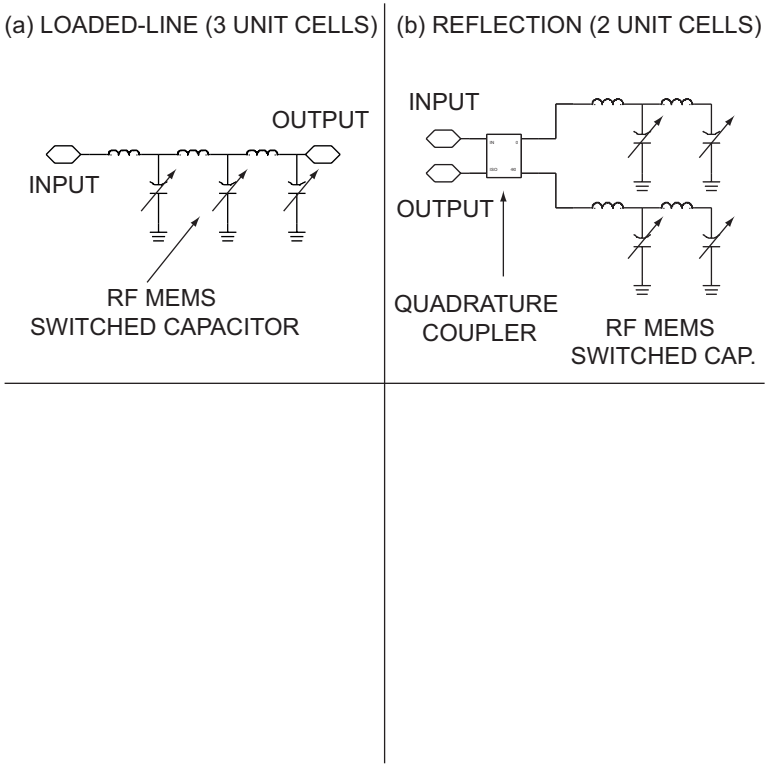

(True-Time-Delay) Phase Shifters

- **Function**: TTD phase shifters provide (TTD) phase shift to steer the beam of an RF beamforming ESA.
- Design trade-offs are necessary in the selection of:
  - Biasing: current-controlled, voltage-controlled (electrodynamic (current flow), electrostatic (no current flow))
  - Design: (distributed) loaded-line [2–5], reflect-type [6], switched LC network (high-pass, low-pass) [7], switched-line [8–11], vector modulator
  - Differential (CPS, slotline) or single-ended (CPW, microstrip) transmission line
  - Phase shift versus time delay
  - Quantization: analog or digital (4b, 5b)
  - RF power amplification: active (unilateral) or passive (reciprocal)

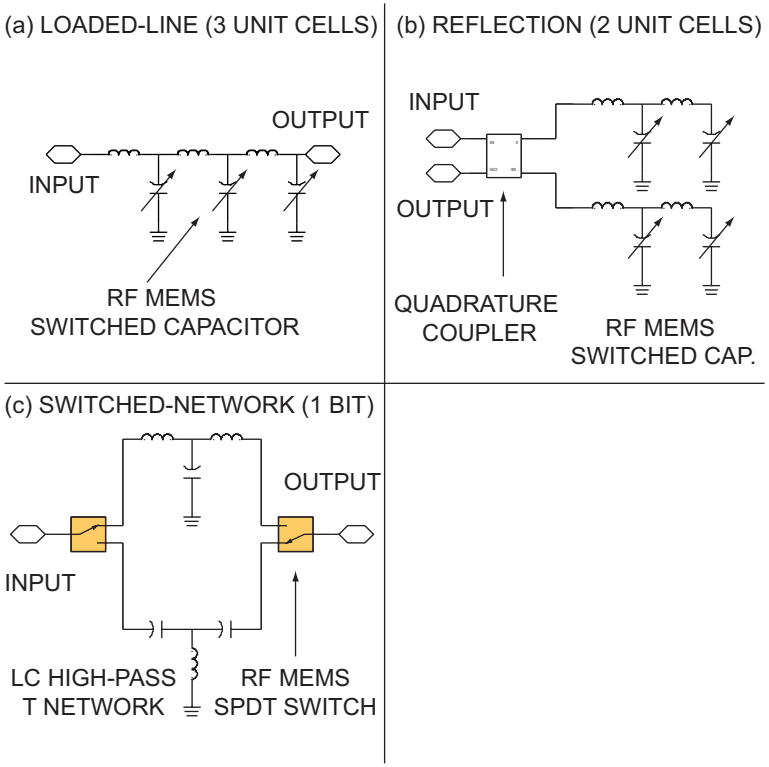

(True-Time-Delay) Phase Shifters

- **Function**: TTD phase shifters provide (TTD) phase shift to steer the beam of an RF beamforming ESA.
- Design trade-offs are necessary in the selection of:
  - Biasing: current-controlled, voltage-controlled (electrodynamic (current flow), electrostatic (no current flow))
  - Design: (distributed) loaded-line [2–5], reflect-type [6], switched LC network (high-pass, low-pass) [7], switched-line [8–11], vector modulator
  - Differential (CPS, slotline) or single-ended (CPW, microstrip) transmission line
  - Phase shift versus time delay
  - Quantization: analog or digital (4b, 5b)
  - RF power amplification: active (unilateral) or passive (reciprocal)

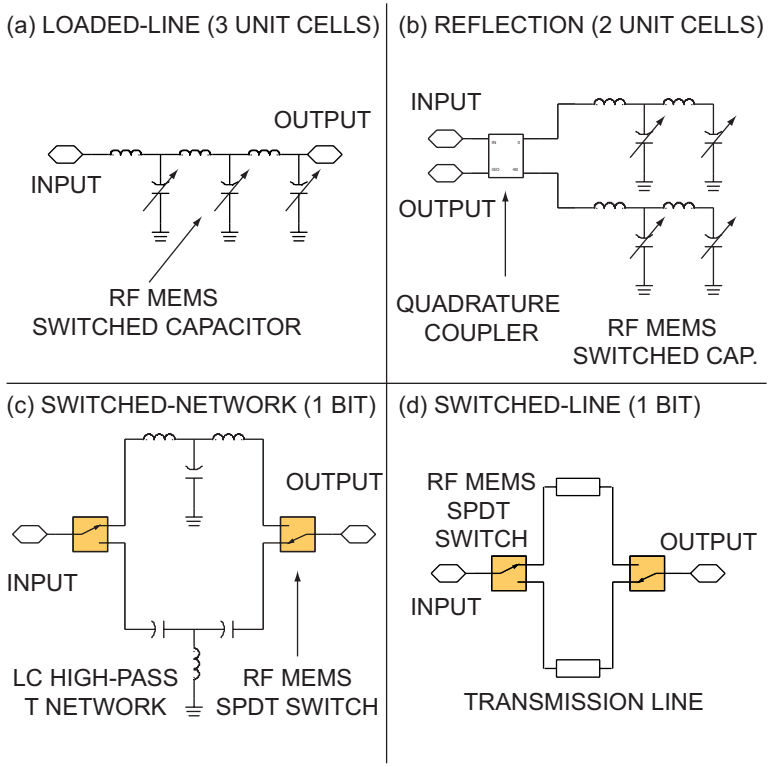

(True-Time-Delay) Phase Shifters

- **Function**: TTD phase shifters provide (TTD) phase shift to steer the beam of an RF beamforming ESA.
- Design trade-offs are necessary in the selection of:
  - Biasing: current-controlled, voltage-controlled (electrodynamic (current flow), electrostatic (no current flow))
  - Design: (distributed) loaded-line [2–5], reflect-type [6], switched LC network (high-pass, low-pass) [7], switched-line [8–11], vector modulator
  - Differential (CPS, slotline) or single-ended (CPW, microstrip) transmission line
  - Phase shift versus time delay
  - Quantization: analog or digital (4b, 5b)
  - RF power amplification: active (unilateral) or passive (reciprocal)

(True-Time-Delay) Phase Shifters

- **Function**: TTD phase shifters provide (TTD) phase shift to steer the beam of an RF beamforming ESA.
- Design trade-offs are necessary in the selection of:
  - Biasing: current-controlled, voltage-controlled (electrodynamic (current flow), electrostatic (no current flow))
  - Design: (distributed) loaded-line [2–5], reflect-type [6], switched LC network (high-pass, low-pass) [7], switched-line [8–11], vector modulator
  - Differential (CPS, slotline) or single-ended (CPW, microstrip) transmission line
  - Phase shift versus time delay
  - Quantization: analog or digital (4b, 5b)
  - RF power amplification: active (unilateral) or passive (reciprocal)
- Phase shifting
  - Bandwidth:

    $$BW_{max} < 0.886\, B_b \frac{c}{L \sin\theta_{max}}$$

  - Frequency squinting:

    $$\theta - \theta_0 = \arcsin\left(\frac{-\beta}{k\, d}\right) - \arcsin\left(\frac{-\beta}{k_0\, d}\right)$$

- TTD phase shifting
  - TTD beam steering:

    $$\theta = \arcsin\left(\frac{c}{d}\, \Delta\tau\right)$$

(True-Time-Delay) Phase Shifters

- **Function**: TTD phase shifters provide (TTD) phase shift to steer the beam of an RF beamforming ESA.
- Design trade-offs are necessary in the selection of:
  - Biasing: current-controlled, voltage-controlled (electrodynamic (current flow), electrostatic (no current flow))
  - Design: (distributed) loaded-line [2–5], reflect-type [6], switched LC network (high-pass, low-pass) [7], switched-line [8–11], vector modulator
  - Differential (CPS, slotline) or single-ended (CPW, microstrip) transmission line
  - Phase shift versus time delay
  - Quantization: analog or digital (4b, 5b)
  - RF power amplification: active (unilateral) or passive (reciprocal)
- Phase shifting
  - Bandwidth:

    $$BW_{max} < 0.886\, B_b \frac{c}{L \sin\theta_{max}}$$

  - Frequency squinting:

    $$\theta - \theta_0 = \arcsin\left(\frac{-\beta}{k\, d}\right) - \arcsin\left(\frac{-\beta}{k_0\, d}\right)$$

- TTD phase shifting
  - TTD beam steering:

    $$\theta = \arcsin\left(\frac{c}{d}\, \Delta\tau\right)$$

(True-Time-Delay) Phase Shifters

- **Function**: TTD phase shifters provide (TTD) phase shift to steer the beam of an RF beamforming ESA.
- Design trade-offs are necessary in the selection of:
  - Biasing: current-controlled, voltage-controlled (electrodynamic (current flow), electrostatic (no current flow))
  - Design: (distributed) loaded-line [2–5], reflect-type [6], switched LC network (high-pass, low-pass) [7], switched-line [8–11], vector modulator
  - Differential (CPS, slotline) or single-ended (CPW, microstrip) transmission line
  - Phase shift versus time delay
  - Quantization: analog or digital (4b, 5b)
  - RF power amplification: active (unilateral) or passive (reciprocal)
- Phase shifting
  - Bandwidth:

    $$BW_{max} < 0.886\, B_b \frac{c}{L\, \sin\theta_{max}}$$

  - Frequency squinting:

    $$\theta - \theta_0 = \arcsin\left(\frac{-\beta}{k\, d}\right) - \arcsin\left(\frac{-\beta}{k_0\, d}\right)$$

- TTD phase shifting
  - TTD beam steering:

    $$\theta = \arcsin\left(\frac{c}{d}\, \Delta\tau\right)$$

(True-Time-Delay) Phase Shifters

- **Function**: TTD phase shifters provide (TTD) phase shift to steer the beam of an RF beamforming ESA.
- Design trade-offs are necessary in the selection of:
  - Biasing: current-controlled, voltage-controlled (electrodynamic (current flow), electrostatic (no current flow))
  - Design: (distributed) loaded-line [2–5], reflect-type [6], switched LC network (high-pass, low-pass) [7], switched-line [8–11], vector modulator
  - Differential (CPS, slotline) or single-ended (CPW, microstrip) transmission line
  - Phase shift versus time delay
  - Quantization: analog or digital (4b, 5b)
  - RF power amplification: active (unilateral) or passive (reciprocal)
- Number of *effective* bits:

$$\tilde{P} = \frac{1}{2}\,\log_2 \pi^2 - \log_2 3\,(S^2_{P_{ATT}} + S^2_{P_{PS}} + \frac{1}{3}\,\frac{\pi^2}{2^{2P}})$$

(True-Time-Delay) Phase Shifters

- **Function**: TTD phase shifters provide (TTD) phase shift to steer the beam of an RF beamforming ESA.
- Design trade-offs are necessary in the selection of:
  - Biasing: current-controlled, voltage-controlled (electrodynamic (current flow), electrostatic (no current flow))
  - Design: (distributed) loaded-line [2–5], reflect-type [6], switched LC network (high-pass, low-pass) [7], switched-line [8–11], vector modulator
  - Differential (CPS, slotline) or single-ended (CPW, microstrip) transmission line
  - Phase shift versus time delay
  - Quantization: analog or digital (4b, 5b)
  - RF power amplification: active (unilateral) or passive (reciprocal)

Table IV: Comparison of State-of-the-Art Distributed Loaded-Line Phase Shifters

	Barker and Rebeiz [2], 1999	Perruisseau-Carrier, et al. [3], 2006	Lakshminarayanan and Weller [4], 2007	Van Caekenberghe, et al. [5], 2008
Design characteristics				
Analog or digital	analog	digital (1 bit)	digital (1 bit)	analog
Differential or single-ended	single-ended	single-ended	single-ended	differential
Drive voltage	< 13 V	20 V	30-45 V	< 7 V
Frequency	40 GHz	20 GHz	12 GHz	10 GHz
Substrate	fused silica $\epsilon_r = 3.78$, $\tan\delta = 0.0002$	silicon $\epsilon_r = 11.7$, $\sigma = 10$ kΩ cm	fused silica $\epsilon_r = 3.78$, $\tan\delta = 0.0002$	borosilicate glass $\epsilon_r = 5.1$, $\tan\delta = 0.006$
RF MEMS technology	fixed-fixed beam varactors	capacitive fixed-fixed beam switches	capacitive cantilever & fixed-fixed beam switches	fixed-fixed beam varactors
Transmission line	CPW	CPW	CPW	slotline
Figures of merit				
Phase shift / length	11.8°/mm	14.7°/mm	35°/mm	5.9°/mm
Phase shift / noise figure	70°/dB	72°/dB	429°/dB	28.2°/dB
Time delay / length	0.8 ps/mm	2 ps/mm	8.1 ps/mm	1.6 ps/mm
Time delay / noise figure	4.9 ps/dB	10 ps/dB	99.3 ps/dB	7.8 ps/dB

RF Components: References

[1] D. M. Pozar, *Microwave Engineering, 2nd Ed.* John Wiley & Sons, 1998.

[2] N. S. Barker and G. M. Rebeiz, "Optimization of distributed MEMS transmission-line phase shifters - U-band and W-band designs," *IEEE Trans. Microwave Theory Tech.*, vol. 48, no. 11, pp. 1957–1966, November 2000.

[3] J. Perruisseau-Carrier, R. Fritschi, P. Crespo-Valero, and A. K. Skrivervik, "Modeling of periodic distributed MEMS application to the design of variable true-time delay lines," *IEEE Trans. Microwave Theory Tech.*, vol. 54, no. 1, pp. 383–392, January 2006.

[4] B. Lakshminarayanan and T. M. Weller, "Optimization and implementation of impedance-matched true-time-delay phase shifters on quartz substrate," *IEEE Trans. Microwave Theory Tech.*, vol. 55, no. 2, part 1, pp. 335–342, February 2007.

[5] K. Van Caekenberghe and T. Vähä-Heikkilä, "An analog RF MEMS slotline true-time-delay phase shifter," *IEEE Trans. Microwave Theory Tech.*, vol. 56, no. 9, pp. 2151–2159, September 2008.

[6] B. Pillans, S. Eshelman, A. Malczewski, J. Ehmke, and C. Goldsmith, "Ka-band RF MEMS phase shifters," *IEEE Microwave Wireless Compon. Lett.*, vol. 9, no. 12, pp. 520–522, December 1999.

[7] M. A. Morton and J. Papapolymerou, "A packaged MEMS-based 5-bit X-band high-pass/low-pass phase shifter," *IEEE Trans. Microwave Theory Tech.*, vol. 56, no. 9, pp. 2025–2031, September 2008.

[8] J. B. Hacker, R. E. Mihailovich, M. Kim, and J. F. DeNatale, "A Ka-band 3-bit RF MEMS true-time-delay network," *IEEE Trans. Microwave Theory Tech.*, vol. 51, no. 1, part 1, pp. 305–308, January 2003.

[9] C. D. Nordquist, C. W. Dyck, G. M. Kraus, I. C. Reines, C. L. Goldsmith, W. D. Cowan, T. A. Plut, F. Austin, P. S. Finnegan, M. H. Ballance, and C. T. Sullivan, "A DC to 10 GHz 6-bit RF MEMS time delay circuit," *IEEE Microwave Wireless Compon. Lett.*, vol. 16, no. 5, pp. 305–307, May 2006.

[10] J. Muldavin, C. Bozler, S. Rabe, and C. Keast, "Fully packaged 4-bit 100 ps RF MEMS time delay," in *IEEE MTT-S International Microwave Symposium Digest, Honolulu, HI*, June 3–8, 2007, pp. 493–496.

[11] A. Stehle, G. Georgiev, V. Ziegler, B. Schönlinner, U. Prechtel, H. Seidel, and U. Schmid, "RF MEMS switch and phase shifter optimized for W-band," *European Microwave Conference, Amsterdam, The Netherlands*, pp. 104–107, October 2008.

Transmitters

Vacuum electronics devices (1906, L. De Forest) [1–4]

- **Principle**: Slow-wave linear-beam tube amplifiers (klystrons, TWTs) provide high-power amplification at microwave frequencies. Fast-wave linear-beam tube amplifiers (gyro-klystrons, gyro-TWTs) provide high-power amplification at millimeter-wave frequencies.
- **Advantages**:
  - Bandwidth: wideband (TWT amplifiers are only wideband at high output power levels.)
  - Efficiency: up to 70%, higher than SSPA
  - Frequency: up to 94 GHz, higher than SSPA
  - Output power: up to 100 kW peak (pulse-Doppler radar) at 94 GHz
  - Gain: high (klystron)
- **Disadvantages**:
  - Phase noise: phase stable, but higher phase noise than SSPA
  - High-voltage technology (kV)
  - Reliability and lifetime: lower than SSPA (graceful degradation)
  - Warm-up delay (hot cathode requirement)
- **Applications**:
  - Passive electronically scanned arrays, reflector systems

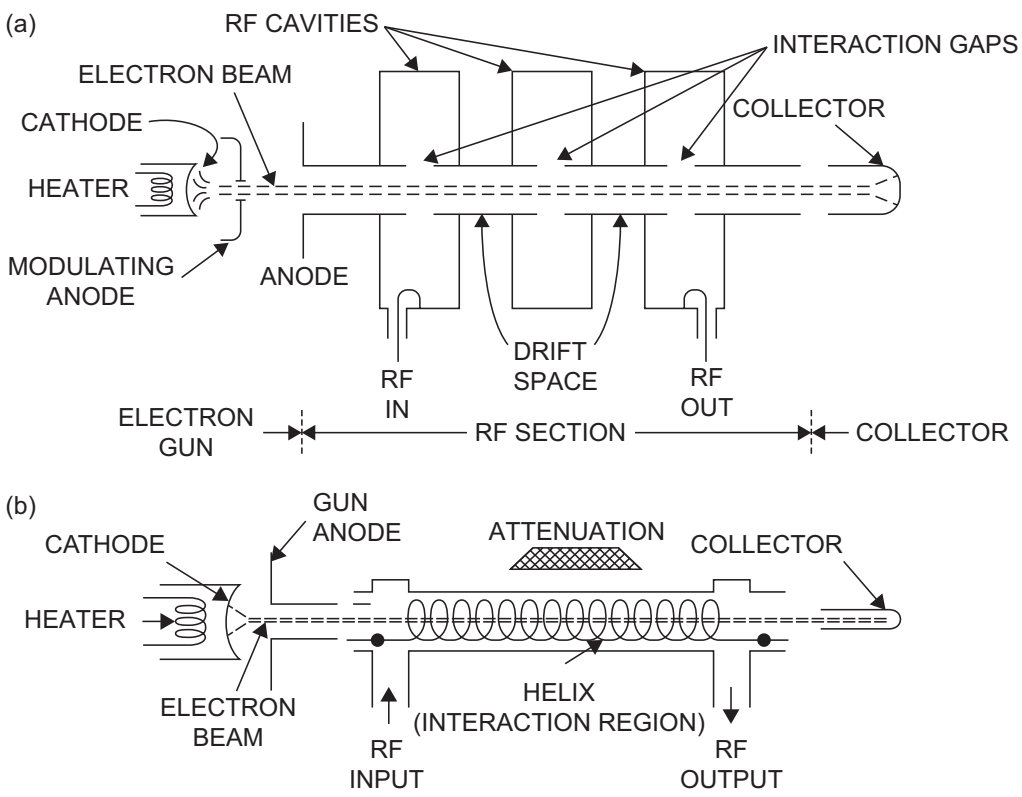

Figure 37: (a) Representation of the principal parts of a three-cavity klystron amplifier (b) Representation of the principle parts of a traveling wave tube showing a helix slow-wave circuit shown for simplicity [4].

RF Components: References

[1] K. Felch, B. Danly, H. Jory, K. Kreischer, W. Lawson, B. Levush, and R. Temkin, "Characteristics and applications of fast-wave gyrodevices," *Proc. IEEE*, vol. 87, no. 5, pp. 752 –781, May 1999.

[2] J. Antonsen, T.M., A. Mondelli, B. Levush, J. Verboncoeur, and C. Birdsall, "Advances in modeling and simulation of vacuum electronic devices," *Proc. IEEE*, vol. 87, no. 5, pp. 804 –839, May 1999.

[3] B. Levush, D. Abe, J. Calame, B. Danly, K. Nguyen, E. Dutkowski, R. Abrams, and R. Parker, "Vacuum electronics: Status and trends," *IEEE Aerosp. Electron. Syst. Mag*, vol. 22, no. 9, pp. 28 –34, Sept. 2007.

[4] M. I. Skolnik, *Radar Handbook, 3rd Ed.* McGraw-Hill, 2008.

RF Technologies

Ferrites

Ferrite phase shifter (1958, Fruchaft)

- **Principle**: Faraday rotation (propagation in direction of bias) and birefringence (propagation transverse to bias) at magnetic resonance (gyrotropism). Examples of ferrites include yttrium iron garnet (YIG), and ferrites composed of iron oxides and various other elements such as aluminum, cobalt, manganese, and nickel
- **Advantages**:
  - Linearity
  - Power handling: up to 100 kW
- **Disadvantages**:
  - Bandwidth: resonant
  - Biasing: large magnetization current
  - Insertion loss: low loss, bound by the Kramer-Krönig relation. The higher the permeability, the higher the attenuation.
  - Size: waveguide
- **Applications**:
  - Control devices: phase shifters, switches and tunable resonators and filters.
  - Directional devices: isolators, circulators, and gyrators.
  - Radar-absorbing materials or coatings.

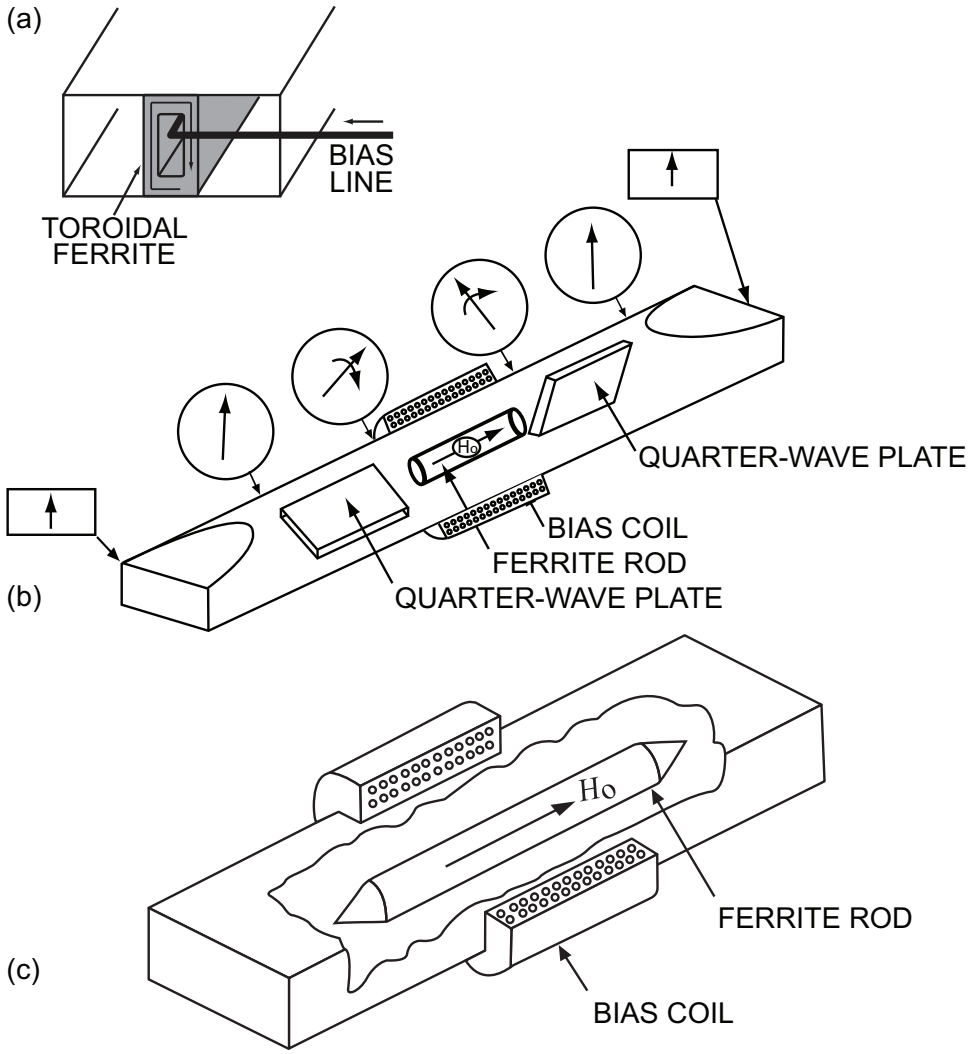

Figure 38: (a) Nonreciprocal latching (remanent) phase shifter, (b) nonreciprocal Faraday rotation phase shifter, and (c) Reggia-Spencer reciprocal phase shifter [1].

Ferroelectrics

Ferroelectricity (1920, J. Valasek)

- **Principle**: Ferroelectricity is a property of certain materials which possess a spontaneous electric polarization that can be reversed by the application of an external electric field. The term is used in analogy to ferromagnetism, in which a material exhibits a permanent magnetic moment. Ferromagnetism was already known when ferroelectricity was discovered in 1920 in Rochelle salt by Valasek. Thus, the prefix ferro, meaning iron, was used to describe the property despite the fact that most ferroelectric materials do not contain iron. Examples include barium strontium titanate (BST), and lead zirconate titanate (PZT)[a]

- **Advantages**:
  - Versatility: volumetric (waveguide) and thin film (circuit)

- **Disadvantages**:
  - Insertion loss: bound by the Kramer-Krönig relation. The higher the dielectric constant, the higher the attenuation.
  - Supply voltage: High voltage

- **Applications**:
  - Continuous transverse stubs (CTS) [2] and electronically scanned reflect arrays

[a] Nematic liquid crystals, such as the Merck nematic mixture BL037, have similar properties [3].

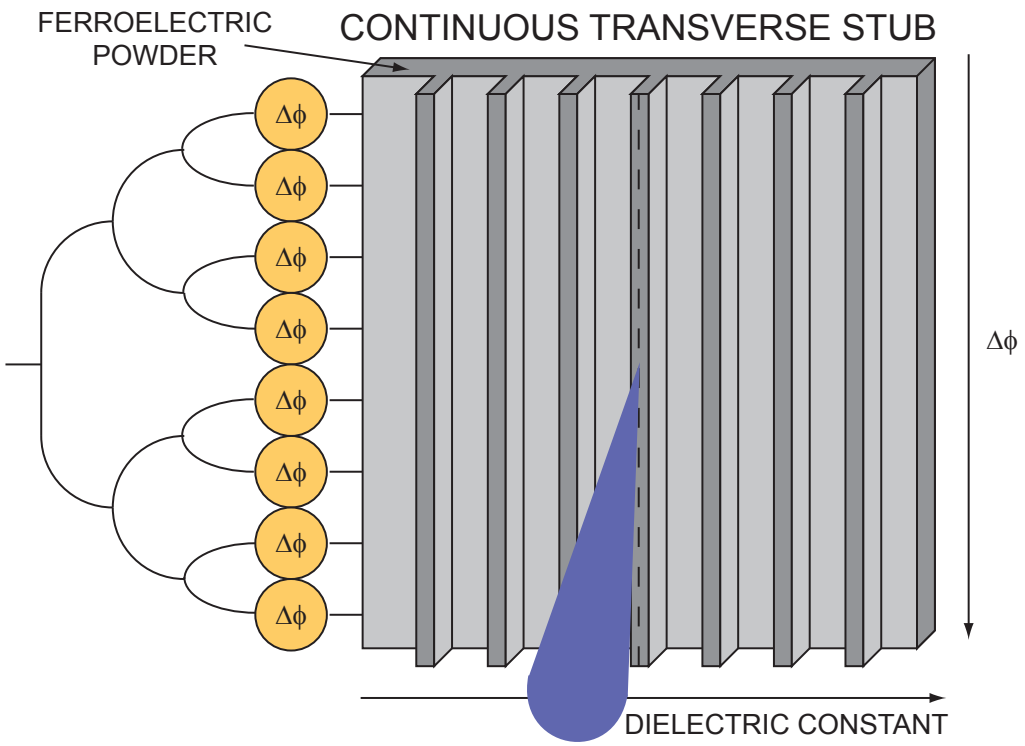

Figure 39: Continuous transverse stub (CTS) filled with a voltage tunable ferroelectric [2].

MOSFET

Enhancement-mode (normally-off) bulk nMOSFET (1960, Kahng and Atalla)

- **Principle**: A MOSFET is a 3-terminal device, in which the n-type surface channel resistance between two of the contacts (source, drain) is capacitively controlled (MOS capacitor) by the third (gate). In CG configuration, it can be used as an SPST switch (ON-state: linear region, OFF-state: cut-off region).

- **Advantages**:
  - Biasing: high-resistivity biasing improves isolation and linearity
  - Power consumption: no static power consumption
  - Switching time: limited by f_T

- **Disadvantages**:
  - BW, IL and isolation: high $R_{ON}\,C_{OFF}$ product. IL inversely related to gate width, which is limited by BW (parasitics) and isolation requirements. Lateral field isolation using deep (DTI) and shallow trench isolation (STI), vertical field isolation using high-resistivity biasing of gate (floating-gate), and buried-Nwell (double-well body floating triple-well RF nMOSFET) or insulator (SOI)
  - Power handling: limited by dielectric breakdown (vertical field, $V_{GS_{MAX}}$), hot electron injection (lateral field, $V_{DS_{MAX}}$) and electromigration ($I_{DS_{MAX}}$).

- **Applications**:
  - SPNT switch topologies: series-shunt ($R_{ON}\,C_{OFF}$), stacked (high-linearity), traveling-wave (wideband)

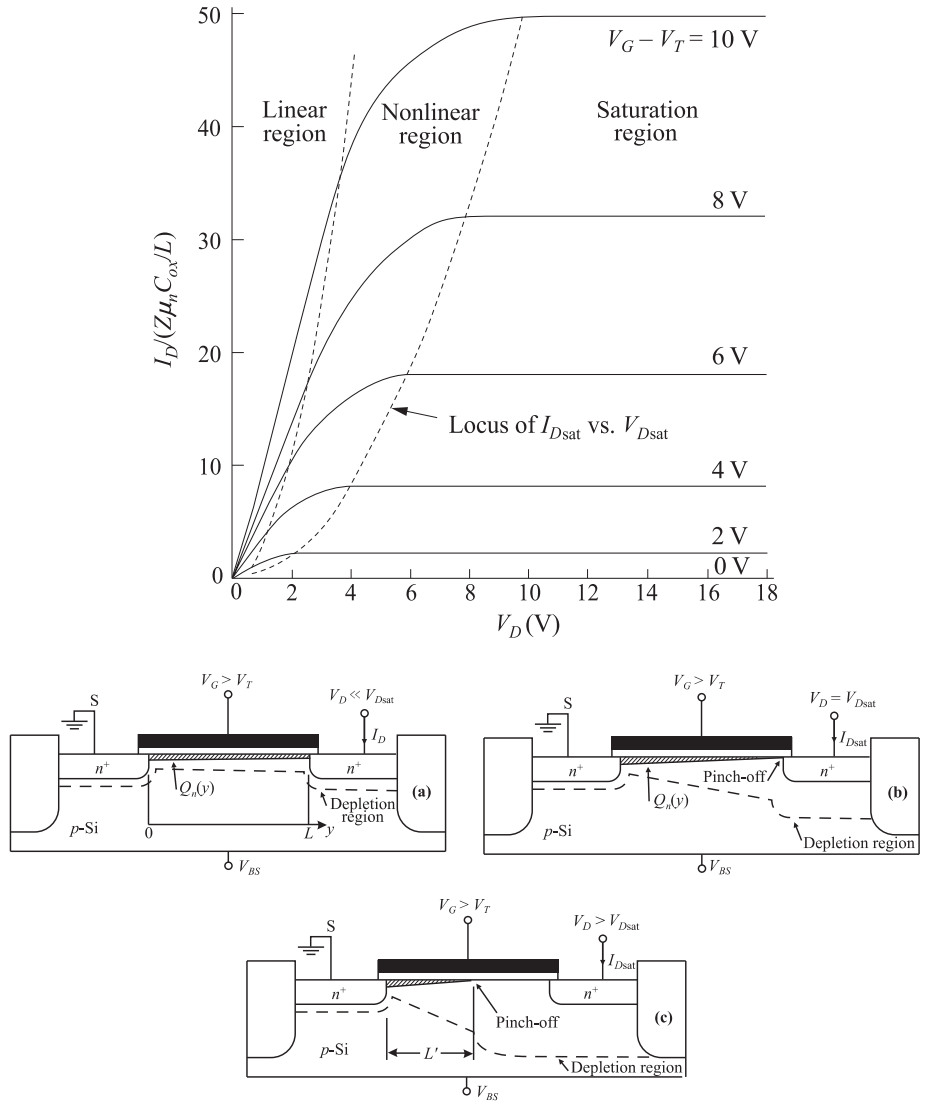

Figure 40: Enhancement-mode (normally-off) bulk nMOSFET operated (a) in the linear region (low V_DS), (b) at onset of saturation, and (c) beyond saturation (effective length is reduced) [4].

pHEMT (MODFET)

AlGaAs/GaAs depletion-mode (normally-on) HEMT (1980, Mimura)

- **Principle**: The unique feature of the modulation doped FET (high-electron mobility transistor) is the heterostructure, in which the wide-energy-gap material is doped and carriers diffuse to the undoped narrow-bandgap layer. At the heterointerface, a 2-D electron gas (2DEG) n-type buried channel is formed [4].

- **Advantages**:
  - Biasing: high-resistivity biasing (floating-gate) improves isolation and linearity
  - BW, IL and isolation: much lower $R_{ON}\,C_{OFF}$ product, due to high electron mobility of minority carriers in 2DEG channel (no $SiO_2 - Si$ interface impurity scattering, strain caused by indium insertion is used to increase the mobility even further in pseudomorphic HEMTs (pHEMTs)). Mesa lateral field isolation, and semi-insulating GaAs or SiC (GaN) substrate.
  - Power consumption: no static power consumption
  - Power handling: high for GaN HEMTs (wide-bandgap) and field-plate GaAs pHEMTs. No doping-induced $SiO_2 - Si$ interface hot electron injection
  - Switching time: limited by f_T

- **Disadvantages**:
  - Cost (cost drivers: epitaxial growth (MBE, MOCVD), mesa (ebeam lithography))

- **Applications**:
  - See MOSFET

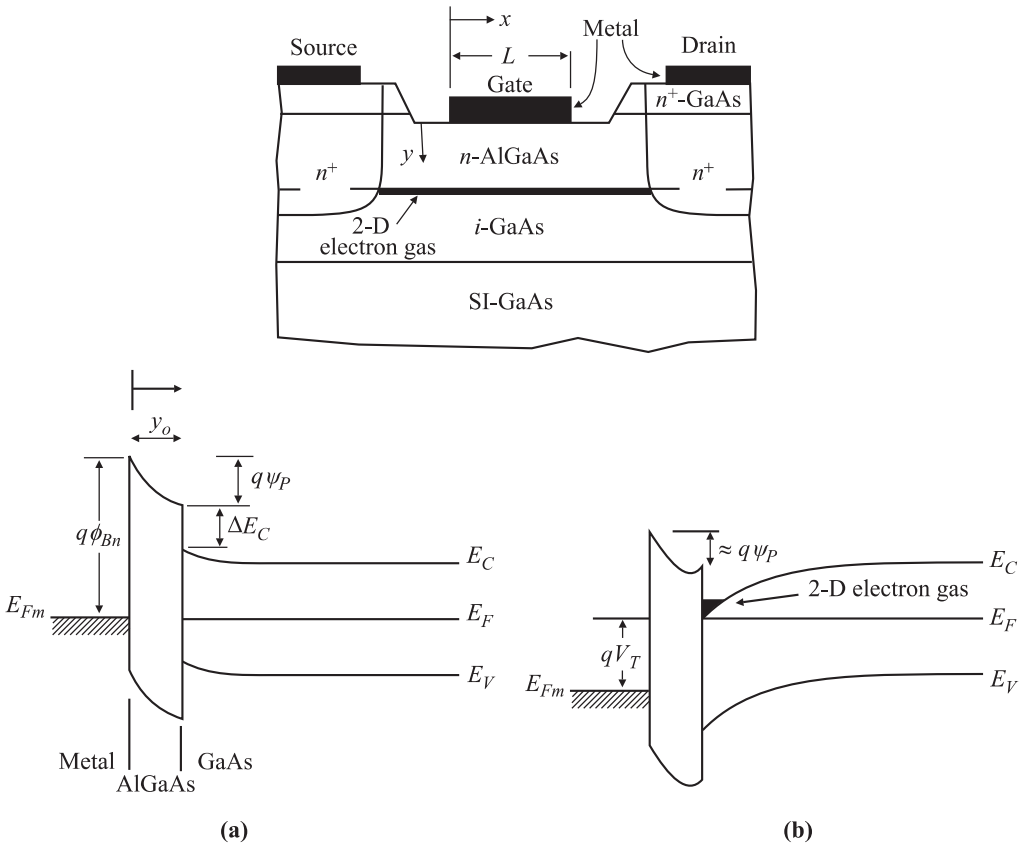

Figure 41: (top) Typical structure of MODFET, using the basic AlGaAs/GaAs system. (bottom) Energy-band diagrams for an enhancement-mode (normally-off) MODFET at (left) equilibrium and (right) onset of threshold [4].

p-i-n Diodes

p-n Diode (1949, W. Shockley)

- **Principle**: A p-i-n diode is a p-n junction with an intrinsic layer (i-layer) sandwiched between the p-layer and the n-layer. In practice, the i-region is approximated by either a high-resistivity p-layer (referred to as π-layer) or a high-resistivity n-layer (ν-layer). It can be used as an SPST switch (ON-state: forward-biased, OFF-state: reverse-biased), and as a varactor (reverse-biased).

- **Advantages**:
  - BW, IL and isolation: lowest $R_{ON}\,C_{OFF}$ product among semiconductors. The $R_{ON}\,C_{OFF}$ product is related to contact resistance and forward-bias DC current (R_{ON}), as well as to width of intrinsic layer (C_{OFF}). R_P is high for vertical p-i-n diodes, lower for lateral p-i-n diodes, which are derived from InGaP or SiGe:C heterojunction bipolar transistors (HBTs).
  - Linearity and power handling: limited by forward and reverse breakdown voltages
  - Rectification: does not rectify like p-n diode

- **Disadvantages**:
  - Biasing: high-resistivity biasing (wideband, power consuming), RF chokes (narrowband)
  - Power consumption: static power consumption. A low R_{ON} requires a high forward-bias DC current.
  - Switching time: faster than FET, RF MEMS

- **Applications**:
  - See MOSFET

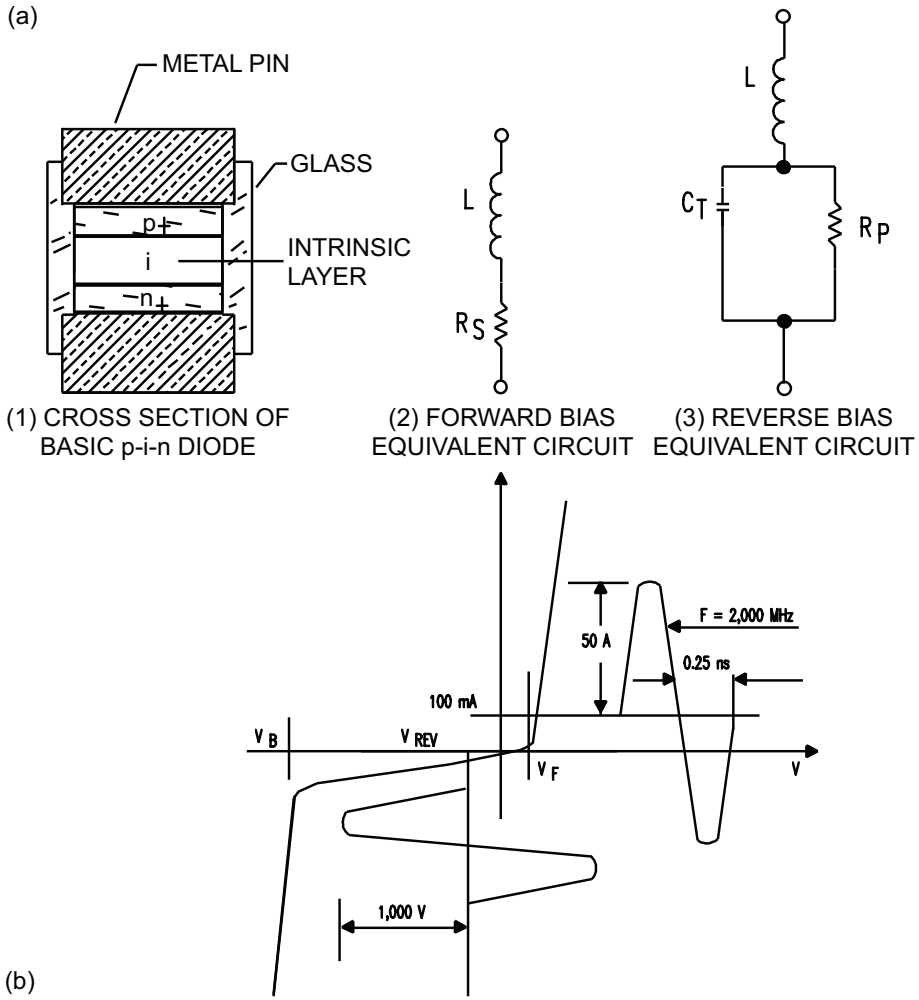

Figure 42: (a) p-i-n Diode and corresponding equivalent circuits, (b) RF voltage and current waveforms superimposed on p-i-n diode IV characteristics [5].

RF Technologies: References

[1] D. M. Pozar, *Microwave Engineering, 2nd Ed.* John Wiley & Sons, 1998.

[2] C. Quan, J. J. Lee, B. M. Pierce, and R. C. Allison, "Wideband 2-D electronically scanned array with compact CTS feed and MEMS phase shifters," U.S. Patent 6,822,615, February 25, 2003.

[3] M. Ismail, W. Hu, R. Cahill, V. Fusco, H. Gamble, D. Linton, R. Dickie, S. Rea, and N. Grant, "Phase agile reflectarray cells based on liquid crystals," *IEE Proceedings—Microwaves, Antennas and Propagation*, vol. 1, no. 4, pp. 809 –814, Aug. 2007.

[4] S. M. Sze and K. K. Ng, *Physics of Semiconductor Devices, 3rd Ed.* John Wiley & Sons, 2007.

[5] The PIN diode circuit designers handbook. Microsemi-Watertown. [Online]. Available: http://www.microsemi.com

RF MEMS

Electrostatically-actuated RF MEMS switch (1979, K. Petersen [3–5, 7, 9, 10, 14])

- **Principle**: The radio frequency microelectromechanical system (RF MEMS) acronym refers to electronic components of which moving sub-millimeter-sized parts provide RF functionality.
- **Advantages**:
  - BW, IL and isolation: intrinsically wideband due to electrostatic biasing and absence of parasitics, low insertion loss (high Q factor) and high isolation, lowest $R_{ON}\,C_{OFF}$ product
  - Cost: fabrication process requires min. 3 masks [11].
  - Linearity
  - Power consumption: no static power consumption
  - Power handling
- **Disadvantages**:
  - Packaging: hermetic
  - Reliability
  - Switching time [6, 8]
- **Applications**:
  - SPNT switches: series-shunt, no need for stacked or traveling-wave topologies

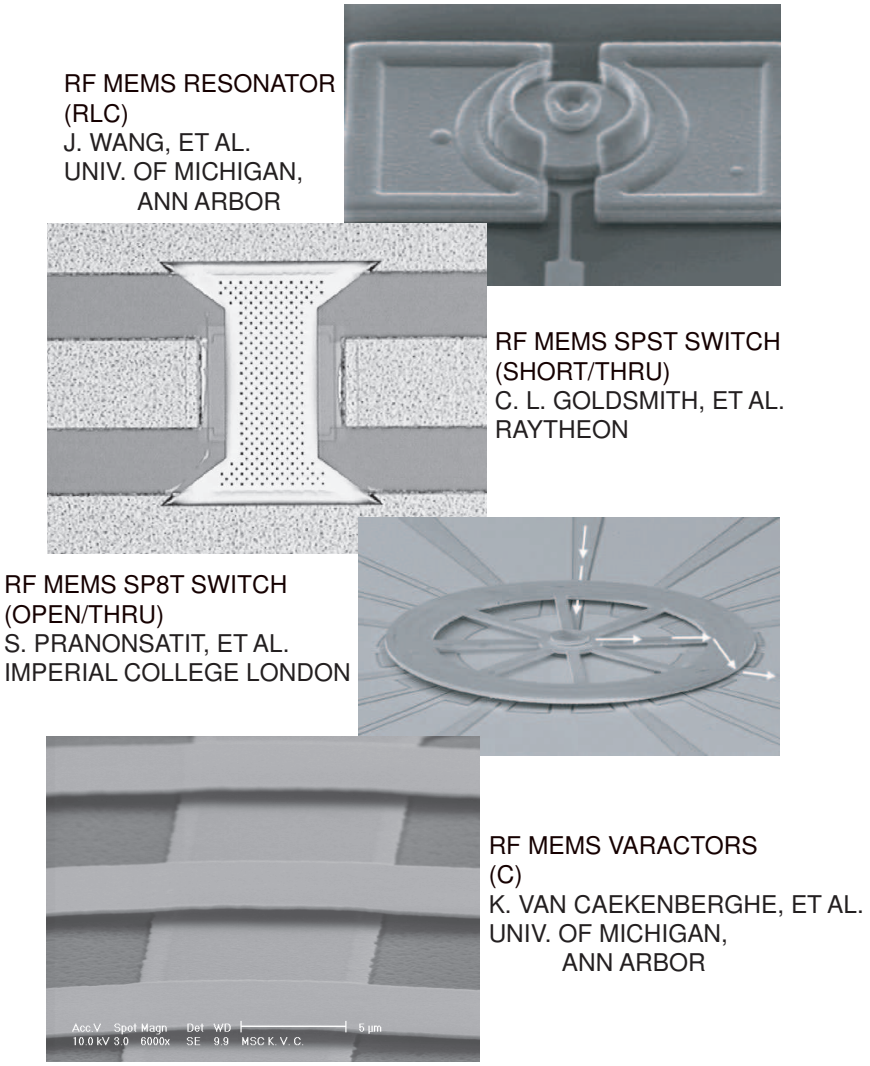

Figure 43: (a) RF MEMS resonator, (b) RF MEMS SPST switch, (c) RF MEMS SPNT switch, and (d) RF MEMS varactors.

Electromechanical model: mass-spring system [10]

- Mass:

$$m = 0.4\,\rho\,l\,w\,t$$

- Spring constant (capacitive fixed-fixed beam):

$$k = 32\,E\,w\left(\frac{t}{l}\right)^3\left(\frac{27}{49}\right) + 8\,\sigma\,(1-\nu)\,w\,\frac{t}{l}\left(\frac{3}{5}\right)$$

- Electrostatic force:

$$F_e = -\frac{1}{2}\,\frac{\epsilon_0\,A\,V_s^2}{g^2}$$

- Pull-in voltage (capacitive fixed-fixed beam):

$$V_p = \sqrt{\frac{8\,k(g_0+t_d/\epsilon_d)^3}{27\,\epsilon_0\,A}}$$

- Hold-down voltage (capacitive fixed-fixed beam):

$$V_h = \sqrt{\frac{2\,k\,g_0\,(t_d/\epsilon_d)^2}{\epsilon_0\,\epsilon_d\,A}}$$

- Switching time (pull-in time):

$$t_s = 3.67\,\frac{V_p}{V_s\,\sqrt{k/m}} \sim \sqrt{\frac{\rho}{E}} \text{ for } V_s = V_p$$

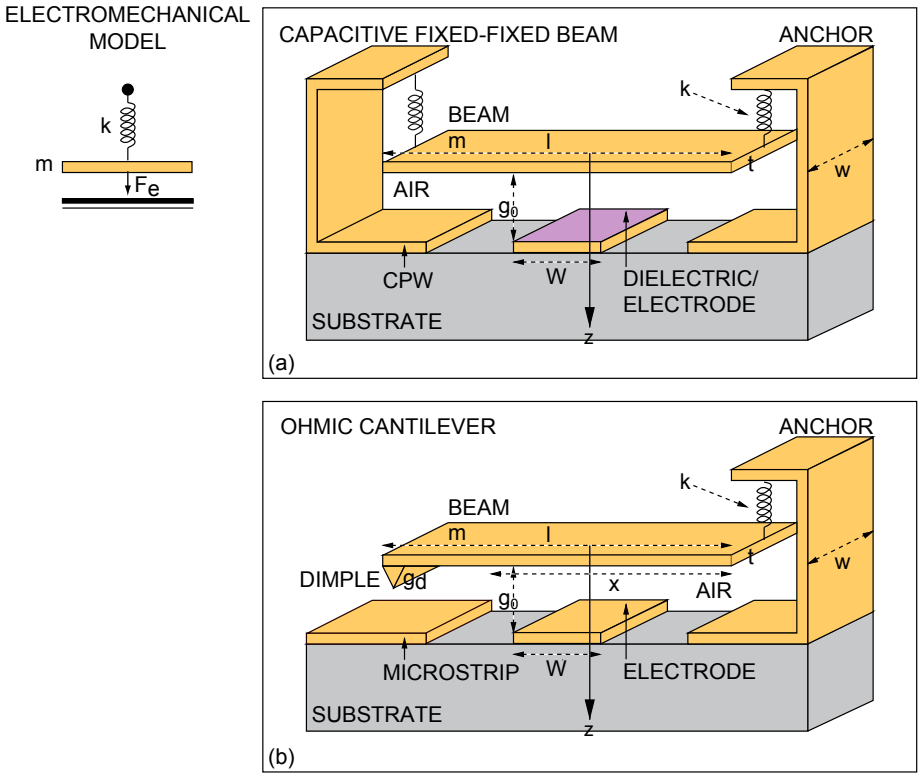

Figure 44: (a) a capacitive fixed-fixed beam RF MEMS switch, connected in shunt to a CPW line, (b) an ohmic cantilever RF MEMS switch, connected in series to a microstrip line.

Electromechanical model: mass-spring system [10]

- Mass:

$$m = 0.4\,\rho\,l\,w\,t$$

- Spring constant (ohmic cantilever):

$$k = 2\,E\,w\left(\frac{t}{l}\right)^3 \frac{1-(x/l)}{3-4\,(x/l)^3+(x/l)^4}$$

- Electrostatic force:

$$F_e = -\frac{1}{2}\,\frac{\epsilon_0\,A\,V_s^2}{g^2}$$

- Pull-in voltage (ohmic cantilever):

$$V_p = \sqrt{\frac{8\,k\,g_0^3}{27\,\epsilon_0\,A}}$$

- Hold-down voltage (ohmic cantilever):

$$V_h = \sqrt{\frac{2\,k\,(g_0-g_d)\,g_d^2}{\epsilon_0\,A}}$$

- Switching time (pull-in time):

$$t_s = 3.67\,\frac{V_p}{V_s\,\sqrt{k/m}} \sim \sqrt{\frac{\rho}{E}} \text{ for } V_s = V_p$$

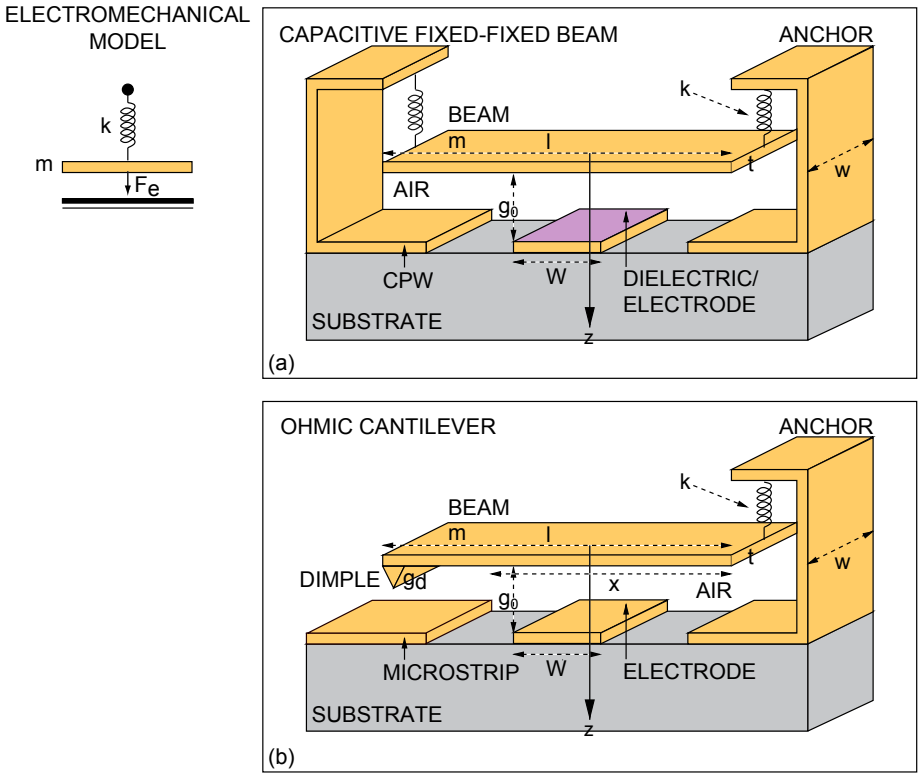

Figure 45: (a) a capacitive fixed-fixed beam RF MEMS switch, connected in shunt to a CPW line, (b) an ohmic cantilever RF MEMS switch, connected in series to a microstrip line.

In reality, RF MEMS beams are not flat but track the underlying topology and are bowed due to residual stress.

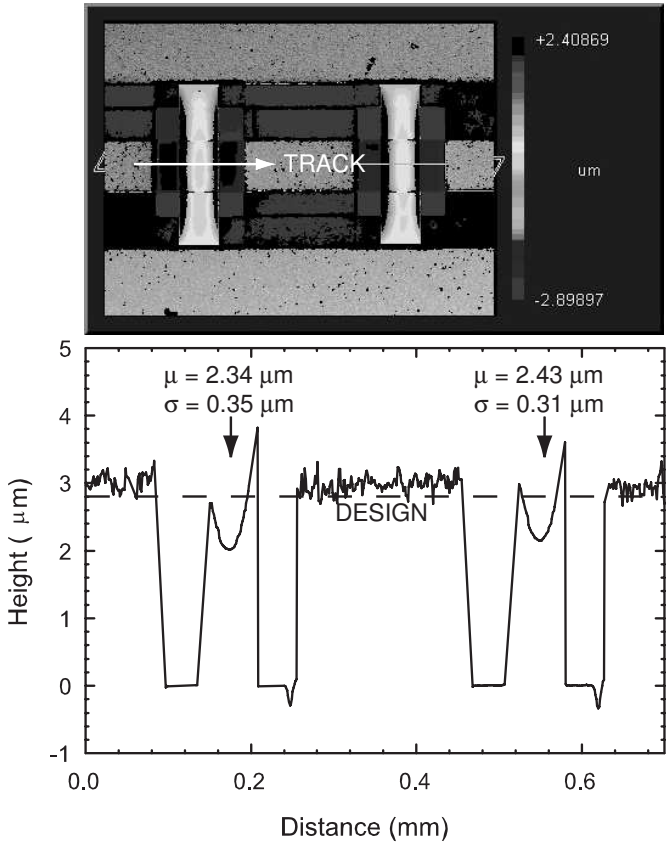

Figure 46: Optical interferometry imagery (top) and surface profile (bottom) of capacitive fixed-fixed beam RF MEMS components fabricated using the conventional fabrication process [1, 2]. The mean and standard deviation of the transverse beam profile are shown.

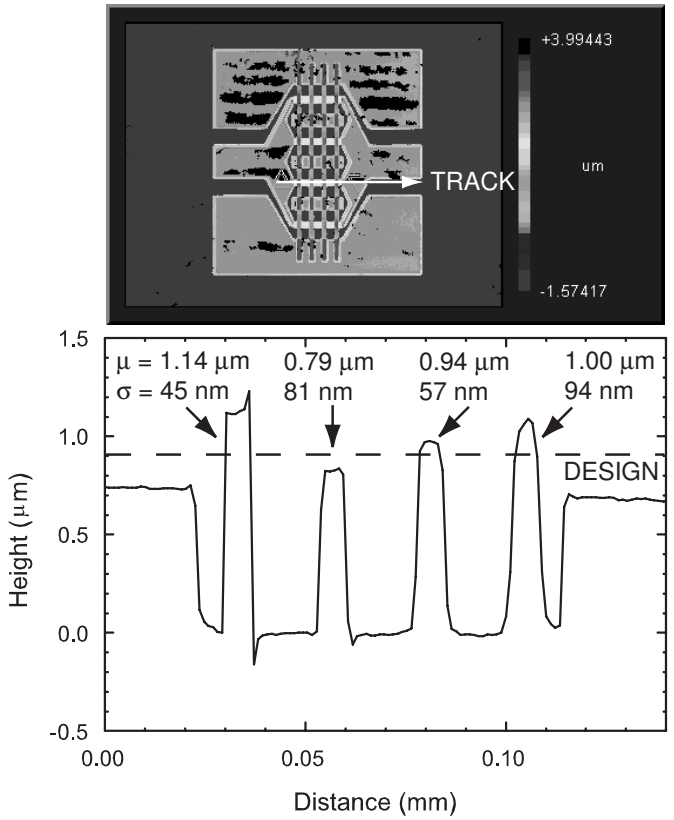

Figure 47: Optical interferometry imagery (top) and surface profile (bottom) of capacitive fixed-fixed beam RF MEMS components fabricated using the self-aligned fabrication process [12]. The mean and standard deviation of the transverse beam profile are shown.

Small signal RF model for S-parameter simulation: C_u/C_d [10]

- Up-state capacitance:

$$C_u = 1.4 \frac{\epsilon_0 A}{g_0 + t_d/\epsilon_d}$$

- Quality factor:

$$Q = \frac{1}{\omega R C_u}$$

- Down-state cap. (capacitive fixed-fixed beam):

$$C_d = 0.65 \frac{\epsilon_0 \epsilon_d A}{t_d}$$

Large signal RF model for harmonic balance simulation (IP3, P1dB): memcapacitor (nonlinear capacitor with hysteresis in the C-V curve) [10, 13]

- Up-state capacitance:

$$C_u = 1.4 \frac{\epsilon_0 A}{g(j\omega) + t_d/\epsilon_d}$$

- Electrostatic force:

$$F_e(j\omega) = -\frac{1}{2} \frac{C_u(j\omega) v^2_{RMS}(j\omega)}{g(j\omega)}$$

- Second law of Newton (frequency domain):

$$g(j\omega) = g_0 + \frac{F_e(j\omega)}{k + j\omega b - \omega^2 m}$$

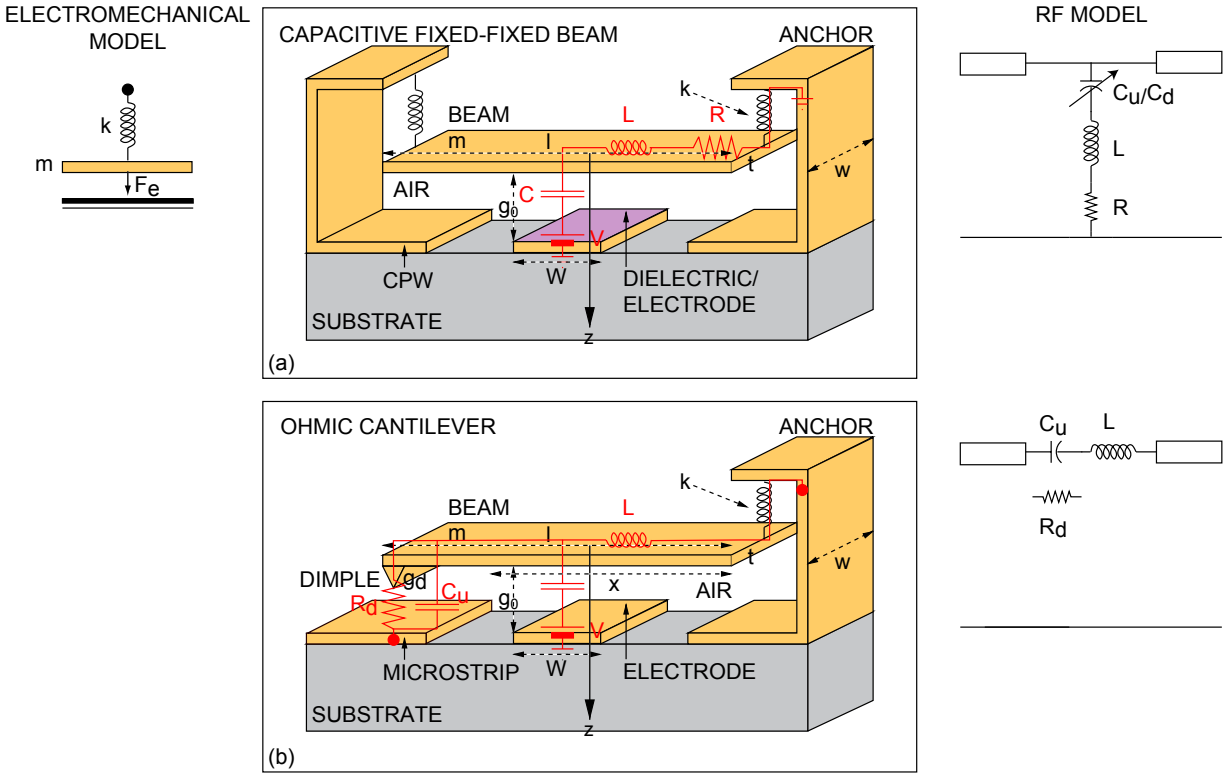

Figure 48: (a) a capacitive fixed-fixed beam RF MEMS switch, connected in shunt to a CPW line, (b) an ohmic cantilever RF MEMS switch, connected in series to a microstrip line.

Small signal RF model for S-parameter simulation: C_u/R_d [10]

- Up-state capacitance:

$$C_u = 1.4 \frac{\epsilon_0 A}{g_0 + t_d/\epsilon_d}$$

- Quality factor:

$$Q = \frac{1}{\omega R C_u}$$

- Down-state resistance (ohmic cantilever):

$$R_d$$

Large signal RF model for harmonic balance simulation (IP3, P1dB): memcapacitor (nonlinear capacitor with hysteresis in the C-V curve) [10, 13]

- Up-state capacitance:

$$C_u = 1.4 \frac{\epsilon_0 A}{g(j\omega) + t_d/\epsilon_d}$$

- Electrostatic force:

$$F_e(j\omega) = -\frac{1}{2} \frac{C_u(j\omega) v^2_{RMS}(j\omega)}{g(j\omega)}$$

- Second law of Newton (frequency domain):

$$g(j\omega) = g_0 + \frac{F_e(j\omega)}{k + j\omega b - \omega^2 m}$$

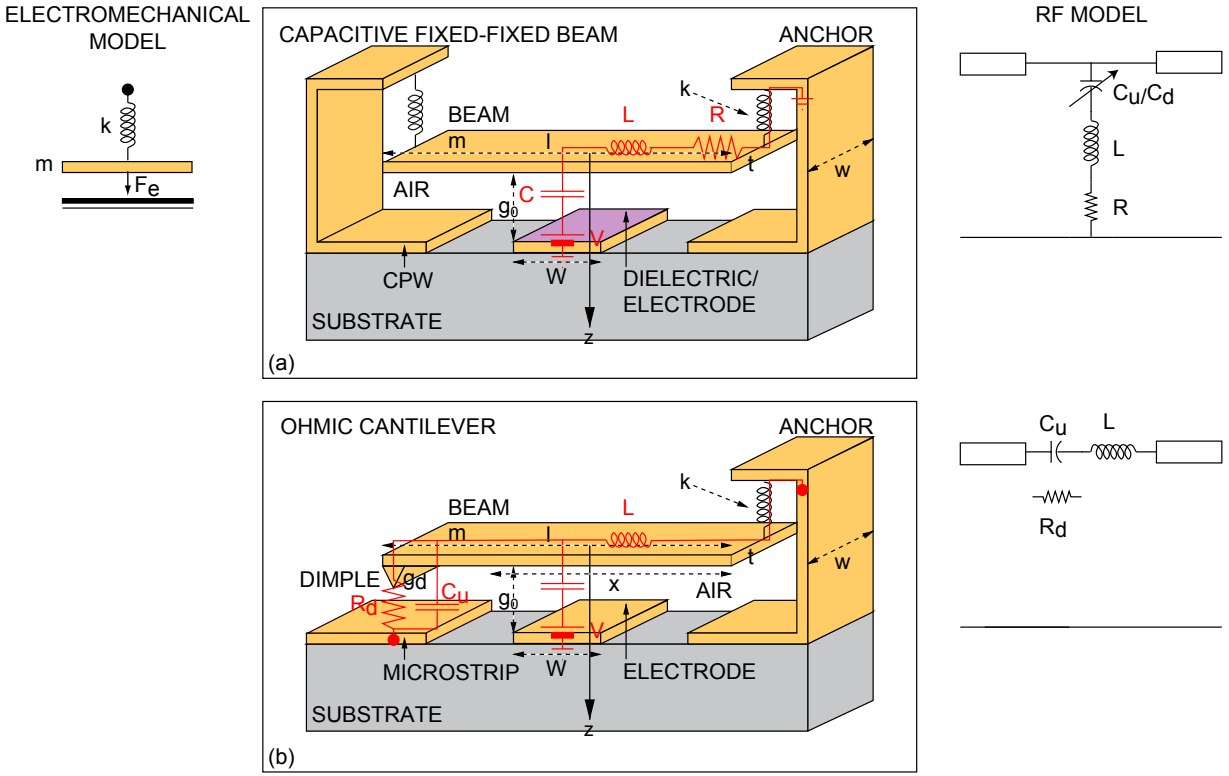

Figure 49: (a) a capacitive fixed-fixed beam RF MEMS switch, connected in shunt to a CPW line, (b) an ohmic cantilever RF MEMS switch, connected in series to a microstrip line.

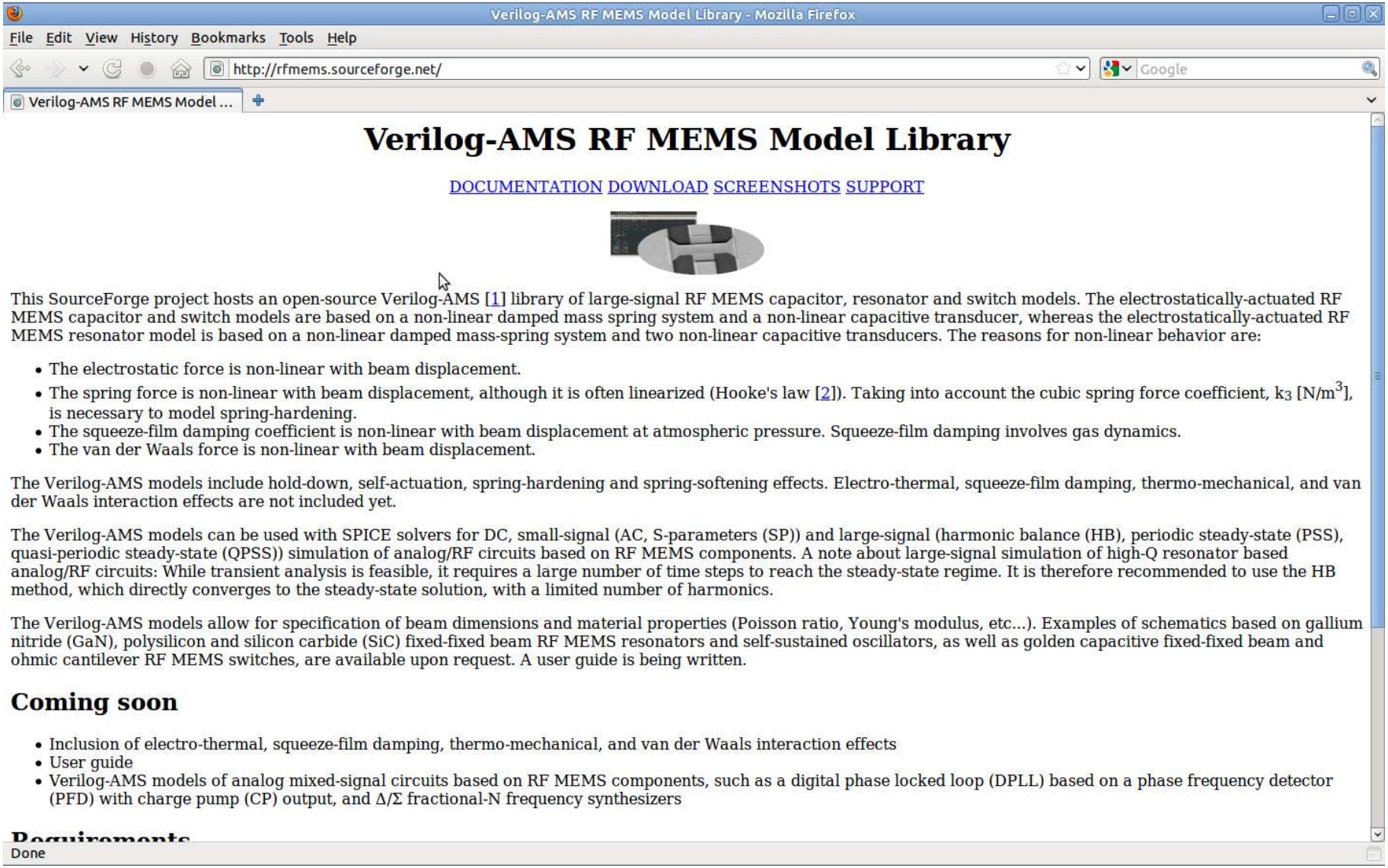

Figure 50: rfmems.sourceforge.net

RF Technologies: References

[1] N. S. Barker and G. M. Rebeiz. Distributed MEMS true-time delay phase shifters and wideband switches. *IEEE Trans. Microwave Theory Tech.*, 46(11):1881–1890, November 1998.

[2] N. S. Barker and G. M. Rebeiz. Optimization of distributed MEMS transmission-line phase shifters - U-band and W-band designs. *IEEE Trans. Microwave Theory Tech.*, 48(11):1957–1966, November 2000.

[3] Charles L. Goldsmith, Bradley M. Kanack, Tsen-Hwang Lin, Bill R. Norvell, Lily Y. Pang, Billy Powers, Jr., Charles Rhoads, and David Seymour. Micromechanical microwave switching.

[4] Charles L. Goldsmith, Zhimin Yao, Susan Eshelman, and David Denniston. Performance of low-loss RF MEMS capacitive switches. *IEEE Microwave Wireless Compon. Lett.*, 8(8):269–271, August 1998.

[5] J. B. Hacker, R. E. Mihailovich, M. Kim, and J. F. DeNatale. A Ka-band 3-bit RF MEMS true-time-delay network. *IEEE Trans. Microwave Theory Tech.*, 51(1, part 1):305–308, January 2003.

[6] Benjamin Lacroix, Arnaud Pothier, Aurelian Crunteanu, Christophe Cibert, Frederic Dumas-Bouchiat, Corinne Champeaux, Alain Catherinot, and Pierre Blondy. Sub-microsecond RF MEMS switched capacitors. *IEEE Trans. Microwave Theory Tech.*, 55(6):1314–1321, June 2007.

[7] Lawrence E. Larson. Micro-machined switch and method of fabrication.

[8] Denis Mercier, Koen Van Caekenberghe, and Gabriel M. Rebeiz. Miniature RF MEMS switched capacitors. In *IEEE MTT-S International Microwave Symposium Digest*, June 2005.

[9] Kurt E. Petersen. Micro-mechanical membrane switches on silicon. *IBM J. Res. & Dev.*, 23(4):376–385, July 1979.

[10] G. M. Rebeiz. *RF MEMS, Theory, Design and Technology*. John Wiley & Sons, 2003.

[11] A. Stehle, C. Siegel, V. Ziegler, B. Schönlinner, U. Prechtel, H. Seidel, and U. Schmid. High-power handling capability of low complexity RF MEMS switch in Ku-band. *Electronics Letters*, 43(24):1367–1368, November 2007.

[12] K. Van Caekenberghe and K. Sarabandi. A self-aligned fabrication process for capacitive fixed-fixed beam RF MEMS components. *J. Microelectromech. Syst.*, 17(3):747–754, June 2008.

[13] Massimiliano Di Ventra, Yuriy V. Pershin, and Leon O. Chua. Circuit elements with memory: Memristors, memcapacitors, and meminductors. *Proc. IEEE*, 97(10):1717–1724, October 2009.

[14] P. M. Zavracky, S. Majumder, and N. E. McGruer. Micromechanical switches fabricated using nickel surface micromachining. *J. Microelectromech. Syst.*, 6(1):3–9, March 1997.